Solar-Terrestrial Centre of Excellence

Annual Report 2019

Belgian Science Policy Office belspo

Royal Observatory of Belgium

RMI

BIRA-IASB

.be

STCE

Solar-**T**errestrial **C**entre of **E**xcellence

https://stce.be/

Ringlaan 3

B-1180 Brussels

Tel.: +32 2 373 0211

Fax: + 32 2 374 9822

Front page: *A view on one of the 17 (!) sessions that was organized during the 16th European Space Weather Week (ESWW16) that took place in Liège, Belgium from 18 till 22 November 2019. There were also 21 Topical Discussion Meetings, and plenty of other activities, making it once again a very successful conference. This ESWW was the last organized by the STCE (for the moment). This space weather conference will continue, but its set-up will now be provided by other institutes. (Credits: Olivier Boulvin)*

Table of Contents

A word from the STCE coordinator

Dear Readers,

I am happy to introduce to you the annual summary report 2019 of the Solar-Terrestrial Centre of Excellence.

The Sun was very quiet in 2019, which is clearly the minimum of the solar cycle, with activity heralding the next cycle gearing up towards the end of the year. Exactly how quiet things were is summarized in the solar-terrestrial highlights at the beginning of the report. It's been many years now since we had large solar events and severe geomagnetic disturbances! But of course we all know that that will change again in the future, and this makes the work of our researchers, forecasters and service providers important for the future. Some highlights of this work are further described in this report, but of course don't forget that we only lift the tip of the curtain! Many more continuous activities are going on in the STCE. It will be our pleasure to present some more of those in the future editions of our annual report.

But back to this year. Once again, the STCE played an important role in bringing the diverse communities interested in space weather together at the annual European Space Weather Week, organized by the STCE in Liège from 18 till 22 November. It was the 14th consecutive time that this was organized in Belgium, but alas also for the time being the last time, since we decided that it is time that ESWW moves around a bit. We are very proud of the heritage that we created by making ESWW grow from a relatively small workshop to a big, mature hallmark conference with attendance by hundreds of scientists, engineers, users,... from scores of countries from all over the world!

But it is not the only meeting we organized in 2019. We celebrated the 50th anniversary of ozone sonde measurements in Uccle with a well-attended symposium. And in Redu we co-organized a symposium at the occasion of PROBA2 becoming a teenager.

And then, of course, we have much to report about the data that we collect and distribute, the instruments that we build and deploy, and the research that we execute and facilitate through the STCE. Not to forgot the space weather forecasts and operations that continue to grow, with e.g. the formal start of PECASUS operations in November. But I will let you read all about that - and more - yourself. Enjoy the reading!

Ronald Van der Linden
General Coordinator of the Solar-Terrestrial Centre of Excellence
Director General of the Royal Observatory of Belgium

Anne Vandersyppe (1959-2019)

Always Loved - Never Forgotten - Forever Missed

Structure of the STCE

The Solar-Terrestrial Centre of Excellence is a project of scientific collaboration that focuses on the Sun, through interplanetary space, up to the Earth and its atmosphere.

The solid base of the STCE is the expertise that exists in the 3 Federal Scientific Institutes of the Brussels Space Pole: the Royal Observatory of Belgium, the Royal Meteorological Institute and the Royal Belgian Institute for Space Aeronomy. The STCE supports fundamental solar, terrestrial and atmospheric physics research, is involved in earth-based observations and space missions, offers a broad variety of services (mainly linked to space weather and space climate) and operates a fully established space weather application centre. The scientists act at different levels within the frame of local, national and international collaborations of scientific and industrial partners.

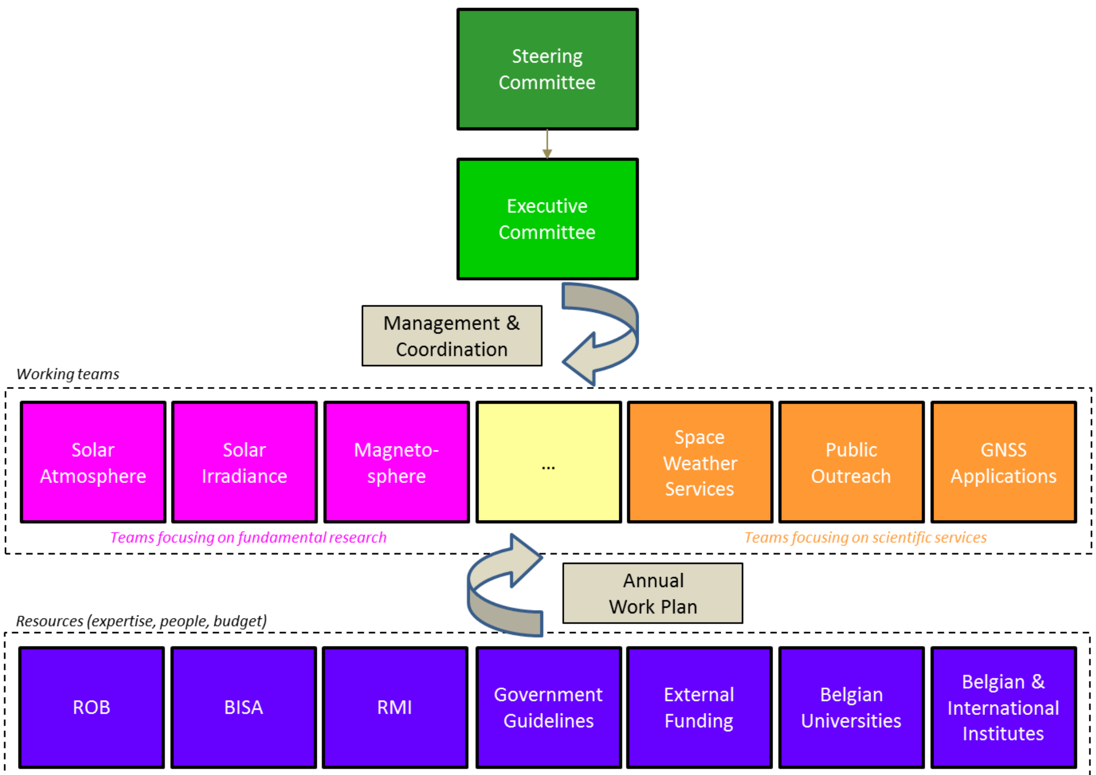

Figure 1: The STCE management structure

The STCE's strengths are based on sharing know-how, manpower, and infrastructure.

In order to optimize the coordination between the various working groups and institutions, as well as the available resources such as ICT, personnel and budget, a management structure for the STCE was put into place, consisting of a steering committee and an executive committee.

The ***steering committee*** takes all the final decisions on critical matters with regard to the STCE. It assures the integration of the STCE into the 3 institutions and the execution of the strategic plans. It is composed of:

- BELSPO Director General "Research Programmes and Applications"

  Dr. Frank Monteny (BELSPO)

- Director General of each of the 3 institutions at the Space Pole

  Dr. Ronald Van der Linden (ROB)
  Dr. Daniel Gellens (RMI)
  Dr. Martine De Mazière (BISA)

The ***executive committee*** assures the global coordination between the working groups and the correct use of the budgetary means for the various projects. It also identifies new opportunities and is the advisory body to the Steering Committee. It is composed of:

- STCE Coordinator

  Dr. Ronald Van der Linden

- Representatives of the research teams in the 3 institutes

  Dr. David Berghmans (ROB)
  Dr. Carine Bruyninx (ROB)
  Dr. Johan De Keyser (BISA)
  Dr. Norma Crosby (BISA)
  Dr. Stanimir Stankov (RMI)
  Dr. Steven Dewitte (RMI)
  Dr. Hugo De Backer (RMI)

A promotional movie giving a flavor of the STCE's tasks, interactions and various research programs can be found via the STCE website (in English, and subtitled in French and Dutch).

Life at the STCE - Scientists studying interaction effects and drag parameters of snowballs. As one can see, they gave themselves completely to their research. (3 inset pictures by Matt West)

Monitoring space weather: solar-terrestrial highlights in 2019

The official annual sunspot number (SN) for 2019, as determined by the WDC-SILSO (World Data Center - Sunspot Index and Long-term Solar Observations), was 3.6. This is a further decrease compared to 2018 (7.0), and it is even lower than the previous deep minimum in 2008 and 2009 when the yearly sunspot number was at 4.2 and 4.8 respectively. The highest daily sunspot number (38) was recorded on 21 March.

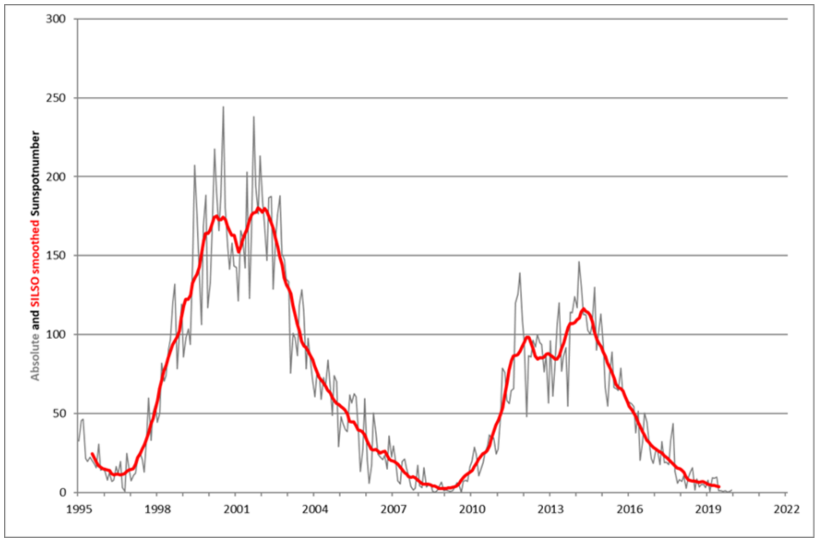

Figure 2: The evolution of the monthly and monthly smoothed SN (1995-2019). Pending the smoothing formula used, Solar Cycle 24 (SC24) reached its maximum of 116.4 in April 2014 (SILSO formula), or 118.2 in March 2014 (Meeus formula).

With 274 days, 2019 has ranked itself on the 4th place in the list of years with the most spotless days since 1849. This number dwarfs that of 2018 (208), and is -again- stronger than the numbers recorded during the years of the previous solar cycle minimum, i.e. 2008 (265 days) and 2009 (262). Only 3 years have produced more spotless days than 2019: 1878, 1901, and the year 1913 which is recordholder with a staggering 311 days. (see SILSO's Spotless Days page). The longest spotless stretch so far this solar cycle transit took place from 14 November 2019 till 23 December 2019, totaling 40 days during which not a single sunspot was visible.

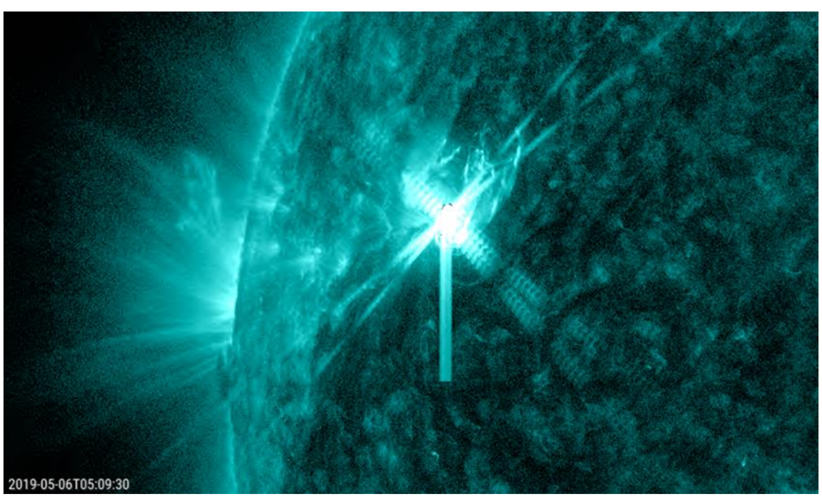

Figure 3: NOAA 2740 was the source of the most powerful flaring event in 2019: a C9.9 on 6 May. The peak of the flare can be seen in this image from SDO/AIA 131. The blooming and diffraction fringes are image artifacts due to pixel saturation and not related to the flare itself (see note 1 in this STCE Newsitem).

Just as in 2018, the Sun did not produce a single M- or X-class flare in 2019. There were also no proton events or Ground Level Enhancements reported. The strongest event was a C9.9 flare generated by NOAA 2740 on 6 May. This region was the source of 12 C-class flares, as many as NOAA 2736 just a few weeks earlier. Combined, these two active regions accounted for three quarters of the total number of C-class flares recorded in 2019.

A moderate to strong geomagnetic storm took place on 14 May, with the estimated K_p reaching 7 and the (Quicklook) Dst index reaching -65 nT (WDC Kyoto). This was the strongest geomagnetic storm of 2019 and it resulted from eruptive activity near the Sun's central meridian on 10 and 11 May. The associated coronal mass ejections (CMEs) reached the earth environment on 14 May, with solar wind speeds up to around 570 km/s and Bz as negative as -15 nT. Further eruptive activity with coronal dimming south of NOAA 2741 took place on 12-13 May, but the main portions of the associated CMEs were mostly directed south of the ecliptic. Of note is that during this solar cycle, no extremely severe geomagnetic storm (K_p = 9) has been observed.

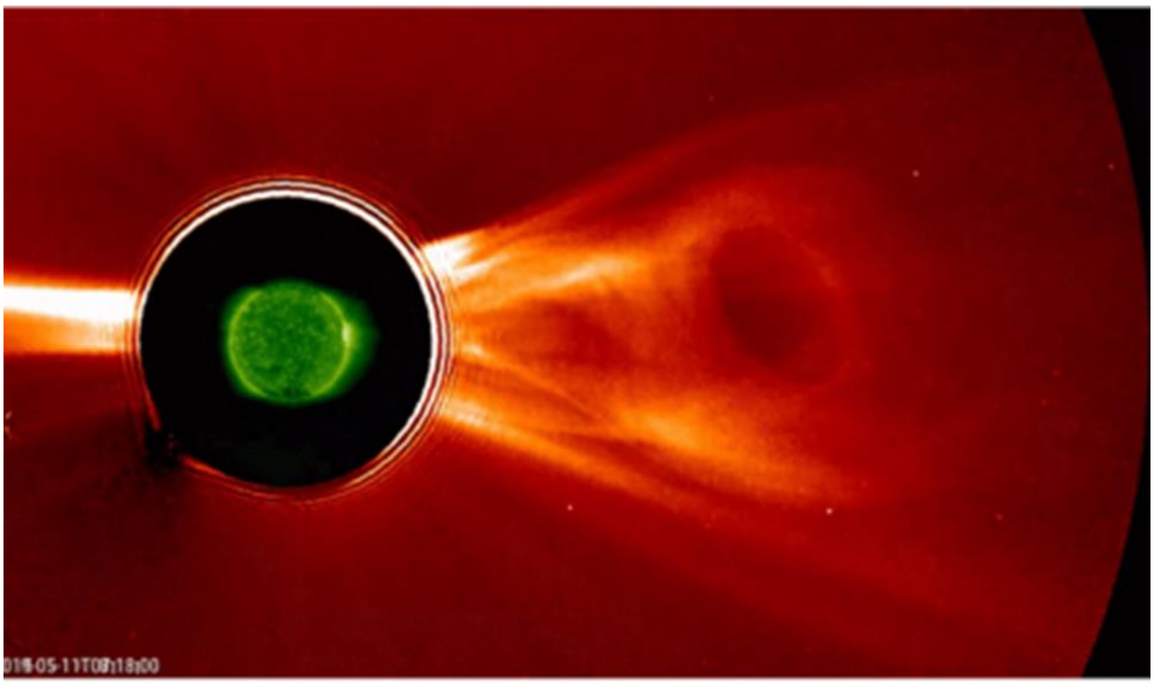

*Figure 4: A view on the 11 May CME which was one of the sources responsible for a moderate geomagnetic storm on 14 May. The picture combines an image of the Sun taken by **STEREO-A** / EUVI 195 in Extreme Ultraviolet (EUV) with a coronagraphic image taken by its COR2 instrument in white light.*

The series of CMEs during the first half of May resulted in a 2-3% decrease of cosmic rays during 8-22 May compared to the rest of the year (Oulu neutron monitor). Due to the ongoing solar cycle minimum, cosmic rays were at very high levels and only slightly lower than during the previous solar cycle minimum transit in 2008-2010. Cosmic rays are known to pose a radiation hazard to passengers and crew on polar flights, and to astronauts. Increased cosmic ray levels affect the composition of the Earth's upper atmosphere, and it is also believed they may help trigger lightning and lightning-associated effects such as sprites.

Early July, a small coronal hole (CH) started to develop in the northern hemisphere, possibly from an extension of the northern polar coronal hole (positive magnetic polarity). One solar rotation later, this CH had substantially grown in size, and during its transit late August it had evolved into a distinct shape resembling the number "7". After its October passage, the CH started to dissolve, but continued to mark its presence in the solar wind until December. Solar wind speeds reached maximum values of 600 or more km/s during each of its transits, with highest values near 800 km/s late August.

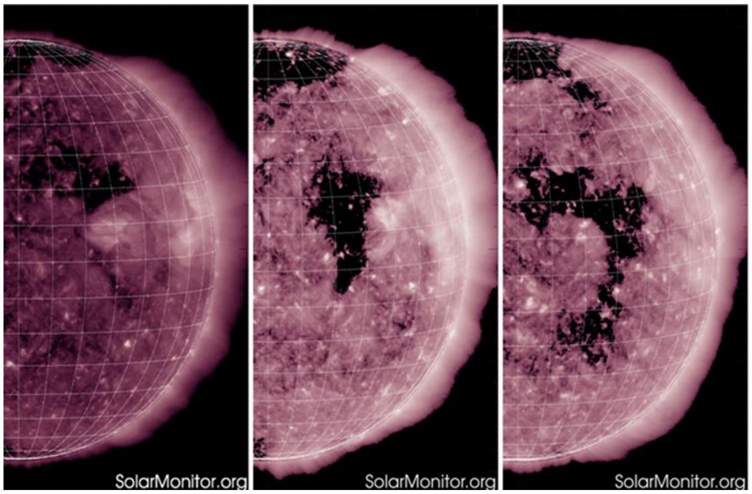

Figure 5: The James Bond of the coronal holes started to develop early July and transformed into a distinct number "7" two solar rotations later (late August). The high speed stream of this CH reached speed values near 800 km/s and drove the high-energy electrons to levels belonging to the highest of this solar cycle.

During that transit, it created also one of the strongest geomagnetic disturbances of the year (31 August-1 September; K_p=6; Dst=-52nT). Fast solar wind streams from coronal holes are known to drive highly energetic (energies of more than 2 MeV) electrons, which can lead to electrostatic discharges (ESD) resulting in malfunctions of a satellite and occasionally even in the satellite failure. The fluxes early September were very high, attaining values close to 90,000 pfu (1 pfu = 1 electron / cm^2 s sr) on 4 September, or 90 times above the alert level! These values belong to the highest > 2 MeV electron fluxes observed during this solar cycle.

The last 2 months of 2019 saw a significant increase in the number of sunspot groups from the new solar cycle 25 (SC25). It concerned all small and short-lived regions. NOAA 2750 was visible early November and produced a B1 flare when it was already spotless on 5 November. Its high southern latitude of -28 degrees and reversed magnetic polarity indicated this was a group of the new solar cycle.

On 24 December, 2 sunspot regions of the new solar cycle were visible on the solar disk at the same time. NOAA 2753, located in the southeast quadrant near latitude -30 degrees, developed late on 23 December. NOAA 2754 was located in the northwest quadrant near latitude +25 degrees, and developed during the morning hours of 24 December. The appearance of these groups halted a period of 40 spotless days that started on 14 November (preliminary SILSO data). It is the longest stretch of spotless days since 1996. The increased number of sunspot groups of the new solar cycle may indicate that the cycle minimum is close and that SC25 is ready to take off.

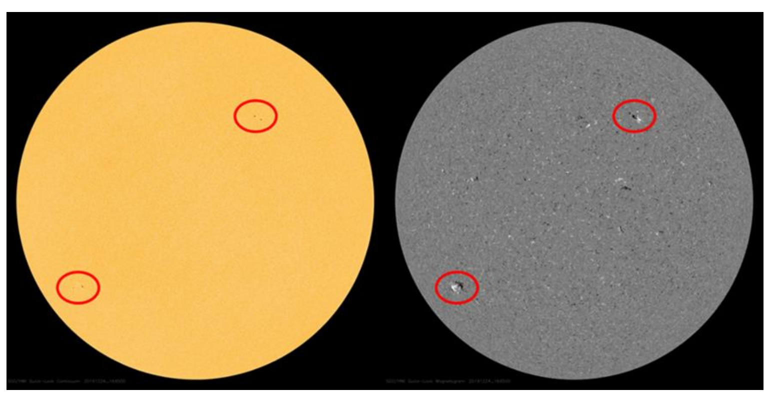

Figure 6: SDO's view of the Sun on 24 December showing two regions of the new solar cycle present at the same time. The continued emergence of regions from SC25 may indicate that solar minimum is very near.

Public outreach meets Science

Space Weather - the key theme at the ESWW conference

The Earth's magnetic field and atmosphere protect us against the solar wind and the highly energetic radiation emitted by the Sun. This fairly continuous particle flow and energy emission can change abruptly in response to solar eruptions and high-speed streams from coronal holes, putting our natural defense mechanisms to the test and initiating space weather processes which impact satellites, navigation, radio communication and can cause an increase of radiation levels. These solar storms can also interfere with the proper functioning of long-distance pipelines and electric power grids. So, it is no surprise that space weather is a hot and important research topic.

Figure 7: Poster for ESWW16.

Scientists need to talk to other scientists, work together and show their research results to each other. These conversations help them to adjust their research and get new insights. The methods to collect data and observations are usually not standardized and can be almost never just taken from the shelf. Innovative and "out of the box" ideas are often necessary. Interaction between scientists is crucial.

Figure 8: Left all alone on the stairs at the end of the ESWW16, the conference bell has tolled for the very last time. Feared by many, it was more effective than using a whip to drive the conference attendees from the break facilities back to the lecture rooms.

The annual European Space Weather Week (ESWW) conference provides such a forum where the worldwide space weather community can gather. At ESWW, the discussion is about how to deal with space weather in science, observations, services and technology and how to bridge the distance between science on the one hand and practical applications and services on the other. The 2019 ESWW was the 16th edition, the 14th edition held in Belgium with the STCE as key player. It took place in Liège from 18-22 November, bringing together no less than 417 participants from 40 different countries. There were 17 open sessions and 21 (!) Topical Discussion meetings on a variety of topics, 2 poster sessions, a tutorial that focused on space weather services, a visit to the Centre Spatial de Liège, live space weather forecasts, and a keynote lecture by Belgian's former astronaut Frank De Winne. More relaxing events were the Medal award ceremony followed by the Welcome reception, the Music Café, and the Space Weather Fair (with beer tasting). The conference dinner, offering delicious food, was concluded with strongly attended casino games. This was the last ESWW organized by the STCE (for now?). The conference will continue, but its set-up will be provided by other institutes. The next one will take place in Glasgow, UK.

Sun-Space-Earth for and by citizens

There's a considerable interest from the broad public in the space weather (SWx) domain. People want to understand what happens around them, what they are actually looking at, and why these things are happening. Understanding is the first step in getting a grip on situations and lives, so we want to optimize our communication on space weather and make the SWx world better understandable.

Figure 9: Ten years and still going strong! A mock-up of the PROBA2 satellite surrounded by its team of passionate researchers and operators adorn its 10th anniversary picture.

The STCE wants to spread the Sun-Space-Earth story that its researchers are looking for in their daily routine. Our scientists are excited to communicate on the knowledge and beauty hidden in the STCE research. In 2019, we celebrated the 10th anniversary of PROBA2, our micro-satellite. Reason enough to share it with the public with this STCE press item.

When the Extreme Ultraviolet Imager, another instrument to which STCE researchers have contributed, was ready to be integrated in the spacecraft Solar Orbiter, we again shared our excitement about this important ESA/NASA mission with the public through a press item.

Some enthusiasts go even further and want to have a concrete contribution in specific science areas. In its 2013 "Green Paper on Citizen Science", the European Commission defined the "citizen science" concept as "*… the general public engagement in scientific research activities when citizens actively contribute to science either with their intellectual effort or surrounding knowledge or with their tools and resources. Participants provide experimental data and facilities for researchers, raise new questions and co-create a new scientific culture. While adding value, volunteers acquire new learning and skills, and deeper understanding of the scientific work in an appealing way. …"* Several scientific tasks are not straightforward to be done by scientists because it is for example time consuming, or split into too many small parts that each have to be executed separately. Help from citizens can be crucial in these cases. We asked them to help us counting sunspots and sunspot groups by looking at old drawings. That way, our solar physicists were able to compare the counting from the past with

*Figure 10: The logo of the citizen science project "Val-U-Sun". The **webpage** is also available in **French** and **Dutch**!*

this recent recounting fairly quickly. If 500 citizens each recount 5 drawings, 2500 drawings are done with only a minimal effort. If 1 scientist has to recount all 2500 drawings, that would take a very long time indeed. Interested in the world of sunspots? Check out the Val-U-Sun webpage!

50 years of ozonesonde measurements at Uccle

Since January 1969, the RMI started the operational launches of ozonesonde instruments, attached to weather balloons. Those instruments, consisting of a very stable pump that sucks the ambient air in electrochemical concentration cells filled with solutions that interact solely with ozone molecules, provide the vertical distribution of the ozone concentrations in the atmosphere between the surface and 30-35 km altitude. In 2019, the time series of those measurements (done thrice a week) reached half a century.

Figure 11: Participants of the scientific symposium celebrating the 50 years of ozonesonde measurements at Uccle.

Therefore, on 19 September 2019, a scientific symposium with world-class leaders in ozone research as speakers (such as e.g. the president of the International Ozone Commission, and the Principal Investigator (PI) of the World Calibration Center for Ozonesondes) was organized on the premises of the Space Pole to celebrate the 50 years of ozonesonde measurements by the RMI. Also the president of the World Meteorological Organization (WMO), who started his career with ozonesonde research, gave a very interesting speech and handed over a certificate to RMI for "the outstanding contribution to the advancement of the Earth Sciences and especially regarding the long-term observations and quality control of the ozone vertical distribution. Since 1969, these observations greatly enhanced the understanding of the atmospheric processes, supported environmental policy and contributed to the activities of the WMO". Since the launch of the STCE in 2006, the instruments needed for those measurements (ozonesondes, radiosondes, balloons, parachutes) are funded by the STCE, as well as one FTE for the scientific exploitation of the ozonesonde time series.

On the two days preceding the celebration event (17 and 18 September 2009), a meeting of the panel on the Assessment of Standard Operating Procedures for OzoneSondes (ASOPOS) was organized in Brussels

Figure 12: The ozonesonde experts of the panel for the Assessment of Standard Operating Procedures of Ozonesondes that held a meeting in Brussels.

by the STCE. This panel, consisting of around 15 ozonesonde experts worldwide, aims at providing more consistent standard operating procedures in the global ozonesonde network to obtain high quality data, comparable between ozone sounding stations at the uncertainty level of 5% and traceable to a common reference instrument. It also identifies the outstanding, partly unsolved, instrumental and procedural issues on ozone soundings. One of the major goals of the Brussels meeting was the preparation of an update of the current GAW (Global Atmospheric Watch of the WMO) report on the Quality Assurance and Quality Control for Ozonesonde Measurements.

Finally, on 20 September 2019, a rather informal meeting, between the different PIs of the European ozonesonde stations, was organized and partly financed by the STCE. Its aim was to streamline the different operation and processing procedures and exchange recent findings and experiences with ozonesondes.

Life at the STCE - Following the ESWW16 conference dinner, some of the STCE researchers tried their luck in some casino games. Note that scientists are not rich: the chips are virtual and courtesy of the organizer!

Fundamental research

Long-term evolution of the solar corona using PROBA2 data

A group of mostly STCE researchers studied the evolution of the solar corona observed throughout solar cycle 24 (from 2010 to 2019), by using PROBA2/SWAP images, PROBA2/LYRA irradiance time series, and the latest version of the International Sunspot Number (ISN) dataset.

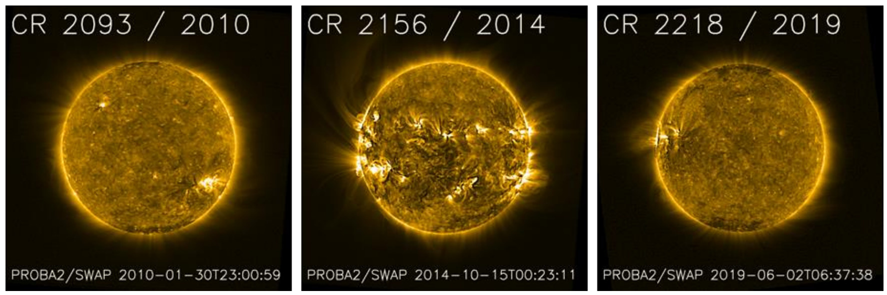

Figure 13: SWAP stacked images showing the solar corona at three moments of time between January 2010 and June 2019.

The SWAP EUV imager is monitoring both the changes on the solar disk and the changes in the large scale off-limb features, which can be seen to vary throughout the solar cycle. These large-scale structures trace out magnetic field lines, which are seen due to hot plasmas trapped on them. In a standard SWAP image, the signal-to-noise ratio in these regions is too small to distinguish individual structures. However, Dr. Dan Seaton developed an image processing method that employs image stacking and median filtering techniques to improve the signal to noise and enhance the signatures of structures in these regions. The evolution of large-scale structures in solar corona throughout SC24 can easily be seen by examining different Carrington rotation (CR) stacked images throughout the PROBA2 mission. A CR is a period of time chosen to represent one rotation of the Sun, allowing the comparison of features such as sunspot groups or active regions. A period of 27.28 days was chosen to represent a single rotation that largely resembles the recurrence time of features near the equator.

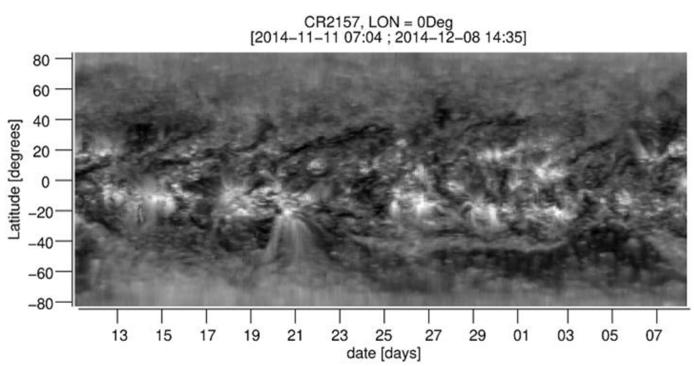

Figure 14: SWAP Synoptic Map of the Sun from 11 November to 8 December 2014. The image is constructed from the central meridian of the CR 2157 stacked images.

Figure 13 compares three stacked images of the Sun taken at different times during the solar cycle. The left image of Figure 13 shows the Sun on 30 January 2010 at the beginning of PROBA2 observations, which corresponds to the period when solar activity was increasing. The central image shows the Sun on 15 October 2014, at one of the peaks in the solar cycle when the Sun exhibited most activity. Finally, the right panel of Figure 13 shows the Sun on 2 June 2019, taken during the minimum phase of the solar cycle. The large-scale off-limb structures can clearly be seen to change between the different phases of the solar cycle, where the overlying structures become more complicated at solar maximum. They were visible from around March 2011 to around March 2016, meaning they were absent at the minimum phase of the solar cycle. A fan-like structure in the northern hemisphere was seen to persist for more than 11

CRs (February 2014 to March 2015) and was observed out to 1.6 solar radii. These complicated field structures are generated by the evolving magnetic field and can drive solar activity and space weather.

From the synoptic maps (see Figure 14) one can see the evolution of the active regions (ARs) over a full CR as well as the evolution of coronal holes (CHs). A SWAP synoptic map (or a latitude-time map) is constructed by extracting 3 degree-wide vertical stripes from individual stacked images. Each stripe is averaged into a single vertical line to remove artifacts in an image that might be created by events such as cosmic rays and Solar Energetic Particles striking the detector, or from radiation from the Earth's radiations belts and the South Atlantic Anomaly. A Carrington Rotation's worth of images are then put together side by side to create an image such as that seen in Figure 14.

By inspecting all the synoptic maps one can see that more ARs started to appear (starting in the north-ern hemisphere) in February 2011 and they became less frequent beginning in December 2016, reaching a very low number from September 2017 onward, indicating the passage from solar minimum to maxi-mum and back again.

The coronal holes at the north pole were present from February 2010 to October 2011, with some short intermittent periods. No CHs were observed between November 2011 and June 2015, with some short intermittent periods also. They started to develop again in July 2015 and remained visible until June 2019 (end of the dataset). At the south pole, the CHs were present from February 2010 to May 2012, with some intermittent periods. No CHs were observed between June 2012 and May 2014. They started to develop again in June 2014 and remained visible until June 2019. The start of the development of the (polar) coronal holes were associated with peaks that were observed at both poles in SWAP intensity data.

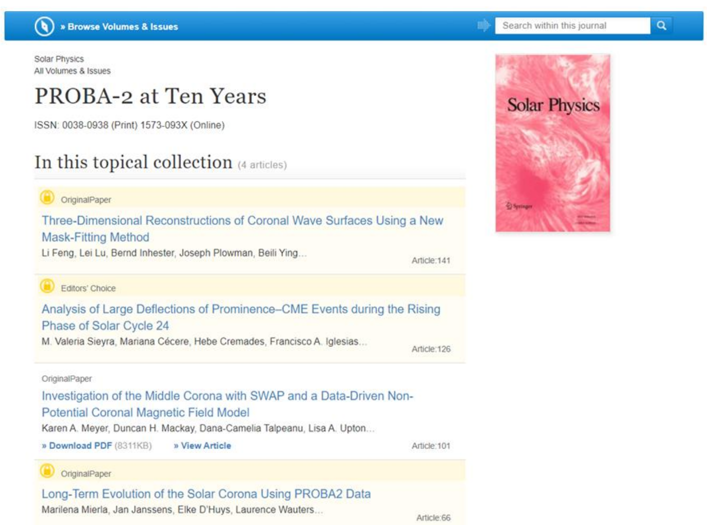

Figure 15: A screenshot from the Topical Collection in the journal "Solar Physics" on 10 years of PROBA2 observations. The paper of which the results are discussed here is number 4 on the list.

When observing the Sun for a long period of time, one can see that features on its surface and in its outer atmosphere do not rotate at the same rate. This is because the Sun is not a solid body, but a big ball of magnetized plasma, whose rotation is variable with position and height in the solar atmosphere. We found that the average rotation speed, for bright regions between latitudes of -40 and +40 degrees was approximately 14 degrees/day. The average rotation rate of bright features at latitudes of +15 , 0 , and −15 degrees was around 15 degrees/day throughout the period studied. We also observed that the three data sets used in this study (SWAP on-disk average brightness; LYRA signal and ISN) had a high degree of correlation (around 0.9), all following the SC evolution.

The present work was published in the journal "Solar Physics" in the frame of the special issue "PROBA2: 10 Years of solar Observations".

Probing coronal waves by radio observations

We continued our investigations of solar radio wave bursts related to some of the most energetic events in the solar atmosphere - solar flares and coronal mass ejections. Using data obtained by the large Ukrainian radio telescope URAN-2 (see Figure 16), some new properties of these radio bursts have been identified.

Figure 16: URAN-2 radio telescope of NASU, Ukraine, observes radio emission generated in the solar corona at heliocentric distances 2-3 solar radii.

The so-called "ALF radio wave bursts" are associated with solar flares and magnetic reconnection events at the coronal base; these are processes that are closely linked to solar activity. The sources of ALF radio waves propagate with Alfvénic velocities rather than with electron beam velocities (as other types of radio waves, such as the "type III bursts" do). This is a remarkable property that indicates that these radio waves have something to do with the overall reconfiguration of the plasma and the magnetic field in the solar corona. We distinguished two types of ALF bursts, (i) sporadic isolated ALF bursts (ALF-I bursts), and (ii) groups of ALF bursts partially overlapping with type III bursts (ALF-II bursts).

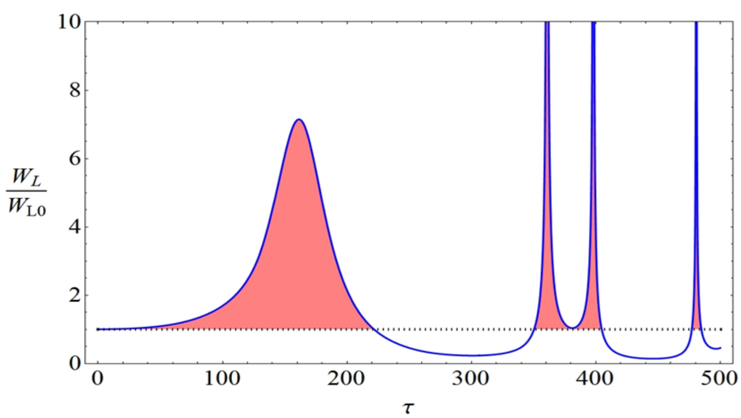

Figure 17: Time evolution of the energy W_L of Langmuir wave propagating through a KAW. In the pink areas the energy of Langmuir waves rises well above its initial background level W_{L0}.

A theoretical framework has been developed to explain the origin of these emissions and their differences. This framework considers two kinds of waves in the solar atmosphere: "Langmuir waves" (LWs) and "kinetic Alfvén waves" (KAWs). First, we demonstrated that LWs and KAWs interact. The energy contained in a LW is not conserved during such interactions and periodically rises well above the background level (see Figure 17 for the case of a pre-existing LW entering the KAW density profile at time τ=0). Then we showed that the ALF-I bursts can be formed by pre-existing LWs that are modified by KAWs, while the ALF-II bursts are formed by LWs generated within KAW density cavities and trapped there. These are situations that one can realistically expect to occur in the corona. In both cases, the high-amplitude LWs (highlighted by the pink shading in Figure 17) undergo a nonlinear conversion into radio waves, thus turning these phenomena into bright radio sources. It is highly probable that this kind of phenomena can be observed by the Parker Solar Probe and Solar Orbiter missions.

SOLARNET-SPRING: homogenization of images from ground-based stations

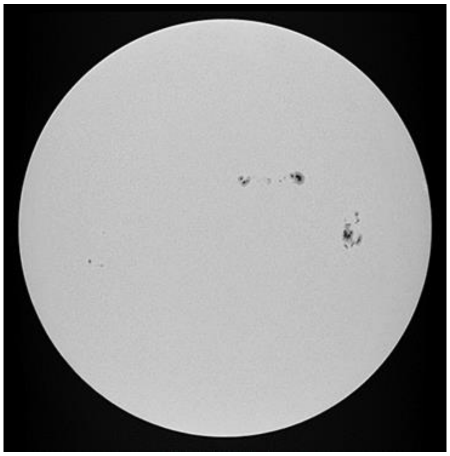

Figure 18: USET White-light image, with many sunspot groups (6 September 2017).

The Uccle Solar Equatorial Table (USET) located on the Space Pole records whole disk images of the Sun since more than a solar cycle. This continuous monitoring is essential for long-term solar activity study and space weather forecast. The possibility to record images in three different wavelengths (broad-band "White-light", Calcium-II K and H-alpha) allows to visualize simultaneously different height of the solar atmosphere (the photosphere and the chromosphere). Hence it covers a broad range of solar activity manifestations such as sunspot groups, plages, solar flares and filaments as illustrated by Figures 18 and 19 showing one of the last periods with strong solar activity from solar cycle 24. These images have been processed with a new home-made image processing pipeline written in Python3 developed in 2018 and 2019. It contains original methods to automatically recenter the disk in the image and correct the limb darkening. This is the required base before the development of more advanced image processing methods.

One limitation of monitoring the Sun with a ground-based instrument is its limited time coverage due to the night-day cycle and the variable observing conditions. In order to mitigate this, a solution is to consider a network of lightweight patrols, such as USET, at different geographical locations. Then, in order to merge the data from different stations and to consider it as a unique, continuous and high-quality image sequence, we need to develop a layer of software to homogenize the images. Indeed, inhomogeneity between images can arise due to a different set-up (optical set-up, filter band-pass,...) or from different observing conditions (clouds, atmospheric turbulence,…). Correcting for these inhomogeneities is important for the scientific exploitation of the images such as the automatic detection of solar flares. This work is foreseen in the context of an EU project in which the ROB is involved, SOLARNET-SPRING, that has started in 2019. The main goals of this project are on the one hand the correction of the atmospheric turbulence with dedicated methods such as lucky imaging, and on the other hand the correction of inhomogeneities arising from different instrumental set-up and weather conditions.

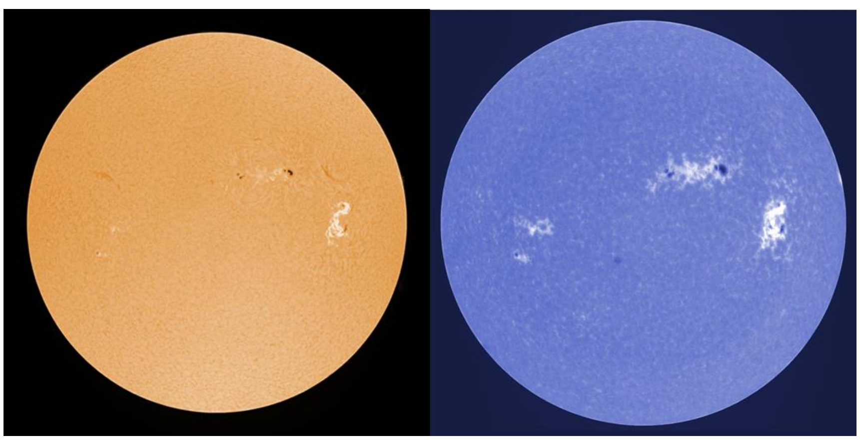

Figure 19: (left) USET H-alpha image with the two bright ribbons of a solar flare. (right) USET CaII-K image with sunspot groups and plages. Both images were taken on 6 September 2017.

In order to develop and test dedicated methods for the image homogenization, there is a need for a good dataset in which the only differences are due to the acquisition method and not to the solar activity. To create this dataset, a multi-stations joint campaign has been organized in July and August 2019 with observatories located in Austria (Kanzelhöhe), and Italy (Rome and Catania) in order to take simultaneous images. Due to the variable weather conditions between the different stations involved, it was difficult to find periods with overlapping data as illustrated on the Figure 20, and the joint campaign needed to be extended on a longer period than expected. This confirmed the need for a network of ground-based stations to have a good temporal coverage.

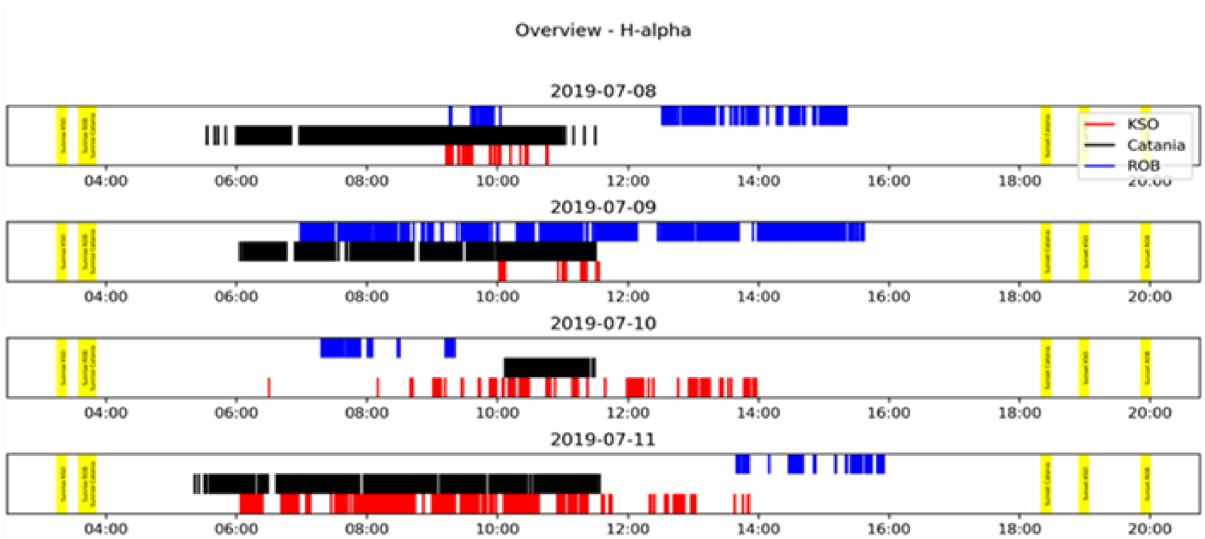

Figure 20: Overlapping period of observations between the different stations participating in the SOLARNET joint campaign in 2019. (Figure from Kanzelhöhe Observatory).

The methods that are currently being developed in the context of the SOLARNET-SPRING project will allow to merge images from different stations, paving the way to the creation of lightweight patrols networks monitoring the Sun. This will provide homogeneous and good temporal coverage data as if it was coming from a single instrument. These high-quality data will be useful for the study of long-term solar activity and for space weather forecasting.

Hazards of space weather to ground based electronic devices

Cosmic rays have been known and researched extensively for more than a century already. However, with the recent technological advancements towards higher automation and device complexity, understanding and monitoring the activity of cosmic rays became of crucial importance because of their potential hazardous effects on instruments as well as on public health.

Imagine that cosmic rays are like tennis balls randomly shot towards the light switch on the wall. The chance of flipping a switch depends on the number of balls (flux intensity) and number of switches (per unit area) representing in our case the number of electronic components of a device. The flux intensity in the case of cosmic ray balls (particles) will depend on the solar activity, and especially on the number of high-energetic solar particles propagating towards the Earth during major solar events. While some of the effects were studied on spaceborne electronic devices, the effects on ground level infrastructure are less known. A sharp increase in the intensity of the solar energetic particles will result in elevated atmospheric radiation levels and a higher intensity of neutrons at ground level (known as Ground Level Enhancement, GLE). This increases the probability of upsetting the operation of an electronic device or even to physically (permanently) damage it.

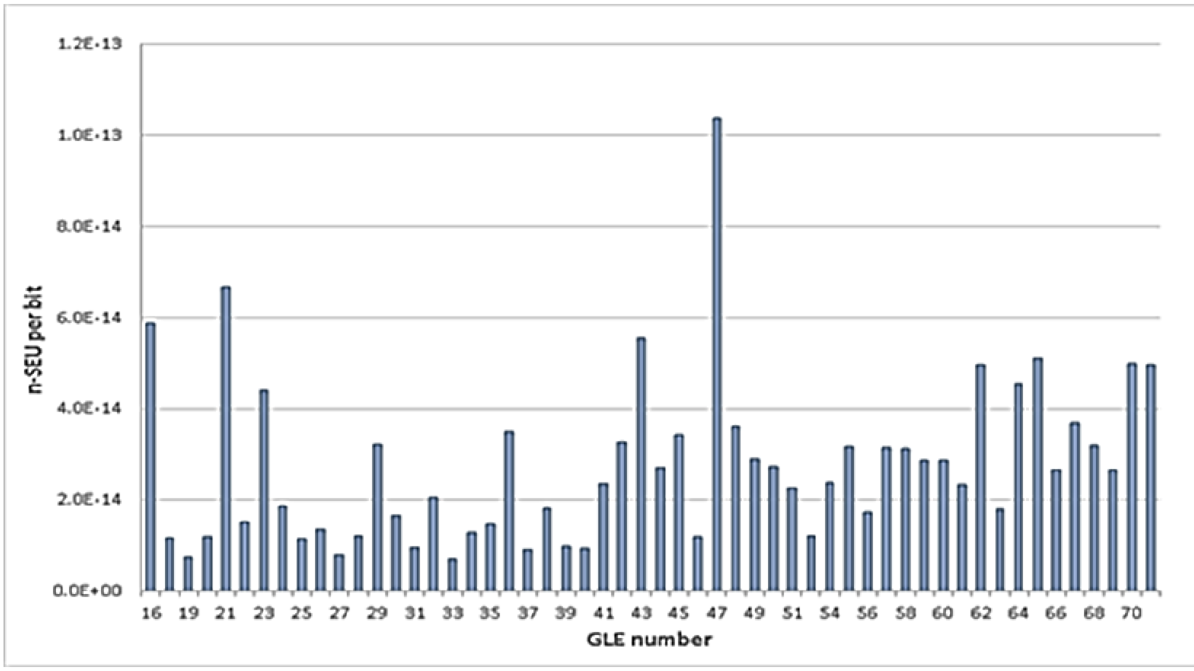

Figure 21: Neutron induced single event upsets (n-SEU) per bit from the calculated peak neutron flux (with energies > 14 MeV) during a GLE. Data from the RMI Neutron Monitor in Dourbes. GLE events detected by the instrument. The n-SEUs per bit are calculated using cross sections data from a commercial 4-megabit SRAM devices with a technology minimum feature size of 400 nm.

With the continuous miniaturization of electronic devices, the probability of upsets and hardware failures increases. Such failures are referred to as Single Event Upsets (SEU) or, when they are caused by neutrons, n-SEU. They are important both at ground level and at low altitudes within the atmosphere. To obtain the frequency or the total n-SEUs under given space weather conditions, we need the neutron flux at the location of interest and the cross section of the processes.

This cross section depends on a large number of parameters and is usually determined experimentally and complemented by computer modelling and simulations. The neutron flux at ground level in quiet and storm conditions is calculated from neutron monitor measurements. Neutron monitors are dedicated instruments to study and predict the probability for severe events, like the one in Dourbes. These instruments continuously measure the intensity of neutrons at ground levels. Due to the complexity of the interactions in the magnetosphere and the atmosphere, it is challenging to calculate the neutron fields at ground level from the measurements of the neutron monitor.

The fluence (the total number of neutrons during the event) and the peak neutron flux (at energies above 14 MeV) are calculated from the count rate using the neutron monitor response function. Finding the latter is a non-trivial problem solved by using Monte Carlo techniques. Other quantities necessary to evaluate the effects of space weather on ground-based electronics are the cross sections for the particular events. These cross sections depend in general on the device construction: scaling (minimum feature size), the fabrication materials, and the typical charge levels associated with a logical state.

Figure 21 shows the calculated frequencies of neutron induced upset events for a commercial off-the-shelf (COTS) device, a 4-megabit SRAM with a minimum feature size of 400 nm. The calculations are performed for the GLEs observed by the Dourbes neutron monitor. The total faults frequency depends on the number of bits within the device. Clearly, the n-SEUs per bit vary significantly from one GLE to another, with a maximum value during the extreme GLE47 on 21 May 1990 that has also the highest recorded Neutron Monitor count rate increase.

To obtain the total number of fails within a device during an entire GLE event, the total number of neutrons (or the neutron fluence) was calculated. The results for the same 4-megabit SRAM device are presented in Figure 22. It is remarkable that total number of n-SEUs fall within a narrower band, that is, the values fluctuate less than the n-SEU per bit, an exception being again the intensive GLE47. Further research is underway to determine what the reasons are for this observation (saturation effects, or another reason related to the interactions between the solar particles and the atmospheric diffusion and sources of secondary neutrons).

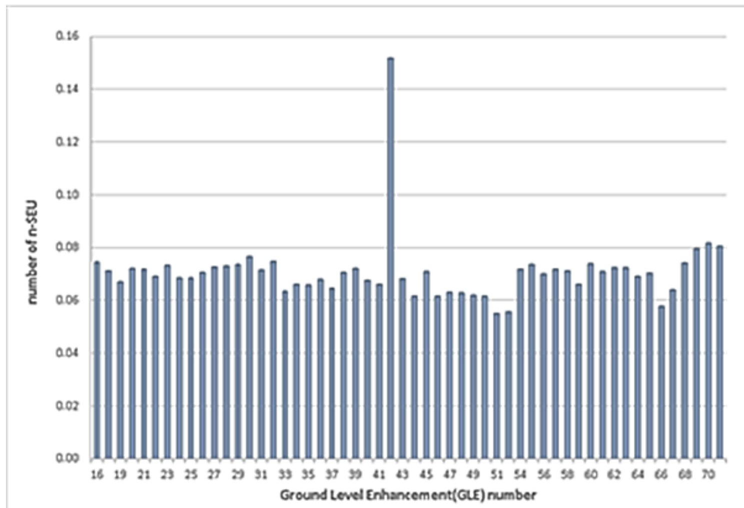

Figure 22: Total number of neutron induced single event upsets in a commercial 4-megabit SRAM during the GLE event observed by the neutron monitor in Dourbes. Besides the peak during GLE47 (21 May 1990) the total number of n-SEUs follows a rather constant value. The explanation of these results is a subject of ongoing research. Probably due to the complex structure of the electronics device, the cross sections for an event may depend on more detailed properties of the neutrons like the angular neutrons distribution etc.

The results presented in Figure 21 and Figure 22 will depend on the device type and the energy dependent cross sections for n-SEU for this device. The latter must be included in the device documentation, especially for devices intended to operate in critical systems at ground levels or at aviation altitudes within the atmosphere. The n-SEUs may cause insignificant error or, in an unlucky event, lead to catastrophic accident. Their occurrence is random. Therefore, the evaluation of their probability, the prediction of space weather conditions that may increase their frequency, and the development of mitigation techniques to compensate for or reduce the consequences of n-SEU and other atmospheric radiation induced device damage has to be continuously improved.

Life at the STCE - On Saturday, 21 September, an "Astronomy Day" was organized at the Space Pole. It was an event where the public could come and discover various aspects of astronomy. During the day, they could visit the various telescopes and experiment stands, attend lectures or do solar observations, whereas the night program had stargazing sessions, BRAMS radio meteor observations, and more. The organization was done in collaboration with associations of amateur astronomers from Brussels, Flanders and Wallonia, and with the support from RMI, BISA and the Planetarium. The occasion was the celebration of the 100th anniversary of the International Astronomical Union. The event was picked up by the media, and a movie featuring some of the activities as well as interviews with some of the researchers can be found at BX1.

Instrumentation and experiments

PROBA2 - 10 years of observations

On 2 November 2019 the PROBA2 ESA micro-satellite celebrated 10-years of operations. PROBA2 is the second of the European Space Agency's (ESA) fleet of PROBA satellites. It hosts 17 new technological developments including two main solar instruments (SWAP and LYRA) designed for studying all events on the Sun that might have implications on the solar-terrestrial connection.

SWAP (**S**un **W**atcher using **A**ctive Pixel System detector and Image **P**rocessing) provides images of the solar corona filtered at a wavelength around 17.4 nm, a bandpass that corresponds to a temperature of roughly 1 million degrees, allowing us to see the hot solar atmosphere while filtering out the relatively cooler solar surface. SWAP observes an exceptionally wide field-of-view (FOV), allowing it to see more structures around the edge of the Sun. A good example is reported in a paper published last year by O'Hara et al. "Exceptional Extended Field-of-view Observations by PROBA2/SWAP on 2017 April 1 and 3". Observing the structured nature of the extended solar atmosphere is one of SWAP's most important tasks.

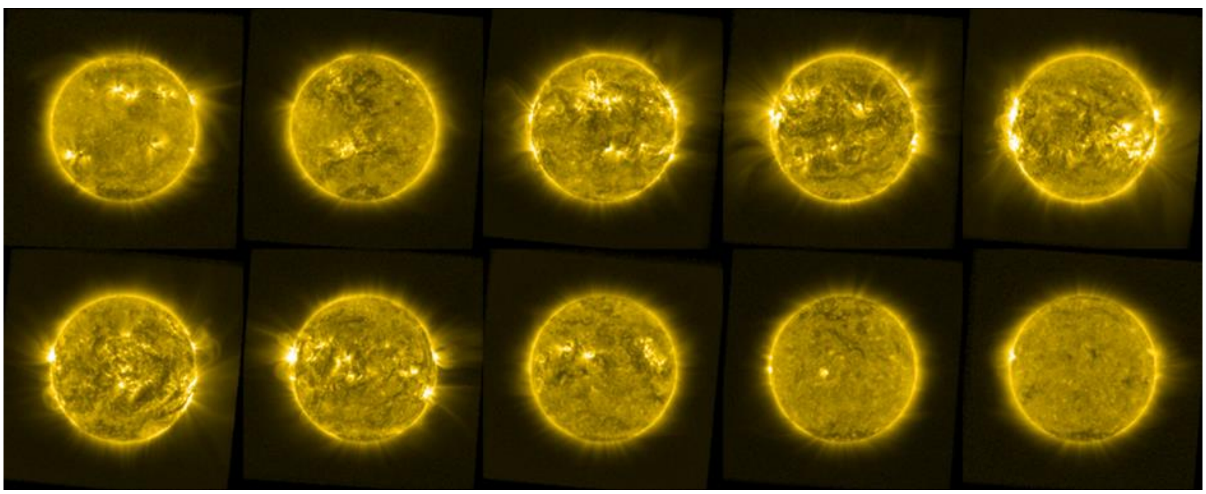

Figure 23: Ten years of SWAP observations, from 2010 to 2014 on the top row and from 2015 to 2019 on the bottom row, showing the changing face of the solar atmosphere.

Figure 23 shows SWAP images from each year of the mission. It has long been known that the Sun undergoes an 11-year activity cycle, where solar activity, such as the magnitude and number of flares and coronal mass ejections, fluctuates. The images in Figure 23 reflect this variability through the changing number of coronal holes (the dark regions) and of active regions (the bright structures), which are often the source of the more dramatic solar activity.

LYRA (**L**arge **Y**ield **RA**diometer) is a solar UV-EUV radiometer, monitoring the Sun through 4 channels relevant to Solar Physics, Space Weather and Aeronomy, and hosts one of the first Lyman-Alpha irradiance monitors. Unlike the SWAP imager, LYRA observes the Sun as a star, that is, as a single data point. The extremely high-cadence (up to 100 measurements per second) of LYRA is required for the detailed study of transient solar events such as solar flares. In particular, LYRA was able to characterize the strongest flare of the current solar cycle, on 6 September 2017, and make rare observations in its Lyman-Alpha and

Herzberg channels (Figure 24). LYRA detected small-amplitude oscillations called quasi-periodic pulsations in its rising phase. Such oscillations can only be made with high cadence observations, like those of LYRA. These observations are shedding new light on the flaring mechanism itself.

Space Weather - SWAP and LYRA were originally designed for studying the Sun and energetic events, such

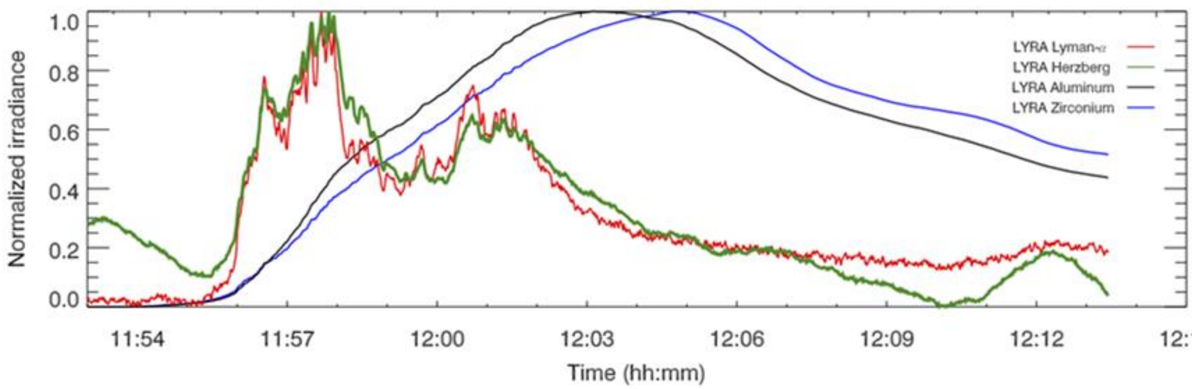

Figure 24: LYRA light curves of the 6 September 2017 X9.3 flare.

as solar flares, coronal holes and CMEs, that might have implications on the solar-terrestrial connection. Naturally, the observations have become an integral part of several solar-monitoring space weather forecasting centres, including the Regional Warning Center at the Royal Observatory of Belgium.

Figure 23 highlighted long-term changes in the Sun. Active regions (the bright structures) and coronal holes (the dark regions) can clearly be seen varying over time, both of which can have implications for space weather on Earth. SWAP and LYRA are also monitoring more transient, energetic and eruptive phenomena such as flares and CMEs, Figure 25 below shows SWAP's ability to track eruptions into the extended solar atmosphere. Two papers, published last year, highlight PROBA2's ability to track space weather events: "Multipoint Study of Successive Coronal Mass Ejections Driving Moderate Disturbances at 1 au" by Palmerio et al. , and "Large non-radial propagation of a coronal mass ejection on 2011 January 24" by Cécere et al.

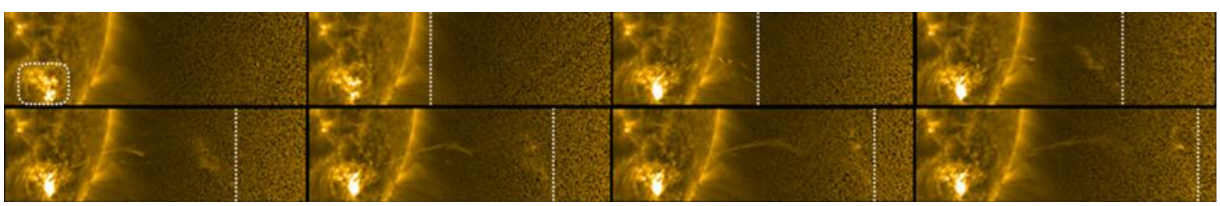

Figure 25: A flare (top left panel) and eruption observed by SWAP on 1 April 2017. The eruption was traced to over 1 solar radius, as highlighted by the dashed line.

Vital Statistics from launch to the 10-year anniversary - PROBA2 was launched under the ESA Technology, Engineering and Quality Directorate (D/TEC). After launch, the ESA Science Directorate (D/SCI) supported the scientific exploitation of the PROBA2 science instruments and the Belgian PI-teams were supported by PRODEX.

By the time of the 10-year anniversary, PROBA2 had:

- been in orbit for 3653 days.
- Orbited the Earth ~53,000 times.
- Produced ~30,000 LYRA data files.
- Produced ~2,090,000 SWAP images.
- Passed our ground stations in Redu, Belgium and Svalbard, Norway (Arctic) 32,453 times.
- Helped produce over 100 peer-reviewed papers (link).
- Run 8 guest investigator programs from 2010 to 2018, and welcomed 64 teams, 81 team members from 16 countries.

What next for the PROBA2 mission? - As discussed above, the Sun undergoes an 11-year activity cycle, and next year will mark the 11^{th} anniversary of the PROBA2 mission and therefore the monitoring of the Sun for a full solar cycle. This landmark period will allow PROBA2 to probe the Sun's evolution over the long term, comparing two solar minimum periods. The instruments themselves are proving robust in the harsh radiation environment. The detectors, which had never been used in space before, still produce a clean signal, with very low levels of noise. SWAP has seen less than 10% degradation in the number of active pixels, a remarkable number after 10 years of operations.

To celebrate 10 years of observations, the PROBA2 team are putting together a 10-year anniversary topical collection of articles (see Figure 15), a follow-up of the successful 2013 Topical Issue that highlighted the scientific and operational achievements after the first two years of the mission. The 10-year PROBA2 anniversary edition reports on the health and status of the mission as well as various studies ranging from the middle corona to solar flares.

Figure 26: Participants at the 7-8 February 2019 symposium in Redu celebrating nearly 10 years of PROBA2 operations and achievements.

With a 2-day PROBA2 Symposium, organized at the ground station in Redu, we celebrated the achievements after nine years of smooth operations by summarizing the findings, reflecting on the experiences, brainstorming on the lessons-learned, and looking into the challenges for the future. PROBA2 is ready for the next 10 years!

A new neutron monitor at Dourbes for SWx research and forecasting

In the beginning of this year, a new instrument designed to monitor the intensity of the cosmic ray particles commenced its full operation at the RMI Geophysical Center in Dourbes. The purpose of this instrument is to monitor continuously the intensity of the cosmic rays striking the Earth's atmosphere. This new instrument is complementary to the already existing neutron monitor that has been measuring the cosmic rays since the early 1960's. Together with the ionosonde and the GNSS receivers, the neutron monitor forms the core of the research equipment for now- and forecasting of the climate in the interplanetary space between the Sun and the Earth known as space weather (SWx). While the intensity of the cosmic rays arriving from the distant parts of the universe is constant, the cosmic rays originating from the Sun are not. The Sun and its activity are the principal driving force of the atmospheric climate as well as the space weather conditions. While our sensations have evolved to sense and feel the changes in the atmospheric weather (the cold, the heat, the humidity, etc.), we are unable to feel anything related to space weather (with the few exceptions of observing the Northern and Southern Lights). One may ask then - why are we interested in it? We live safely on the surface of the planet protected by its atmosphere and geomagnetic field against the violet radiation fields and streams of high energetic particles in the outer space.

Figure 27: Construction of the new neutron monitor at Dourbes - from design to assembly, testing and start of the continuous monitoring of cosmic rays intensities.

The answer can be found if we look around us: our everyday life is now unimaginable without devices like smart phones, the navigation services, car and office computers, telecommunications and network. Even more - computers are in charge of the control and security of the train transport, airplanes, traffic lights, factory automation, power plants, and just about everything else. The computers and other electronic devices play an important role in our everyday life not only as an entertainment, but also as a means to improve the quality and security of our life. However, they all contain microchips and electronic circuits that are susceptible to the cosmic ray particles, which may introduce faults and changes during normal operation, which in turn can result in important failures in - among others- power grid failures, airplane safety operation, and endanger our life by excess radiation exposure during long-haul flights, particularly on polar routes.

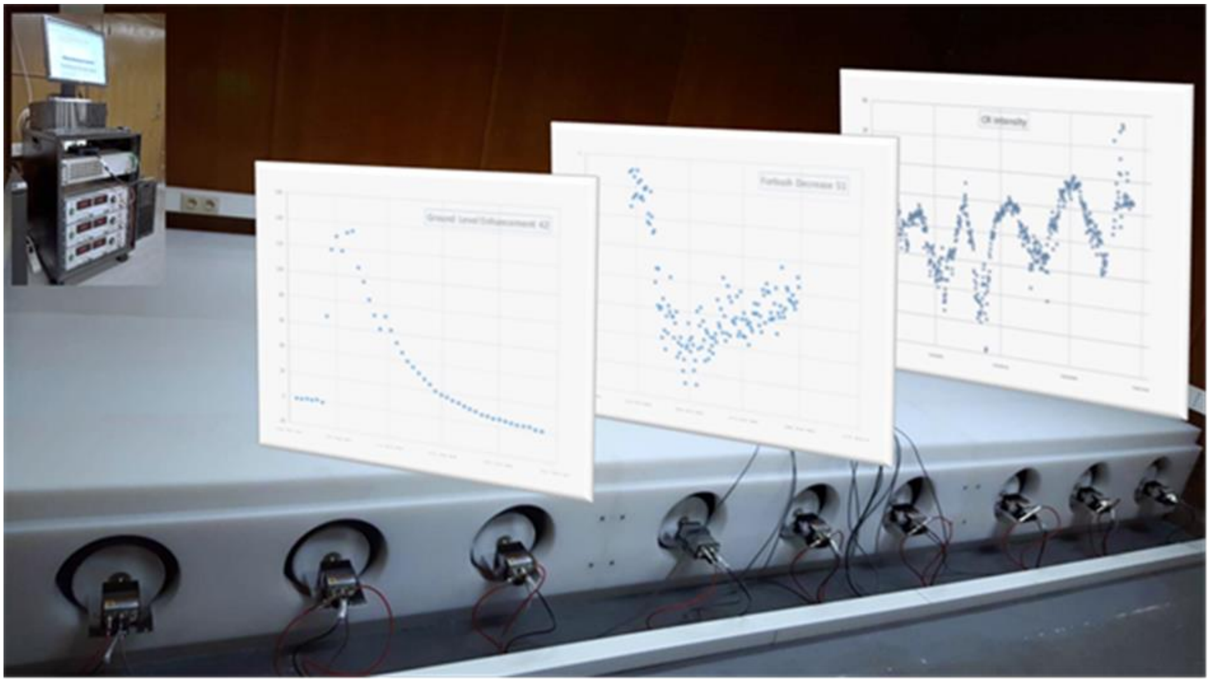

Figure 28: The new neutron monitor at Dourbes for SWx research and forecasting. The neutron monitor allows surface observations of Solar Energetic Particles (SEP) like ground level enhancement (GLE) and Forbush decrease. They provide an indirect means for monitoring the solar activity and the space radiation conditions. It provides real-time information about the atmospheric radiation levels and the neutron fields at the location of the instrument. The neutron monitor is a part of the international network of neutron monitors (NMDB) indispensable for SWx alerts and forecasting services.

How does the neutron monitor works? The cosmic rays from outer space (the primary component) and the Sun produce a large number of secondary particles on entering the atmosphere. Great fractions of these particles are neutrons. While neutrons are omnipresent due to the natural radioactivity, the neutron monitor is designed to detect the neutrons produced by the cosmic rays. A standard neutron monitor consists of 18 neutron detectors. In order to amplify the incident radiation, the detectors are surrounded by lead material which produces on average 9-10 more neutrons within the instrument. These neutrons are too fast to be "captured" by the detector and need to be slowed down in a similar way that neutrons are moderated and conditioned in a nuclear reactor.

Observing the intensity of the neutrons at ground level reveals, both directly and indirectly, the state of our Sun - the periodicity of the solar activity is readily visible in the cosmic ray intensity measurements. Besides these periodic observations - the neutron monitor also detects the random swings in the mood of the Sun - the solar storms. This however is of little use when trying to protect ourselves from the dangers that the space weather poses to our technological society. Because of the very high energies (and velocities) of the cosmic ray particles and the complex interactions in the space surrounding the Earth, a network of neutron monitors has the potency of forecasting in advance the arrival of the solar storms with sufficient lead time. This will allow us taking the necessary measures and preventing expensive damages and accidents. Forecasting of dangerous solar storms is the main objective of the space weather research efforts.

RMI has many decades of experience in monitoring the intensity of the cosmic rays. It is one of the few institutes with access to a modern neutron monitor and as such will be able to continue the 55 years of constant measurements of the cosmic ray intensity at mid-latitudes in the following decades.

Moreover, neutron monitors are built to be "eternal" in the sense that they have to provide continuous series of measurements for decades. They are very robust and simple instruments based on significant theoretical and research efforts and remain the state-of-the-art instrument for the monitoring of the complex phenomena responsible for the space weather climate.

Analysis of the performance of the SLP Instrument in a plasma chamber

The Sweeping Langmuir Probe instrument SLP will fly on board the triple unit CubeSat PICASSO, an ESA in-orbit demonstrator. This instrument, fully developed at BIRA-IASB with substantial STCE support, comprises four small cylindrical probes mounted at the tip of the solar panels. The measurement principle is based on the conventional Langmuir probe theory: by sweeping the potential of one probe with respect to the plasma potential and measuring the current collected, the instrument will acquire a current-voltage (I-V) characteristic from which several plasma parameters are retrieved: the electron density and temperature, ion density and S/C (spacecraft) potential. SLP will perform in-situ measurements of those plasma parameters in the ionosphere along the PICASSO orbit, at about 500 km altitude.

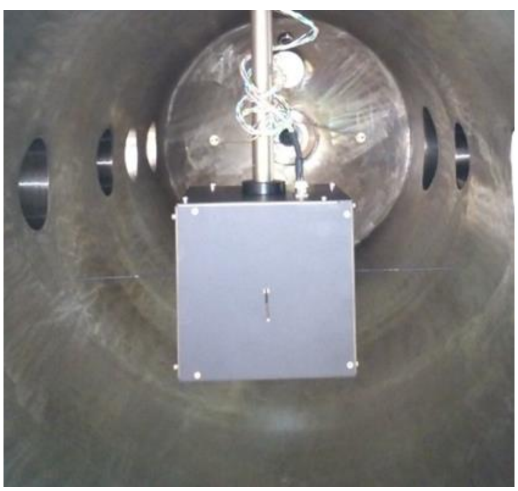

Figure 29: Picture of the electrically representative PICASSO mock-up in the plasma chamber.

The measurement principle of Langmuir probe instruments is relatively simple but the accurate computation of the plasma parameters is a much more challenging task because of many possible biases. Those biases are not only due to the imperfections of the instrument, but also arise from the complex coupling between the probes, the plasma and the S/C. For this reason, SLP, accommodated on an electrically representative PICASSO mock-up, has been tested in a plasma chamber at ESA/ESTEC, Noordwijk (The Netherlands) in February 2019, as shown in Figure 29. The aim was to validate the performance of the instrument in a relevant environment and to study, inter alia, two important elements for the proper interpretation and processing of the acquired data: the effects of a) the miniaturization of the probes and b) the contamination of the surface of the probes.

Most Langmuir probes used in space, and a fortiori on board nano-satellites, have a relatively small diameter so that the Orbital-Motion-Limited (OML) collection theory can be applied. Nevertheless, the OML theory requires that the length of the probe is infinite, making the end-effect negligible. Given the limited length of the probes of SLP and of other Langmuir probes instruments flying on CubeSats, this requirement cannot be fulfilled. Therefore, the OML theory cannot be applied directly for such

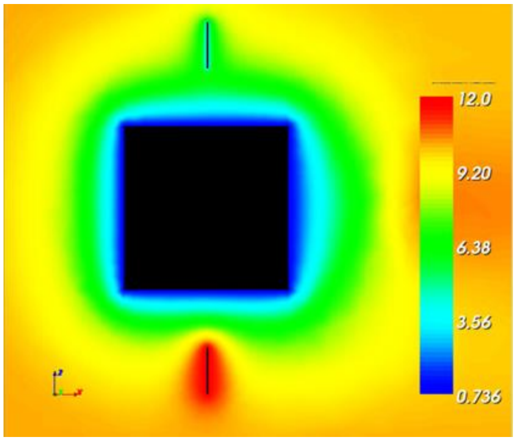

Figure 30: Electron density around the S/C mock-up when a 7.6 V is applied on the bottom probe (log scale, in part/m³).

instruments because the volume where the particles are attracted is not a true cylinder but rather an ellipsoid, as can be seen in the simulated electron density depicted in Figure 30 (top view of the PICASSO mock-up, with only two probes). As a result, the measured I-V characteristic is not as predicted by the OML theory, but tends to be like the one of a spherical probe. It should be noted that the intensity of this effect varies as a function of the plasma parameters encountered along the orbit. Due to these results, a modified computation method will be used so that for each measurement the deviation from the expected theoretical curve will be assessed and corrected for.

Surface contamination is a serious issue for Langmuir probe operation. When a probe is covered by a thin contamination layer, this layer act as a capacitor C with a resistor R in parallel that will charge and discharge with an RC time constant during or between consecutive sweeps. This will decrease or increase the actual potential in contact with the plasma. When performing a series of measurements, the charging effect will induce a drift in the I-V characteristic from one sweep to another as can be seen in Figure 31 for three consecutive two-way sweeps (from negative to positive and back to negative bias voltages). If the contamination effect is not taken into account properly, it can be misinterpreted as an increase of the electron temperature. The contamination-induced error on the temperature has been found to be of the order of 50 % for series of nine consecutive sweeps.

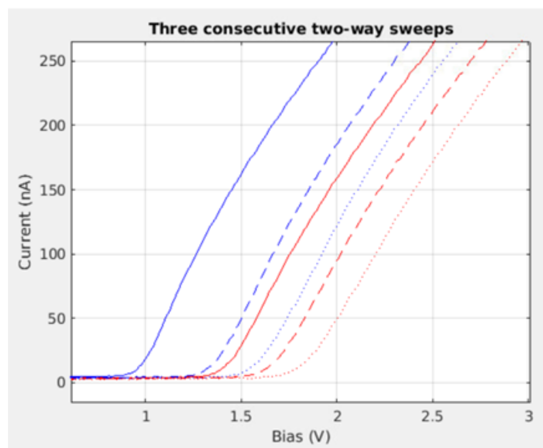

Figure 31: I-V characteristics of three consecutive two-ways sweeps. The increasing and decreasing parts of the sweeps are in blue and red, respectively. The first, second and third sweeps are in solid, dashed and dotted lines.

This test campaign allowed the assessment of the performance of SLP, including on board processing capabilities, in a relevant environment. It gave insights into fundamental aspects that are essential to correctly interpret the measurement data not only for SLP but also for any Langmuir probe instrument on board satellites, especially those on board nanosatellites, which are more and more considered for scientific missions.

Status report from the VLF receiver for plasmaspheric radio waves

Thanks to a strong interaction with BELSPO and the International Polar Foundation (IPF), the VLF radio receiver instrument at the Princess Elisabeth station in Antarctica is now working well. A scientist of IPF successfully fixed the problems with strong electromagnetic noise in the VLF antenna data. As a result of this detective work, the source of the noise has been localized and it has been removed. Data collection will resume by the end of 2020.

The collaboration regarding the data analysis of the VLF antenna in Humain, consisting of two rhombus-shaped loops in perpendicular planes held up by the central mast and 4 tension wires, continues. The study involves the source location of whistlers, very low frequency (VLF) electromagnetic (radio) waves generated by lightning. A new method for identifying the source regions of these whistlers detected at Humain has been developed, by calculating the ratio of lightning discharges (from the World Wide Lightning Location Network data) transmitted into ground detectable whistlers as a function of location. The results show that the source region of whistlers corresponding to each station is around the magnetic conjugate point (two points on the Earth's surface connected by a geomagnetic field line) of the respective station. The size of the source region is typically less than 2000 km in radius with a small fraction of sources extending to up to 3500 km. A paper on this topic has been published.

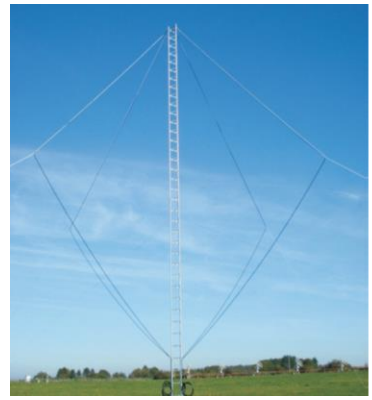

Figure 32: VLF antenna in Humain. The antenna consists of two rhombus-shaped loops in perpendicular planes, held up by the central mast and 4 tension wires.

The Belgian ALC network

In 2019, RMI continued to maintain and to expand its network of ALC (automatic lidars and ceilometers) that now consists of 4 fully operational ALC and a new one of which the installation in the south of Belgium is still pending. This ALC network with its high sensitivity offers the opportunity to monitor the vertical profile of aerosols on a continuous temporal scale. It benefits for the aviation and also for the air pollution monitoring.

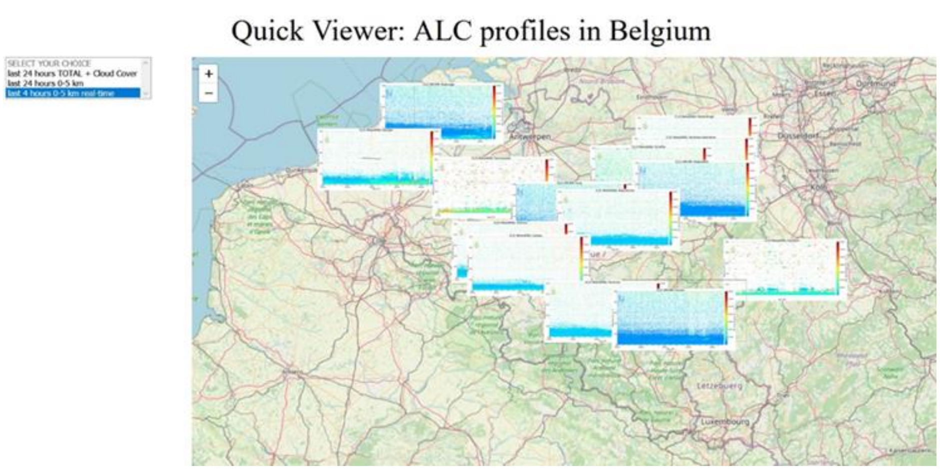

Figure 33: The dynamic graphical user interface with the 14 operational ALC sending data in near-real time.

RMI has expanded this ALC network, after at least 6 years of discussions with the Belgian Defense and its weather services (Meteo Wing). The RMI now receives the ALC data from the 10 ALC of Belgian Defense in near-real time (10 minutes). The data profiles of these ALC will permit to monitor the aerosol clouds over Belgium with a better spatial distribution. In order to use these new data series in a homogeneous way with the already existing ALC data, a dynamic graphical user interface (Figure 33) was created allowing quick access to the forecasters. This interface will be completed in the future with other parameters (boundary layer height, fog prediction…) needed for weather forecasts.

RMI has settled all administrative steps in order to be able to exchange these new ALC data with the data-hub operated by E-PROFILE. E-PROFILE is part of the EUMETNET managing in near real-time the European network of ALC for the monitoring of vertical profiles of aerosols including volcanic ash. In addition to the aerosol cloud monitoring, the boundary layer height can be retrieved from vertical profiles of aerosols measured by ALC. It is a key parameter that an ALC network can provide to improve weather forecasts, air quality prediction, and climate model parameterization. In this framework, RMI participates in the PROBE project (COST-Action: CA18235 - PROfiling the atmospheric Boundary layer at European scale) that started at the end of 2019.

JUICE mission: development and validation of the laboratory facility for MAJIS

MAJIS (Moons And Jupiter Imaging Spectrometer) is part of the science payload of the ESA L-Class mission JUICE (Jupiter ICy Moons Explorer) to be launched in 2022 with an arrival at Jupiter in 2030. JUICE is planned to perform detailed observations of the giant gaseous planet Jupiter and three of its largest moons Ganymede, Callisto and Europa for at least three years. The MAJIS instrument is composed of two imaging array spectrometers combining two spectral channels: the visible and near infrared (VIS-NIR: 0.50 µm - 2.35 µm), and the infrared (IR: 2.25 µm - 5.54 µm). The objectives of its mission are mainly to characterize the Jovian atmosphere and magnetosphere, and to collect information about the surface composition of the icy moons.

Figure 34: The targets of the JUICE/MAJIS mission: Jupiter and its icy moons.

The subsystems of all space instrumentation, and particularly detectors, need to be characterized in a laboratory before their integration at instrument level, launch and operations in space. In this context, the Space Pole in Uccle was a key contributor for the characterization of the MAJIS VIS-NIR channel. Figure 35 summarizes the full electro-optical characterization that will be executed on both the Spare (SM) and the Flight (FM) models of the VIS-NIR detectors.

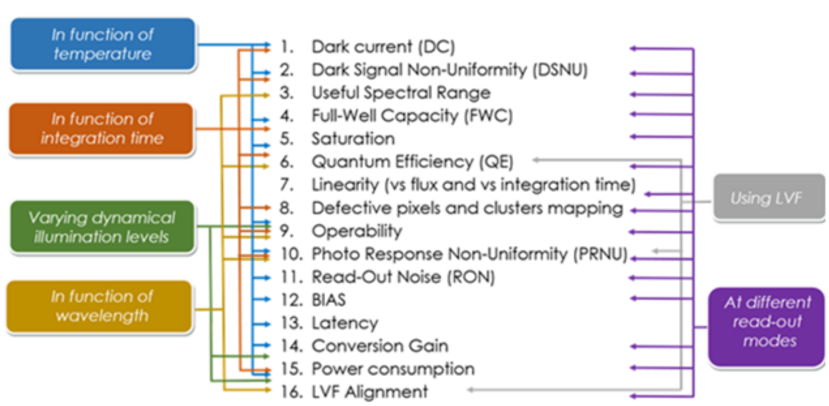

Figure 35: MAJIS VIS-NIR detectors characterization measurements.

This work will be performed in 2020 in one laboratory of the Space optoelectronic and optical Technology and Calibration Laboratories (STCL). It is a joint structure between BIRA-IASB, KSB-ORB and KMI-IRM whose purpose is to provide facilities and expertise, namely to support the characterization of sub-systems for space instrumentation. This part of the project is funded and supported by BELSPO and ESA (PRODEX Office), and supervised by CNES (Centre National d'Etudes Spatiales, France). The characterization must be carried out in accordance with the requirements of the MAJIS prime team from IAS (Institut d'Astrophysique Spatiale, France).

During the year 2019, scientists and engineers from BIRA-IASB developed and validated the MAJIS facility in their laboratory to prepare and ensure the characterization of the VIS-NIR detectors. For invaluable equipment such as flight model detectors dived in a simulated space environment (high vacuum and cold temperatures between -157°C to -120°C), the facility must guarantee a high level of cleanliness and safety conditions. For that reason, the facility was optimized in terms of security system, thermal-vacuum equipment and optical system. This facility (Figure 36) includes a cryo-cooling system, a customized detector mount designed to thermalize the detector inside a vacuum chamber, and well-designed optical equipment (quartz-halogen lamp, double monochromator, integrating sphere, filtering system) to illuminate the detector under specific conditions (beam uniformity, monochromatic light) for its characterization. Optics and Thermic Ground Support Equipment (OGSE, TGSE) manage the equipment for automatic and remote-control operations of the bench.

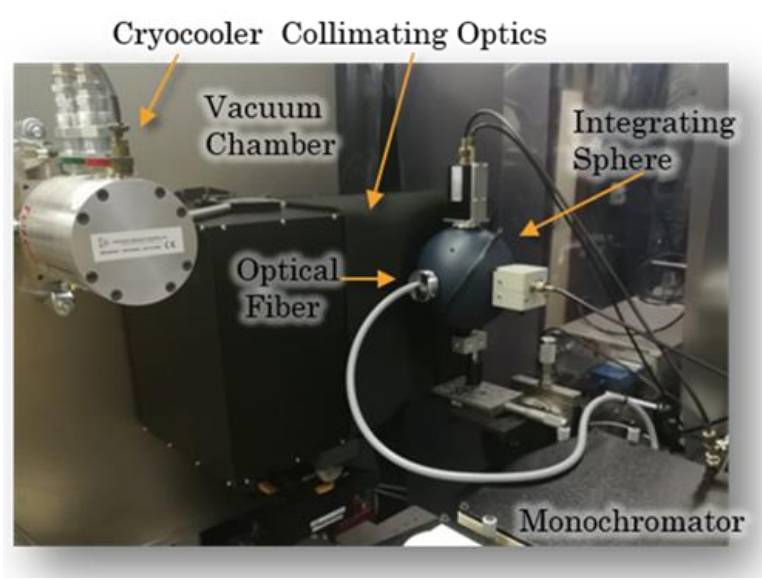

Figure 36: VIS-NIR facility external equipment (left) and cryogenic detector mount (right) inside the vacuum chamber.

The thermal vacuum validation of the facility was successfully done in the autumn of 2019 using Structural Model (STM) and Engineering Model (EM) of the detectors. During these campaigns, the Quality Assurance was provided by the B.USOC. The next steps for 2020 are additional validations of the facility, and particularly the characterization campaigns of both the MAJIS flight and spare models.

Life at the STCE - Many colleagues from the space pole took part in one or more of the numerous climate demonstrations that took place in 2019. These climate marches regularly mobilized several tens of thousands of teenagers and other sympathizers. At the Space Pole, it became a more regular practice to think about the consumption of energy (light, heating, laptop screens,…), of water (restrooms,…), of the necessity to travel abroad when a meeting could be held online as well, about recycling material,…

Applications, modeling and services

PECASUS - The European answer to ICAO's SWx call

Figure 37: The civil aviation is particularly interested in all SWx conditions affecting high frequency (HF) radio communications, GNSS-based navigation and surveillance, and radiation exposure at flight levels.

Sporadic and massive eruptions of highly energetic matter and radiation from the Sun can trigger space weather processes in the Earth's atmosphere and magnetosphere causing problems in radio communication and navigation systems and an increase of harmful radiation levels at flight altitude. The aviation sector has grown considerably over the last decades. The airspace has become crowded, north-polar flights were opened, flight altitudes increased for long distance flights,... As planes have become more sophisticated, they also have become more vulnerable to space weather (SWx). Also, measures to guarantee the safety of onboard personnel and passengers against these space weather conditions remain an issue. Therefore, the International Civil Aviation Organization (ICAO) wants to be informed on space weather that is expected to affect communications, navigation and surveillance systems and/or pose a radiation risk to flight crew members and passengers.

In 2017, ICAO launched a call for a space weather safety program to meet this need. In particular, they wanted -on a 24/7 base- that space weather centres or consortiums informed civil aviation whenever space weather conditions could have an impact on high frequency (HF) radio communications, GNSS-based navigation and surveillance, and radiation exposure at flight levels. For no less than 9 parameters, ranging from ionospheric scintillation to short-wave fades, moderate and severe thresholds were established for which advisories (coded messages for pilots and aviation services) were required to be sent. According to ICAO regulations, space weather advisories shall be issued only when very strong space weather events occur, but the advisories need to be sent within minutes after the threshold exceedance.

Figure 38: Another meeting to finetune the services offered by PECASUS and the two other consortiums to ICAO. Cookbook, dashboard, advisory,… all became household terms.

Already in 2001, the ROB started operating a space weather room where researchers continuously collect, analyze and interpret solar data. Indeed, the Solar Influences Data analysis Center (SIDC) issues every day a space weather bulletin that gives an update on how the Sun behaves, what the impact of a possible solar storm is and what can be expected for the coming days. For sudden changes in space weather conditions, PRESTO alerts are issued as soon as possible. So, in response to the ICAO call, the STCE teamed up with scientific institutes in other European countries, jointly creating the Pan-European Consortium for Aviation Space weather User Services - PECASUS for short. Finland has the lead in this consortium, but

relies on Belgium to collect and process data from all over the world. Indeed, the STCE's expertise in solar observations and research combined with the experience of the GNSS and solar particle radiation group proved to be crucial. PECASUS was selected as one of the three ICAO global space weather centres.
This did not come without significant efforts from all involved, and required numerous onsite and online

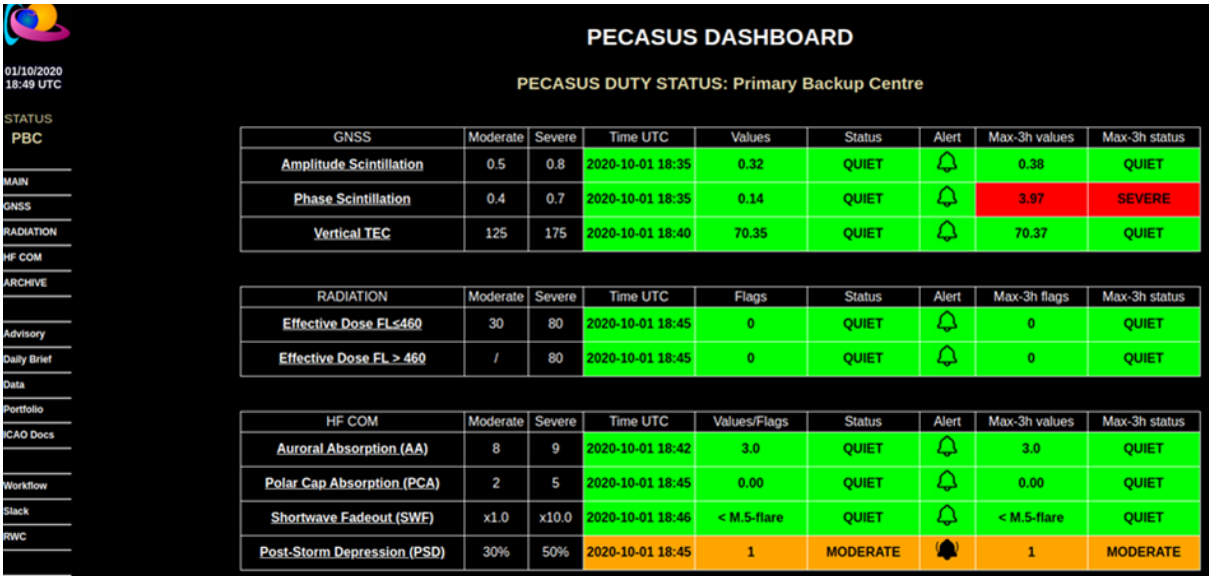

GNSS	Moderate	Severe	Time UTC	Values	Status	Alert	Max-3h values	Max-3h status
Amplitude Scintillation	0.5	0.8	2020-10-01 18:35	0.32	QUIET		0.38	QUIET
Phase Scintillation	0.4	0.7	2020-10-01 18:35	0.14	QUIET		3.97	SEVERE
Vertical TEC	125	175	2020-10-01 18:40	70.35	QUIET		70.37	QUIET

RADIATION	Moderate	Severe	Time UTC	Flags	Status	Alert	Max-3h flags	Max-3h status
Effective Dose FL≤460	30	80	2020-10-01 18:45	0	QUIET		0	QUIET
Effective Dose FL > 460	/	80	2020-10-01 18:45	0	QUIET		0	QUIET

HF COM	Moderate	Severe	Time UTC	Values/Flags	Status	Alert	Max-3h values	Max-3h status
Auroral Absorption (AA)	8	9	2020-10-01 18:42	3.0	QUIET		3.0	QUIET
Polar Cap Absorption (PCA)	2	5	2020-10-01 18:45	0.00	QUIET		0.00	QUIET
Shortwave Fadeout (SWF)	x1.0	x10.0	2020-10-01 18:46	< M.5-flare	QUIET		< M.5-flare	QUIET
Post-Storm Depression (PSD)	30%	50%	2020-10-01 18:45	1	MODERATE		1	MODERATE

Figure 39: The finetuned PECASUS dashboard to monitor the 9 different parameters. An orange colour indicates that the moderate threshold for that parameter has been exceeded (currently, or over the last 3 hours), whereas a red colour indicates the severe threshold has been exceeded. In both case, the operator needs to check the conditions and send out an advisory as required.

meetings both internally as with the international consortium members. Specific guidelines for the operators had to be written, dealing with relevant issues such as when and how to write an advisory, or what to do when the data are lacking or corrupted. To support the monitoring and interpretation of the space weather data, a dashboard for the parameters was created with colours depicting the various conditions (missing data, thresholds exceeded,...) and links to maps of the underlying data. There's even a sound alert if a threshold has been exceeded. The dashboard also allows the writing of the advisories (a performant tool on itself), and provides links to relevant documents and discussion forums. A memorandum with the Meteo Wing of the Belgian Defense was agreed to assure the 24/7 requirement, and an internal shift system was put on rails. The STCE also developed and provides tailored info and training courses to the end-users of the PECASUS services that have to interpret the Space Weather Advisories.

```
SWX ADVISORY
STATUS:              TEST
DTG:                 20170907/1437Z

SWXC:                PECASUS
ADVISORY NR:         2019/28

SWX EFFECT:          HF COM MOD
OBS SWX:             07/1434Z DAYLIGHT SIDE
FCST SWX  +6 HR:     07/2100Z DAYLIGHT SIDE
FCST SWX +12 HR:     08/0300Z NOT AVBL
FCST SWX +18 HR:     08/0900Z NOT AVBL
FCST SWX +24 HR:     08/1500Z NOT AVBL
RMK:                 SOLAR FLARE HF COM ABSORPTION EVENT IN
                     PROGRESS. FURTHER FLARING AND PERIODIC
                     LOSS OF HF COM ON THE DAYLIGHT SIDE EXP.
NXT ADVISORY:        20170907/2034Z
```

Figure 40: An example of a test advisory written in preparation of the official PECASUS start. The test campaign concerned September 2017, a period of enhanced solar activity.

The PECASUS Global Space Weather Center for aviation started its 24/7 operations on 7 November 2019. The Finnish Meteorological Institute (FMI) leads the consortium, which comprises the ICAO member states Finland, Belgium, UK, Austria, Germany, Italy, Netherlands, Poland, Cyprus, and South-Africa. Besides PECASUS, the two other services providing advisories are the Space Weather Prediction Center of NOAA (SWPC) and the ACFJ consortium formed by Australia, Canada, France and Japan.

The three centres are doing space weather monitoring in two week shifts with one of the centres serving as the On Duty Center (ODC) and the others as Primary and Secondary backup-centers (PBC, SBC). The ICAO space weather service started at the time of solar activity minimum and hence calm space weather conditions prevailed. However, intensive solar storms may still take place during the years of solar activity minimum, so the SWX centres remain vigilant all the time. During the next few years, the solar activity is expected to increase substantially with the approaching sunspot maximum of solar cycle 25.

A new empirical model of the Mars ionospheric total electron content

Radio-science experiments are used to obtain motions of spacecraft or assets (e.g. lander, rover,…) around or on planets or moons in space (Figure 41). One usually performs Doppler measurements alone on the radio signal between the Earth and the asset to reconstruct its position and velocity variations. Ranging is also used for obtaining ephemerides of planets or moons. For a spacecraft around Mars or an asset on the Martian surface, dedicated radio frequency bands for space communications are determined by the International Telecommunication Union (ITU). The frequencies used are in UHF (0.3-3.0 GHz), S-band (2.0-4.0 GHz), X-band (8.0-12.0 GHz), and in the future, Ka-band (26.5-40 GHz). At present most of the spacecraft use UHF for inter-satellite links and X-band for Earth-Mars links. Previously, landers such as Viking or Pathfinder used the S-band.

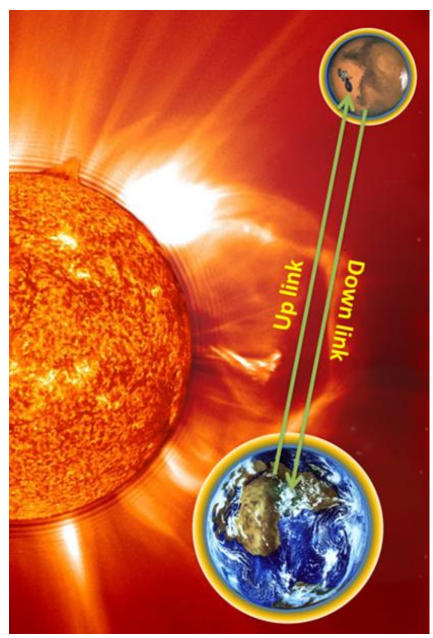

Figure 41: Schematic diagram of the radio science experiments using ground antenna at Earth and satellite or rover on Mars.

Concerning recent and future missions, the NASA lander InSight (Interior Exploration using Seismic Investigations, Geodesy and Heat Transport), which landed successfully in November 2018, conducts a radio-science experiment called RISE (Rotation and Interior Structure Experiment, Folkner et al. 2018). The lander signal in X-band is routinely tracked from Earth, with the goal of measuring the rotational movements of the red planet, and to study its deep interior. A very similar and complementary radio-science experiment called LaRa (Lander Radio science, Dehant et al. 2009, 2011, 2019), was also designed to refine the rotation model of Mars and to further constrain its interior. LaRa is part of the scientific payload of the Russian surface platform of the ESA-Roscosmos ExoMars 2020 mission to be launched on 2022. The X-band measurements provided by these two missions have unprecedented accuracy (and low power level in the case of LaRa). In particular, at least centimeter accuracy in the position determined from the phase delay is required. Doppler measurements from RISE and LaRa instruments are at a precision as high as 0.02 $mm.s^{-1}$ at 60 second integration time corresponding to the instrument precision requirement.
However, the impact of a liquid core on Martian Orientation Parameters is lower than 0.004 $mm.s^{-1}$ in the X-band (Yseboodt

et al. 2017) and could be detected from data timeseries. To reach this accuracy, the ionospheres of Mars and Earth as well as the interplanetary plasma contributions need to be corrected for along the line-of-sight effects. Because the ionosphere and plasma effects depend on the frequency, an adequate combination of radio signals on two frequencies allows scientists to obtain corrected radio links (see Mars Express radio science experiment in Pätzold et al. 2005). However, landers have usually only one frequency disabling the correction for these effects. This is also the case for the radio-science experiments RISE and LaRa which use only one S-band frequency. It is thus important to consider the ionospheric effect on radio signals using external models to correct for ionospheric and plasma effects.

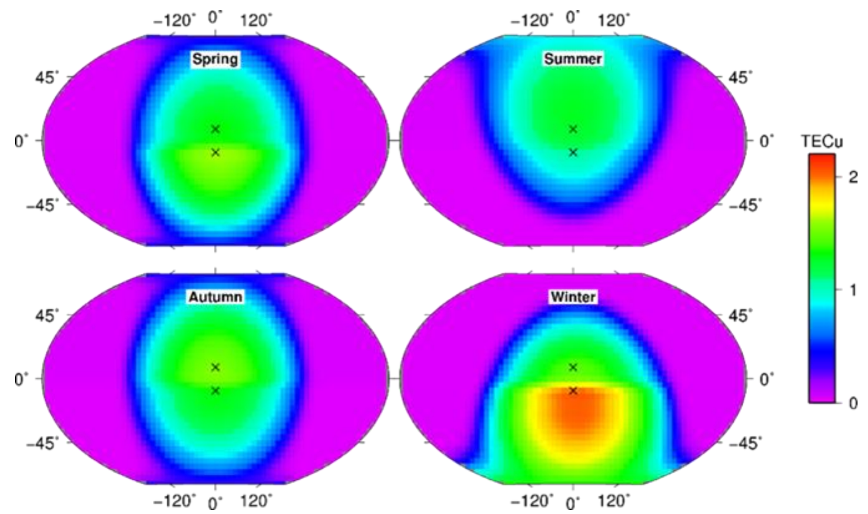

Figure 42: Global maps of Mars vTEC. The different maps correspond to the different outputs of the MoMo model for different seasons (in the North hemisphere) at local noon at the meridian origin. The F10.7P is fixed for a high solar activity level (170 sfu) corresponding to (F10.7P)‾ of 70 sfu for spring, 61 sfu for summer, 79 sfu for autumn and 88 sfu for winter. The black crosses represent the location of two assets on the Mars surface (N10° and S10° in latitude; 0° in longitude).

In that frame, we developed a new empirical model of the Mars Total Electron Content (TEC) called MoMo (Model of Mars Ionosphere). The model provides values for the vertical TEC (vTEC) for a given solar zenith angle, solar activity, solar longitude (Ls) in the two Mars hemispheres. The model has been validated with external radio occultation data for high SZA (Solar Zenith Angle) and with the IPIM (IRAP Plasmasphere Ionosphere Model) physical complex model for low SZA. One of the main motivations for this work was to provide Mars ionosphere corrections for radio-science experiments. We showed that, even if the expected noise of the radio-science instruments is large compared to the Mars ionospheric contribution, it is recommended to correct for this contribution, as its seasonal variations are of the same periods as those of the geophysical parameters determined by the experiments. It is advised to apply ionospheric corrections even during moderate solar activity level, above all for long term studies (i.e. more than one Mars sidereal year), such as those aiming at studying the deep interior of the planet.

The model provides key radio-science quantities like phase delay and Doppler shift, which can be used to calibrate radio science data like those acquired by RISE on the ongoing InSight mission, by LaRa on the future mission ExoMars 2020 mission, or by historical lander missions (Viking, Pathfinder, Mars Exploration Rover (MER)), especially for the Mars ephemeris calculations. From our results, the effect is of the order of 10^{-3} mm.s^{-1} in Doppler observables especially around sunrise and sunset. Consequently, this new model could be used to support the data analysis of any radio-science experiment and especially for present InSight/RISE and future ExoMars LARA instruments aimed at better understand the deep-interior of Mars. This work has been published in the Journal of Space Weather and Space Climate (2019).

Advanced GNSS Tropospheric Products for Monitoring Severe Weather and Climate

About 9 years ago, ROB collaborated with international colleagues to elaborate an EU project proposal aiming at coordinating new and improved capabilities from parallel developments in GNSS (Global Navigation Satellite Systems, such as the American Global Positioning System (GPS) and the European Galileo), meteorological and climate communities: the COST Action ES1206, Advanced GNSS Tropospheric Products for Severe Weather Events and Climate (GNSS4SWEC). This 4-year project (2013-2017) was selected for funding, and in the course of the project, STCE members took leading roles at all levels (from leading research in all working groups to project management). STCE members were particularly active in the following research topics:

- Developing new and advanced products for monitoring the atmospheric water vapour on a wide range of temporal and spatial scales, from real-time monitoring and forecasting severe weather, to the highest quality post-processed products suitable for climate research;
- Studying the atmospheric water vapour anisotropy based on new GNSS products and 3D tomography reconstruction;
- Inter-comparing ground-based, satellite-based, and in-situ water vapour observations and using them to study the long-term variability of the water vapour;
- Tackling the pioneering work of the homogenisation of GNSS-derived water vapour time series as a mandatory step prior to using them for climate applications.

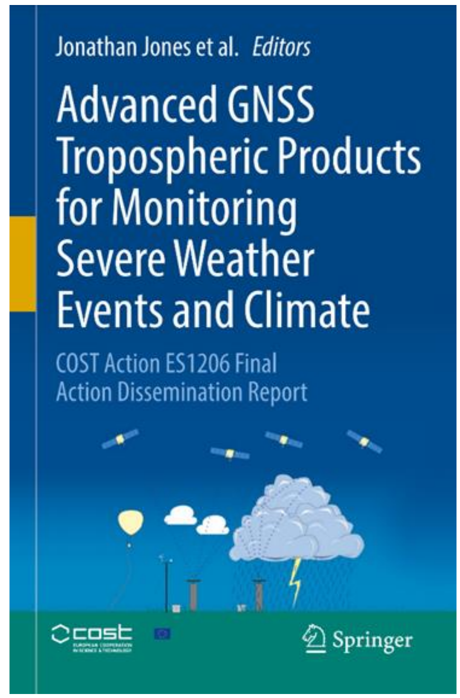

Figure 43: Frontpage of the book published by Springer in 2019, representing the state-of-the-art in GNSS meteorology in Europe.

At the end of the project, the management committee decided to collect the contributions of all project participants in a book in order to summarize the main outcomes of the COST Action ES1206. STCE members contributed largely to this book, both as authors and as editors. This book (Jones et al., 2019) was published by Springer in 2019 and outlines in its 563 pages the present state-of-the-art in GNSS-meteorology in Europe, a summary of advanced GNSS processing techniques and tropospheric products, a unique set of case studies, experiments and data sets for monitoring severe weather and climate; hence including the main contributions of the last years from the STCE to the European research and services in this field.

SSA SWx Service Network coordinated communication exercises

Effective communication is a key factor in ensuring that consistent messages reach their intended audience. Regarding space weather, this is a huge challenge as its impact on society can be both regional and global, and as information may need to be tailored to different end-user communities with different communication standards.

Since 2017, the SSA Space Weather Service Network has initiated a series of coordinated communication exercises with the aim to develop and test a timely and coordinated communication within its extended network in case of a major space weather event and/or a significant media interest. The exercises are performed during normal working hours over a few days (typical duration of a major event) and follow a specific communication protocol. The target is to timely report, and in a consistent way, on the evolution of the space weather event and possible impacts on technology and human health ranging from satellite operation, space walks, aircraft operation and on-board crew and passengers up to critical infrastructure on the ground. To test the readiness of the participants to act, events are simulated based on data from past events and launched in the network without pre-announcement.

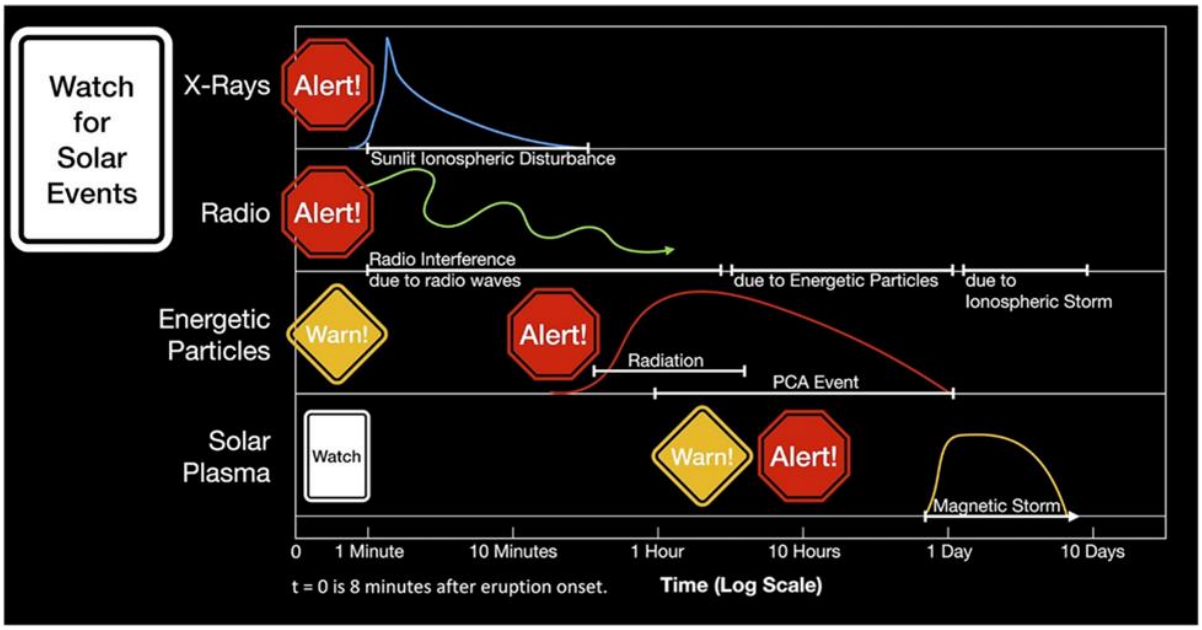

Figure 44: A forecaster's timeline. SWx forecasters are always watching for solar events as potential predictors of near-term technological impacts. This diagram provides a rough phenomenological timeline from X-ray and radio noise producing flares (top) to energetic particles (i.e., SEPs of both eruptive and CME origin) and the arrival of CME solar plasma. Watches, Warnings, and Alerts are invaluable tools for forecasters to disseminate critical space weather information. Adapted from SWPC's "Time Scale for Solar Effects". (Redmon et al. 2018)

Once an event of significant strength takes place, the network experts in the different fields, operators from the SSA Space Weather Coordination Centre (SSCC) and ESA key personnel join in daily telecons to evaluate and update the situation with an overview of the past 24 hours, actual conditions and expectations for the following days. The operators/forecasters closely monitor the space weather activity. At the end of each day, the team of experts and operators agree on a message to be sent out to the ESA communication office that will further disseminate the information via various channels to the outside world in case of a real situation. The exercise continues until the situation has evolved back to nominal conditions.

In its role as lead of the SSCC activities and as SSA Space Radiation Expert Service Centre (R-ESC) coordinator, the BIRA-IASB space weather team contributes to these exercises. This includes providing expertise on particle radiation storms and their effects on technology and human health, as well as coordinating the common efforts of the R-ESC expert groups present in the network.

Figure 45: SSCC room and operators

The goal of the SSCC is to coordinate the whole protocol, contact the experts making sure a representative from each domain is participating, organize and chair the daily discussions and consolidate the overall information delivered in the messages during the exercises guaranteeing that it is as reliable and accurate as possible to be useful for the end-users.

Aside from this activity the SSCC team also organizes user support campaigns in various application fields like aviation and GNSS services, but also for ESA mission operations (Gaia, Mars Express, BepiColombo, …). These campaigns are performed in close collaboration with the end user. Building close relationships with the end user helps to better understand what information they need and how they want to receive it.

Life at the STCE - The year 2019 seemed to be an endless series of meetings, workshops and courses. A well-attended workshop on Cosmic rays took place in one of the BISA meeting rooms on 23 April (upper left). The STCE Annual meeting took place on 6 June, and brought the PECASUS project to everybody's attention (upper right). There were 3 installments of the Space Weather Introductory Course (SWIC), here showing participants intensively occupied with an URSIgram exercise (lower left). And there were many, many training courses given to all involved in the PECASUS-project, such as this one on 5 November to operators from the MeteoWing (lower right).

Publications

This overview of publications consists of three lists: the peer-reviewed articles, the presentations and posters at conferences, and the public outreach talks and publications for the general public. It does not include non-refereed articles, press releases, the daily, weekly and monthly bulletins that are part of our public services,… These data are available at the [STCE-website]() or upon request.

Authors belonging to the STCE have been highlighted in the list of peer reviewed articles.

Peer reviewed articles

1. Asvestari, E.; Heinemann, S.G.; Temmer, M.; Pomoell, J.; Kilpua, E.; **Magdalenic, J.; Poedts, S.**
Reconstructing Coronal Hole Areas With EUHFORIA and Adapted WSA Model: Optimizing the Model Parameters
Journal of Geophysical Research: Space Physics, 124, 11, 8280-8297, 2019, DOI: 10.1029/2019JA027173

2. Barnes, D.; Davies, J.; Harrison, R.; Byrne, J.; Perry, C.; Bothmer, V.; Eastwood, J.; Gallagher, P.; Kilpua, E.; Moestl, C.; **Rodriguez, L.**; Rouillard, A.; Odstrcil, D.
CMEs in the Heliosphere: II. A Statistical Analysis of the Kinematic Properties Derived from Single-Spacecraft Geometrical Modelling Techniques Applied to CMEs Detected in the Heliosphere from 2007 to 2017 by STEREO/HI-1
Solar Physics, 294, 5, 2019, DOI: 10.1007/s11207-019-1444-4

3. Barthélemy, M.; **Lamy, H.**; Vialatte, A.; Johnsen M.G.; **Cessateur, G.**; Zaourar, N.
Measurement of the polarization in the auroral N^2_+ 427.8 nm band
Journal of Space Weather and Space Climate, 9, A26, 2019, DOI: https://doi.org/10.1051/swsc/2019024

4. **Bergeot, N.**; Witasse, O.; **Le Maistre, S.**; Blelly, P.-L.; Kofman, W.; Peter, K.; **Dehant, V.; Chevalier, J.-M.**
MoMo: a new empirical model of the Mars ionospheric total electron content based on Mars Express MARSIS data
Journal of Space Weather and Space Climate, 9, A36, 2019, DOI: 10.1051/swsc/2019035

5. Besliu-Ionescu, D.; **Talpeanu, D.-C.**; **Mierla, M.**; Maris Muntean, G.
On the prediction of geoeffectiveness of CMEs during the ascending phase of SC24 using a logistic regression method
Journal of Atmospheric and Solar-Terrestrial Physics, 193, 105036, 2019, DOI: 10.1016/j.jastp.2019.04.017

6. **Bruyninx, C.; Legrand, J.; Fabian, A.; Pottiaux, E.**
GNSS Metadata and Data Validation in the EUREF Permanent Network
GPS Solutions, 23, 106, 2019, DOI: 10.1007/s10291-019-0880-9

7. **Decraemer, B.; Zhukov, A.N.**; Van Doorsselaere, T.
Three-dimensional Density Structure of a Solar Coronal Streamer Observed by SOHO/LASCO and STEREO/COR2 in Quadrature
The Astrophysical Journal, 883, 2, 152, 2019, DOI: 10.3847/1538-4357/ab3b58

8. Galy, C.; Thizy, C.; Stockman, Y.; Galano, D.; Rougeot, R.; Melich, R.; **Shestov, S.**; Landini, F.; **Zukhov, A.N.**; Kirschner, V. ; Horodyska, P.; Fineschi, S.
Straylight analysis on ASPIICS, PROBA-3 coronagraph
Proceedings of the SPIE, 11180, 111802H, 2019, DOI: 10.1117/12.2536008

9. Gonzalez-Herrero, D.; Micera, A.; Boella, E.; Park, J.; **Lapenta, G.**
ECSIM-CYL: Energy Conserving Semi-Implicit particle in cell simulation in axially symmetric cylindrical coordinates
Computer Physics Communications, 236, 153-163, 2019, DOI: 10.1016/j.cpc.2018.10.026

10. Hinterreiter, J.; **Magdalenic, J.**; Temmer, M.; Verbeke, C.; **Jebaraj, I.C.**; Samara, E.; Asvestari, E.; Poedts, S.; Pomoell, J.; Kilpua, E.; **Rodriguez, L.; Scolini, C.**; Isavnin, A.
Assessing the Performance of EUHFORIA Modeling the Background Solar Wind
Solar Physics, 294, 12, 170, 2019, DOI: 10.1007/s11207-019-1558-8

11. Janssens, J.; Berghmans, D.; Vanlommel, P.; Andries, J.
Space Weather: The Impact on Security & Defense
Schrogl KU. (eds) Handbook of Space Security. Springer, Cham., 2019, DOI: https://doi.org/10.1007/978-3-030-22786-9_94-1

12. Jones, J.; Guerova, G.; Douša, J.; Dick, G.; de Haan, S.; **Pottiaux, E.;** Bock, O.; Pacione, R.; **van Malderen, R.** (Eds.)
Advanced GNSS Tropospheric Products for Monitoring

Severe Weather Events and Climate - COST Action ES1206 Final Action Dissemination Report
Springer, 1st ed. 2020, XXI, ISBN 978-3-030-13900-1, DOI: 10.1007/978-3-030-13901-8

13. Katsavrias, Ch.; Sandberg, I.; Li, W.; **Podladchikova, O.**; Daglis, I.; Papadimitriou, C.; Aminalragia-Giamini, S.
Highly relativistic electron flux enhancement during the weak geomagnetic storm of April-May 2017
Journal of Geophysical Research, 124, 6, 4402-4413, 2019, DOI: 10.1029/2019JA026743

14. Kilpua, E.K.J.; Good, S.W.; Palmerio, E.; Asvestari, E.; Lumme, E.; Ala-Lahti, M.; Kalliokoski, M.M.H.; Morosan, D.E.; Pomoell, J.; Price, D.J.; **Magdalenic, J.**; Poedts, S.; Futaana, Y.
Multipoint Observations of the June 2012 Interacting Interplanetary Flux Ropes
Frontiers in Astronomy and Space Sciences, 6, 50, 2019, DOI: 10.3389/fspas.2019.00050

15. Koronczay, D.; Lichtenberger, J.; Clilverd, M.A.; Rodger, C.J.; Lotz, S.I.; Sannikov, D.V.; Cherneva, N.V.; Raita, T.; **Darrouzet, F.; Ranvier, S.**; Moore, R.C.
The source regions of whistlers
Journal of Geophysical Research Space Physics, 124, 7, 5082-5096, 2019, DOI: 10.1029/2019JA026559

16. Krupar, V.; **Magdalenic, J.**; Eastwood, J.P.; Gopalswamy, N.; Kruparova, O.; Szabo, A.; Němec, F.
Statistical Survey of Coronal Mass Ejections and Interplanetary Type II Bursts
The Astrophysical Journal, 882, 2, 92, 2019, DOI: 10.3847/1538-4357/ab3345

17. Lamy, H.
Properties of meteoroids from forward scatter radio observations
Chapter 3 in Hypersonic Meteoroid Entry Physics (Eds. G. Colonna, M. Capitelli, A. Laricchiuta), IOP Publishing, Bristol, UK, 3-1 to 3-22, 2019, DOI: 10.1088/2053-2563/aae894ch3

18. Leka, K.D.; Park, S.-H.; Kusano, K.; **Andries, J.**; Barnes, G.; Bingham, S.; Bloomfield, D.S.; McCloskey, A.E.; **Delouille, V.**; and 16 co-authors
A Comparison of Flare Forecasting Methods. II. Benchmarks, Metrics, and Performance Results for Operational Solar Flare Forecasting Systems
The Astrophysical Journal Supplement Series, 243, 2, 36, 2019, DOI: 10.3847/1538-4365/ab2e12

19. Leka, K.D.; Park, S.H.; Kusano, K.; **Andries, J.**; Barnes, G.; Bingham, S.; Bloomfield, D.S.; McCloskey, A.E.; **Delouille, V.**; and 16 co-authors
A Comparison of Flare Forecasting Methods. III. Systematic Behaviors of Operational Solar Flare Forecasting Systems
The Astrophysical Journal, 881, 2, 101, 2019, DOI: 10.3847/1538-4357/ab2e11

20. Lilensten, J.; Belehaki, A.; Watermann, J.; **Janssens, J.**; Henri, A.
JSWSC: recent developments and further advances
Journal of Space Weather and Space Climate, 9, E2, 2019, DOI: 10.1051/swsc/2019011

21. Lopez, R.A.; Shaaban, S.M.; Lazar, M.; Poedts, S.; Yoon, P.H.; **Micera, A.;** Lapenta, G.
Particle-in-cell simulations of the whistler heat-flux instability in the solar wind conditions
The Astrophysical Journal Letters, 882, 1, L8, 2019, DOI: 10.3847/2041-8213/ab398b

22. Mathieu, S.; von Sachs, R.; Ritter, C.; **Delouille, V.; Lefèvre, L.**
Uncertainty Quantification in Sunspot Counts
The Astrophysical Journal, 886,1, 7, 2019, DOI: 10.3847/1538-4357/ab4990

23. Middleton, K.F.; Anwand, H.; Bothmer, V.; … ; **Nicula, B.**; … ; **West, M.**; and 16 co-authors
SCOPE: a coronagraph for operational space weather prediction: phase A/B1 design and breadboarding
Proceedings of the SPIE, 11180, 111803A, 2019, DOI: 10.1117/12.2536037

24. O'Hara, J.; Mierla, M.; Podladchikova, O.; D'Huys, E.; West, M.
Exceptional Extended Field-of-View Observations by PROBA2/SWAP on 2017 April 1 and 3
The Astrophysical Journal, 883, 1, 59, 2019, DOI: 10.3847/1538-4357/ab3b08

25. Opgenoorth, H.; Wimmer-Schweingruber, R.; Belehaki, A.; **Berghmans, D.**; Hapgood, M.; Hesse, M.; Kauristie, K.; Lester, M.; Lilensten, J.; Messerotti, M.; Temmer, M.
European Space Weather Activities: Assessment and Recommendations for a Consolidated European Approach to Space Weather - as Part of a Global Space Weather Effort
Journal of Space Weather and Space Climate, 9, A37, 2019, DOI: 10.1051/swsc/2019033

26. Palmerio, E.; **Scolini, C.**; Barnes, D.; **Magdalenic, J.; West, M.; Zhukov, A.N.; Rodriguez, L.; Mierla, M.**; Good, S.; Morosan, D.; Kilpua, E.; Pomoell, J.; Poedts, S.
Multipoint Study of Successive Coronal Mass Ejections Driving Moderate Disturbances at 1 au
The Astrophysical Journal, 878, 1, 37, 2019, DOI: 10.3847/1538-4357/ab1850

27. **Pierrard V.; Lopez Rosson, G.; Botek, E**.
Dynamics of Megaelectron Volt Electrons Observed in the Inner Belt by PROBA-V/EPT

Journal of Geophysical Research: Space Physics, 124, 3, 1651-1659, 2019, DOI: 10.1029/2018JA026289

28. Podladchikova, T.; Veronig, A.; Dissauer, K.; Temmer, M.; **Podladchikova, O.**
Three-dimensional Reconstructions of Extreme-ultraviolet Wave Front Heights and Their Influence on Wave Kinematics
The Astrophysical Journal, 877, 2, 68, 2019, DOI: 10.3847/1538-4357/ab1b3a

29. Sarkar, R.; Srivastava, N.; **Mierla, M.; West, M.; D'Huys, E.**
Evolution of the Coronal Cavity From the Quiescent to Eruptive Phase Associated with Coronal Mass Ejection
The Astrophysical Journal, 875, 2, 101, 2019, DOI: 10.3847/1538-4357/ab11c5

30. **Scolini, C.; Rodriguez, L.; Mierla, M.**; Pomoell, J.; Poedts, S.
Observation-based modelling of magnetised Coronal Mass Ejections with EUHFORIA
Astronomy and Astrophysics, 626, A122, 2019, DOI: 10.1051/0004-6361/201935053

31. **Shestov, S.V.; Zhukov, A.N.**; Seaton, D.
Modeling and removal of optical ghosts in the PROBA-3/ASPIICS externally occulted solar coronagraph
Astronomy and Astrophysics, 622, A101, 2019, DOI: 10.1051/0004-6361/201834584

32. Thompson, A.M.; Smit, H.G.; Witte, J.C.; … ; **Van Malderen**, **R.**; … and 27 co-authors
Ozonesonde Quality Assurance: The JOSIE-SHADOZ (2017) Experience
Bulletin of the American Meteorological Society, 100, 1, 155-171, 2019, DOI: 10.1175/BAMS-D-17-0311.1

33. **Verbeeck, C.; Kraaikamp, E.**; Ryan, D.F.; **Podladchikova, O.**
Solar flare distributions: lognormal instead of power law?
The Astrophysical Journal, 884, 1, 50, 2019, DOI: 10.3847/1538-4357/ab3425

34. Waets, A.; Cipriani, F.; **Ranvier, S.**
LEO Charging of the PICASSO Cubesat and Simulation of the Langmuir Probes Operation
IEEE Transactions on Plasma Science, 47, 8, 3689-3698, 2019, DOI: 10.1109/TPS.2019.2920136

Presentations and posters at conference

1. Anciaux, M.; Lamy, H.; Martínez Picar, A.; Ranvier, S.; Calders, S.; Calegaro, A.; Verbeeck, C.
The BRAMS receiving station V2.0
International Meteor Conference 2019, Bollmannsruh, Germany, 3-6 October 2019

2. Asvestari, E.; Heinemann, S.; Pomoell, J.; Temmer, M.; Kilpua, E.; Magdalenic, J.; Poedts, S.
Reconstructing coronal holes with EUHFORIA
EGU General Assembly 2019, Vienna, Austria, 7-12 April 2019 (poster)

3. Bechet, S.; Clette, F.
Data homogenization for a network of ground-based synoptic imaging telescopes
ML-Helio, Amsterdam, The Netherlands, 16-20 September (poster)

4. Belehaki, A.; Galkin, I.; Borries, C.; Pintor, P.; Altadill, D.; Sanz, J.; Miguel Juan, J.; Buresova, D.; Verhulst, T.; Mielich, J.; Katamzi-Joseph, Z.; Watermann, J.; Haralambous, H.; Unger, S.
Travelling Ionospheric Disturbances nowcasting, TechTIDE: Warning and Mitigation
2019 URSI AP-RASC, New Delhi, India, 9-15 March 2019

5. Belehaki, A.; Blanch, E.; Altadill, D.; Tsagouri, I.; Borries, C.; Buresova, D.; Galkin, I.; Zornosa, M.J.; Segarra, A.; and the TechTIDE consortium (incl. Verhulst, T. and Stankov, S.)
Real-Time identification of Travelling Ionospheric Disturbances-The TechTIDE project
AGU Fall Meeting, San Francisco, California, USA, 9-13 December 2019

6. Bergeot, N.; Pierrard, V.; Darrouzet, F.; Chevalier, J.-M.
Comparison between empirical and physical models of the topside ionospheric-plasmaspheric electron content above Antarctica
2019 URSI AP-RASC, New Delhi, India, 9-15 March 2019

7. Bergeot, N.; Chevalier, J.-M.; Pinat, E.
Ionosphere/plasmasphere system in polar region and mid-latitude
Workshop: Interhemispheric Comparison of the Ionosphere-Plasmasphere System, SANSA, Hermanus, South Africa, 19-21 November 2019

8. Bergeot, N.; Witasse, O.; Le Maistre, S.; Blelly, P.-L.; Kofman, W.; Peter, K.; Dehant, V.; Chevalier, J.-M.
A new empirical model for Mars Ionosphere to correct radio signal experiments
EPSC-DPS Joint Meeting 2019, Geneva, Switzerland, 15-20 September 2019

9. Bergeot, N.; Habarulema, J.B.; Chevalier, J.-M.; Pinat, E.; Cilliers, P.J.
GNSS-based empirical models for inter-hemispheric comparison of the ionosphere-plasmasphere system at mid-latitude
20th International Beacon Satellite Symposium, Olsztyn, Poland, 19-23 August 2019

10. Bergeot, N.; Pierrard, V.; Darrouzet, F.; Chevalier, J.-M.; Pinat, E.
Ionosphere-Plasmasphere empirical model over Antarctica region
20th International Beacon Satellite Symposium, Olsztyn, Poland, 19-23 August 2019 (talk and poster)

11. Bergeot, N.; Alfonsi, L.
RESOURCE: an International Activity Addressed to Space Weather Monitoring at High Latitudes
2019 URSI AP-RASC, New Delhi, India, 9-15 March 2019 (poster)

12. Berghmans, D.; Andries, J.; Dominique, M.; Dammasch, I.; Bonte, K.
PROBA2 space weather services at the SSA Solar Weather Expert Service Center
PROBA-2 Symposium: 9 Years of Proba-2 Operations, Redu, Belgium, 7-8 February 2019 (invited talk)

13. Berghmans, D.
SolO/EUI timeline
24th EUI Consortium Meeting, Brussels (ROB), Belgium, 17 September 2019 (invited talk)

14. Berghmans, D.; Rochus, P.; and the EUI Consortium
Status EUI
25th Solar Orbiter Science Working Team (SWT-25), Noordwijk, The Netherlands, 16 October 2019

15. Berghmans, D.
Product/Quality Assurance, verification, validation
PROBA-3 Science Working Team Meeting 8, Göttingen, Germany, 25-26 September 2019

16. Berghmans, D.; Rochus, P.; and the EUI Consortium
Status EUI
24th Solar Orbiter Science Working Team (SWT-24), Firenze, Italy, 2 April 2019

17. Berghmans, D.; D'Huys, E.; Zhukov, A.N.; Auchère, F.
From PROBA2/SWAP to Solar Orbiter/EUI: Exploring the outer edge of the EUV corona
AGU Fall Meeting, San Francisco, California, USA, 9-13 December 2019 (invited talk)

18. Borries, C.; Belehaki, A.; Tsagouri, I.; Galkin, I.; Sanz, J.; Juan, M.; Altadill, D.; Buresova, D.; Mielich, J.; Verhulst, T.; Stankov, S.; Haralambous, H.; Segarra, A.; Blanch, E.
Travelling Ionospheric Disturbances studied in the EU H2020 TechTIDE project
International Workshop on GNSS Ionosphere, Neustrelitz, Germany, 23-25 September 2019

19. Broock, E.; West, M.; Mierla, M.; Podladchikova, E.; Rodriguez, L.
Multi-point Measurements of Solar Eruptions at Locations Throughout the Heliosphere
ESWW16, Liège, Belgium, 18-22 November 2019 (poster)

20. Bruyninx C.; Pottiaux E.; Pacione R.; Fabian A.; Legrand J.
On the Future High-Precision European GNSS CORS Infrastructure
EGU General Assembly 2019, Vienna, Austria, 7-12 April 2019 (invited talk)

21. Bruyninx, C.; Legrand, J.; Fabian, A.; Pottiaux, E.; Roosbeek, F.
EPN Data Quality in a Multi-GNSS Environment
EUREF 2019 Symposium, Tallin, Estonia, 22-24 May 2019

22. Bruyninx, C.; Pottiaux, E.; Fabian, A.; Legrand, J.; Pacione, R.; Kenyeres, A.
On the Future High-Precision European GNSS CORS Infrastructure
EUREF 2019 Symposium, Tallin, Estonia, 22-24 May 2019

23. Bruyninx, C.; Legrand, J.; Fabian, A.; Pottiaux, E.
Towards Operational Data Quality Monitoring of EPN Stations
EGU General Assembly 2019, Vienna, Austria, 7-12 April 2019

24. Buresova, D.; Belehaki, A.; Miguel Juan, J.; Sanz Subirana, J.; Chum, J.; Altadill, D.; Blanch, E.; Segarra, A.; Watermann, J.; Kouba, D.; Galkin, I.; and the TechTIDE consortium (including Verhulst, T. and Stankov, S.)
Monitoring and analysis of the TIDs triggered by magnetic storms and their impact on EGNOS availability degradation
20th International Beacon Satellite Symposium, Olsztyn, Poland, 19-23 August 2019

25. Calders, S.; De Donder, E.; Messios, N.
Using the SPENVIS-NG application programming interface to assess the impact of space weather on satellites
ASEC, Los Angeles, California, USA, 13-17 May 2019 (poster)

26. Calders, S.; Draulans, S.; Calders, T.; Lamy, H.
The Radio Meteor Zoo: identifying meteor echoes using artificial intelligence
International Meteor Conference 2019, Bollmannsruh, Germany, 3-6 October 2019

27. Chabanski, S.; O'Hara, J.; Vansintjan, R.; Liber, C.; Glover, A.
ESA SSA SWE Network Service Dashboards and How to Combine Products to Provide Added Value to the User
ESWW16, Liège, Belgium, 18-22 November 2019

28. Chevalier, J.-M.; Bergeot, N.; Pinat, E.
Space Weather Monitoring based on GNSS at the Royal Observatory of Belgium
Workshop: Interhemispheric Comparison of the Ionosphere-Plasmasphere System, SANSA, Hermanus, South Africa, 19-21 November 2019

29. Cilliers, P.; Alfonsi, L.; Correia, E.; Bergeot, N.; Dovis, F.; Linty, N.; Ward, J.
Multi-constellation GNSS observation of ionospheric scintillation at SANAE-IV in Antarctica
20th International Beacon Satellite Symposium, Olsztyn, Poland, 19-23 August 2019

30. Cisneros-González, M.; … ; Ketchazo, C.; and 19 others
Validation tests of the calibration bench for the characterization of MAJIS/JUICE VIS-NIR detectors
EPSC-DPS Joint Meeting 2019, Geneva, Switzerland,15-20 September 2019

31. Cisneros-González, M.; Bolsée, D.
Characterization of MAJIS VIS-NIR detectors, Description of Calibration Facility
S-SAIL, Lisboa, Portugal, 27-28 June 2019

32. Clette, F.
Reconstructing the full sunspot number database
Space Climate 7: The future of solar activity, Canton Orford, Québec, Canada, 8-11 July 2019 (poster)

33. Clette, F.
The new Sunspot Number: What are the key changes?
Solar Cycle 25 Prediction Panel, Boulder, Colorado, USA, 5 March 2019 (invited talk)

34. Clette, F.; Lefèvre, L.; Bechet, S.
The Sunspot Number database: progresses in data recovery and digitization
ISSI Team Meeting 2: Recalibration of the Sunspot Number series, Bern, Switzerland, 19-23 August 2019

35. Clette, F.
Common data and software repository. A premature idea?
ISSI Team Meeting 2: Recalibration of the Sunspot Number series, Bern, Switzerland, 19-23 August 2019

36. Clette, F.
Welcome, introduction, meeting goals and ground rules
ISSI Team Meeting 2: Recalibration of the Sunspot Number series, Bern, Switzerland, 19-23 August 2019

37. Clette, F.; Lefèvre, L.
Reconciling the Sunspot and Group Numbers
VARSITI Closing Symposium, Sofia, Bulgaria,10-14 June 2019

38. Daglis, I.A.; Katsavrias, C.; Sandberg, I.; Podladchikova, O.; Li, W.; Papadimitriou, C.; Tsironis, C.; Aminalragia-Giamini, S.
Long-lived relativistic electron flux enhancement during a weak geomagnetic storm
EGU General Assembly 2019, Vienna, Austria, 7-12 April 2019

39. Dammasch, I.; Dominique, M.; Machol, J.
PROBA2/LYRA soft x-ray response after ten years in space
Degradation and Inter-calibration of EUV instruments Solar EUV Irradiance Workshop, Uccle (BISA), Brussels, 14-18 October 2019

40. Decraemer, B.; Zhukov, A.N.; Van Doorsselaere, T.
Large-scale streamer wave events observed from multiple vantage points
5th UK-Ukraine-Spain Meeting on solar physics and space science, Kyiv, Ukraine, 26-30 August 2019

41. Darrouzet, F.; De Keyser, J.; Lemaire, J.F.; Décréau,P.M.E.; Gallagher, D.L.
Plasmasphere observations with Cluster completed by new data from an old mission, Dynamics Explorer-1
EGU General Assembly 2019, Vienna, Austria, 7-12 April 2019

42. Darrouzet, F.; De Keyser, J.; Lemaire, J.F.; Decreau, P.M.E.; Gallagher, D.; Verbanac, G.; Bandic, M.; Zhelavskaya, I.S.
Plasmasphere observations with Cluster data supplemented with data from the Dynamics Explorer-1 and Van Allen Probes missions
29th Cluster workshop, Lanzarote, Canary Island, Spain, 7-11 October 2019

43. De Donder, E.; Calegaro, A.; Chabanski, S.; Liber, C.; Vansintjan, R.; O'Hara, J.; Glover, A.
Space Weather Bulletins as part of a User Test Campaign for Aviation
ESWW16, Liège, Belgium, 18-22 November 2019 (poster)

44. Defise, J.-M.; Berghmans, D.; Seaton, D.; D'Huys, E.; West, M.; Mierla, M.
Summary of SWAP scientific Results
PROBA-2 Symposium: 9 Years of Proba-2 Operations, Redu, Belgium, 7-8 February 2019 (invited talk)

45. Delouille, V.; Barra, V.
Generation of magnetograms using image-to-image translation of EUV images
ML-Helio, Amsterdam, The Netherlands, 16-20 September (poster)

46. Delouille, V.; Mampaey, B.; Nicula, B.; Andries, J.; Vansintjan, R.; de Patoul, J.
Sharing Solar Data with ESCAPE and SOLARNET
IVOA Interoperability Meeting, Paris, France, 12-17 May 2019

47. Dierckxsens, M.; Zychova, L.; Crosby, N.; Calders, S.
The Operational Performance of the COMESEP SEPForecast Tool
EGU General Assembly 2019, Vienna, Austria, 7-12 April 2019 (poster)

48. Dierckxsens, M.
The ESA SSA Space Weather Space Radiation Expert Service Centre
IRENE Space Radiation Modelling and Data Analysis Workshop 2019, Sykia, Greece , 29-31 May 2019

49. Dolla, L.; Zhukov, A.N.
Observations planning and Science Activity Plan of PROBA-3/ASPIICS
ASPIICS Science Operations Workshop, Göttingen, Germany, 23-24 September 2019

50. Dolla, L.; Nicula, B.; Shestov, S.; Zhukov, A.N.
FITS header keyword definitions for PROBA-3/ASPIICS
ASPIICS Science Operations Workshop, Göttingen, Germany, 23-24 September 2019

51. Dolla, L.; Dominique, M.; Marqué, C.
Quasi-Periodic Pulsations
PROBA-2 Symposium: 9 Years of Proba-2 Operations, Redu, Belgium, 7-8 February 2019

52. Dominique, M.; and the LYRA team
Analysis of the spectral degradation of the PROBA2/LYRA instrument
Degradation and Inter-calibration of EUV instruments (Solar EUV Irradiance Workshop), Uccle (BISA), Brussels, 14-18 October 2019

53. Dominique, M.; Zhukov, A.N.; Dolla, L.; Wauters, L.; Dammasch, I.; Heinzel, P.; Thiemann, E.
Joint observation of the X9.3 and X8.2 flares on 6 and 10 September 2017 by SDO/EVE, PROBA2/LYRA, and MAVEN/EUVM
RAS Meetings, London, UK, 12 April 2019

54. Dominique, M.; and the LYRA team
Summary of LYRA Scientific Results
PROBA-2 Symposium: 9 Years of Proba-2 Operations, Redu, Belgium, 7-8 February 2019

55. Dominique, M.
Solar flare studies with the LYRA instrument onboard PROBA2
Thesis, Public PhD Defense, Leuven, Belgium, 26 February 2019

56. Dominique, M.; Thiemann, E.; Dammasch, I.
Using cubesats to monitor the evolution of the thermospheric temperature and O and N2 densities, as well as their response to solar events, using the occultation technique
ESWW16, Liège, Belgium, 18-22 November 2019 (poster)

57. Dominique, M.; Zhukov, A.N.; Thiemann, E.; Dolla, L.; Heinzel, P.; Wauters, L.; Dammasch, I.
Analysis of the quasi-periodic pulsations in the X9.3 and X8.3 flares on 6 and 10 September 2017 observed by SDO/EVE, PROBA2/LYRA and MAVEN/EUVM
AGU Fall Meeting, San Francisco, California, USA, 9-13 December 2019 (poster)

58. El Fadhel, A.; Karatekin, Ö.; Witasse, O.; Asmar, S.; Bergeot, N.; Van Hove, B.
Radio Occultations Using CubeSats to probe the planetary atmospheres
EPSC-DPS Joint Meeting 2019, Geneva, Switzerland, 15-20 September 2019

59. Georgoulis, M.; Patsourakos, S.; Samara, E.
Magnetic Impact of Propagating Interplanetary Coronal Mass Ejections in the Solar and Stellar Habitability Zones
AGU Fall Meeting, San Francisco, California, USA, 9-13 December 2019

60. Gissot, S.; Berghmans, D.; Auchere, F.; Schuehle, U.; Giordanengo, B.; Laubis, C.; Gottwald, A.
Expected degradation of the Extreme Ultraviolet Imager onboard Solar Orbiter
Degradation and Inter-calibration of EUV instruments (Solar EUV Irradiance Workshop), Uccle (BISA), Brussels, 14-18 October 2019

61. Gonzalez, A.; Delouille, V.; Jacques, L.
Non-parametric PSF estimation from celestial transit solar images using blind deconvolution
Wavelet and Beyond - A celebration for Alexandre Grossmann and Yves Meyer, Orsay, France, 12-14 June 2019 (poster)

62. Harri, A.M.; Kauristie, K.; Andries, J.; Gibbs, M.; Beck, P.; Berdermann, J.; Perrone, L.; van den Oord, B.; Berghmans, D.; Bergeot, N.; De Donder, E.; Latocha, M.; Dierckxsens, M.; Haralambous, H.; Stanislawska, I.M.; Wilken, V.; Romano, V.; Kriegel, M.; Österberg, K.
PECASUS, European Space Weather Service Network for Aviation
AGU Fall Meeting, San Francisco, California, USA, 9-13 December 2019 (talk and poster)

63. Hayakawa, H.; Clette, F.
Hisako Koyama's Sunspot Observations and their Digitization
ISSI Team Meeting 2: Recalibration of the Sunspot Number series, Bern, Switzerland, 19-23 August 2019

64. Hervo, M.; Haefele, A.; Ruefenacht, R.; Turp, M.; Lampin, J.L.; Haeffelin, M.; Mattis, I.; Hopkin, E.; Kotthaus, S.; Thomas, W.; Mortier, A.; Laffineur, Q.; de Haij, M.J.; Itsvan, S.; Martin, D.; Skrivankov, P.
Long-Range Smoke Transport: Monitoring with the New European Automatic Lidar Network—E-PROFILE
99th American Meteorological Society Annual Meeting, Phoenix, Arizona, USA, 6-10 January 2019 (poster)

65. Jebaraj, I.C.; Christopher, I.; Magdalenic, J.; Scolini, C.; Rodriguez, L.; Poedts, S.; Kilpua, E.; Krupar, V.; Pomoell, J.; Temmer, M.
Origin of the two shock waves associated with the September 27/28, 2012 event
EGU General Assembly 2019, Vienna, Austria, 7-12 April 2019 (poster)

66. Janssens, J.
Very low likelihood of a power grid black-out in Belgium during an extremely severe geomagnetic storm
ESWW16, Liège, Belgium, 18-22 November 2019 (poster)

67. Janssens, J.
Status manuscripts Journal of SWSC
ESWW16, Liège, Belgium, 18-22 November 2019 (invited talk)

68. Jebaraj, I.C.; Magdalenic, J.; Scolini, C.; Podladchikova, T.; Pomoell, J.; Dissauer, K.; Veronig, A.; Krupar, V.; Kilpua, E.; Poedts, S.
Complex shock wave signatures associated with CME on September 27/28, 2012
CESRA 2019, Potsdam, Germany, 8-12 July 2019

69. Jebaraj, I.C.; Magdalenic, J.; Scolini, C.; Podlachikova, T.; Dissauer, K.; Pomoell, J.; Rodriguez, L.; Kilpua, E.; Krupar, V.; Veronig, A.; Poedts, S.
A new approach to interpret interplanetary radio observations for forecasting shock arrival at Earth
ESWW16, Liège, Belgium, 18-22 November 2019 (poster)

70. Jebaraj, I.C.; Magdalenic, J.; Scolini, C.; Pomoell, J.; Rodriguez, L.; Kilpua, E.; Poedts, S.
Can radio triangulation help in understanding complex shock wave signatures
CESPM 2019, Hvar, Croatia, 6-10 May 2019 (poster)

71. Jebaraj, I.C.; Magdalenic, J.; Scolini, C.; Rodriguez, L.; Kilpua, E.; Krupar, V.; Poedts, S.
Complex radio emissions associated with the September 27, 2012 CME/flare event
SHINE 2019, Boulder, Colorado, USA, 4-9 August 2019

72. Karatekin, Ö.; El Fadhel, A.; Krishnan, A.; Van Hove, B.; Witasse, O.; Bergeot, N.
Analysis of radio-occultation data from Mars Express
EPSC-DPS Joint Meeting 2019, Geneva, Switzerland, 15-20 September 2019

73. Kauristie, K.; Andries, J.; Bergeot, N.; Beck, P.; Berghmans, D.; Cesaroni, C.; Crosby, N.; De Donder, E.; Dierckxsens, M.; Gibbs, M.; Haralambous, H.; Harri, A.-M.; Latocha, M.; Perrone, L.; Romano, V.; Spogli, L.; Stanislawska, I.; Hammond, K.; Tomasik, L.; van den Oord, B.; Vanlommel, P.; Wilken, V.; Kriegel, M.; McKinnell, L.-A.; Österberg, K.
PECASUS, one of the global Space Weather Centers supporting ICAO
ESWW16, Liège, Belgium, 18-22 November 2019 (talk and poster)

74. Klein, K.L.; Fuller, N.; Steigies, C.; Bütikofer, R.; Sapundjiev, D.; Kryakunova, O.; and the NMDB consortium
The NMDB database as a support for the monitoring of the radiation exposure aboard aircraft
ESWW16, Liège, Belgium, 18-22 November 2019

75. Koukras, A.; Marqué, C.; Downs, C.; Dolla, L.
Analysing the kinematics of EUV waves by combining simulations and multi-instrument observations
Nasa Heliophysics Summer School, Boulder, Colorado, USA, 23-30 July 2019 (poster)

76. Koukras, A.; Dupuis, R.; Ricour, B.; Dolla, L.
Flare Prediction using Deep Learning with multiple wavelength SDO data
ESWW16, Liège, Belgium, 18-22 November 2019 (poster)

77. Koukras, A.; Marqué, C.; Downs, C.; Dolla, L.
Analysing the kinematics of EUV waves by combining simulations and multi-instrument observations
CESPM 2019, Hvar, Croatia, 6-10 May 2019 (poster)

78. Koukras, A.; Marqué, C.; Downs, C.; Dolla, L.
Analysing the kinematics of EUV waves by combining simulations and multi-instrument observations
SHINE 2019, Boulder, Colorado, USA, 4-9 August 2019 (talk and poster)

79. Koukras, A.; Dupuis, R.; Ricour, B.; Dolla, L.
Flare Prediction using Deep Learning with multiple wavelength SDO data
ML-Helio, Amsterdam, The Netherlands, 16-20 September 2019 (poster)

80. Laffineur, Q.; Debal, F.; Mangold, A.; Reyniers, M.; Delobbe, L.; De Backer, H.
Observation of narrow bands of heavy snow: two rare cases of snowfall impacted by industrial heat rejection in Europe
11th International Symposium on Tropospheric Profiling, Toulouse, France, 20-24 May 2019

81. Lamy, H.; Anciaux, M.; Ranvier, S.; Calders, S.; Calegaro, A.; Verbeeck, C.; Martínez Picar, A.; Johannink, C.; De Keyser, J.
Study of combined radio and optical observations of meteors with the BRAMS and CAMS-BeNeLux networks
EGU General Assembly 2019, Vienna, Austria, 7-12 April 2019 (poster)

82. Lamy, H.; Anciaux, M.; Ranvier, S.; Calders, S.; Calegaro, A.; Verbeeck, C.; Martínez Picar, A.; Johannink, C.; De Keyser, J.
Radio and optical observations of meteors with the BRAMS and CAMS-BeNeLux networks
AGU Fall Meeting, San Francisco, California, USA, 9-13 December 2019 (poster)

83. Lamy, H.; Anciaux, M.; Ranvier, S.; Martínez Picar, A.; Calders, S.; Calegaro, A.; Verbeeck, C.
Calibration of the BRAMS interferometer
International Meteor Conference 2019, Bollmannsruh, Germany, 3-6 October 2019

84. Lanabere, V.; Dasso, S.; Démoulin, P.; Janvier, M.; Rodriguez, L.; Masías-Meza, J.J.
Magnetic twist profile inside magnetic clouds derived with a superposed epoch analysis
Workshop FReSWeD 2019 Towards Future Research on Space Weather Drivers, San Juan, Argentina, 2-7 July 2019

85. Lanabere, V.; Dasso, S.; Démoulin, P.; Janvier, M.; Rodriguez, L.; Masías-Meza, J.J.
Finding the distribution of the twist profile in Magnetic Clouds using a superposed epoch analysis
Chapman Conference on Scientific Challenges Pertaining to Space Weather Forecasting Including Extremes, Pasadena, California, USA, 11-15 February 2019 (poster)

86. Lefèvre, L.; Mathieu, S.
VAL-U-SUN: Goals and progresses
ISSI Team Meeting 2: Recalibration of the Sunspot Number series, Bern, Switzerland, 19-23 August 2019

87. Lefèvre, L.
Sunspot Number recalibration: Methods, errors, best practices
ISSI Team Meeting 2: Recalibration of the Sunspot Number series, Bern, Switzerland, 19-23 August 2019

88. Lefèvre, L.; Clette, F.
IAGA Resolution: International Sunspot Number: support to WDC SILSO
27th IUGG General Assembly, Montreal, Canada, 8-18 July 2019

89. Lefèvre, L.; Mathieu, S.; Clette, F.
The Sunspot Number series: reconciling past and present with modern tools
27th IUGG General Assembly, Montreal, Canada, 8-18 July 2019

90. Lefèvre, L.; Mathieu, S.; Clette, F.
The Sunspot Number series: advanced statistics to model sunspot counts
27th IUGG General Assembly, Montreal, Canada, 8-18 July 2019

91. Lefèvre, L.; Mathieu, S.; von Sachs, R.; Delouille, V.; Clette, F.
Advanced Statistics to model the Sunspot Number series
Space Climate 7: The future of solar activity, Canton Orford, Québec, Canada, 8-11 July 2019

92. Magdalenic, J.; Jebaraj, I.C.
Homologous halo CMEs of a flower-like morphology
CESPM 2019, Hvar, Croatia, 6-10 May 2019

93. Magdalenic, J.; Jebaraj, I.C.
Homologous halo CMEs of a flower-like morphology
EGU General Assembly 2019, Vienna, Austria, 7-12 April 2019

94. Magdalenic, J.; Marqué, C.; Fallows, R.; Mann, G.; Vocks, C.
Structured type III radio bursts observed by LOFAR
CESRA 2019, Potsdam, Germany, 8-12 July 2019 (poster)

95. Magdalenic, J.; Jebaraj, I.C.; Harra, L.; Matthews, S.; Berghmans, D.; Krupar, V.
Active region jets on August 25, 2011
CESRA 2019, Potsdam, Germany, 8-12 July 2019 (invited talk)

96. Marqué, C.
Impact of solar radio bursts on technology
CESRA 2019, Potsdam, Germany, 8-12 July 2019 (invited talk)

97. Martínez Picar, A.; Marqué, C.; Ergen, A.; Magdalenic, J.
SAFIRE: An SDR-based Solar Flux Monitor System
CESRA 2019, Potsdam, Germany, 8-12 July 2019 (poster)

98. Martínez Picar, A.; Marqué, C.; Magdalenic, J.
Towards the First Light of SPADE
SKA General Science Meeting and Key Science Workshop 2019, Cheshire, UK, 8-12 April 2019 (poster)

99. Mathieu, S.; von Sachs, R.; Ritter, C.; Delouille, V.; Lefèvre, L.
Modelling of Sunspot counts time series
ML-Helio, Amsterdam, The Netherlands, 16-20 September 2019 (poster)

100. Mathieu, S.; Delouille, V.; Lefèvre, L.; Ritter, C.; Von Sachs, R.
Modélisation et estimation du nombre de taches solaires
GRETSI 2019: XXVIIème Colloque francophone de traitement du signal et des images, Lille, France, 26-29 August 2019 (poster)

101. Messios, N.; Calders, S.; De Donder, E.
Paving the way for the next SPENVIS system
ASEC, Los Angeles, California, USA, 13-17 May 2019

102. Messios, N.
Geant4 Tools in SPENVIS - A User Perspective
14th Geant4 Space Users' Workshop, Xylokastro, Greece, 21-23 October 2019

103. Micera, A.; Boella, E.; Zhukov, A.N.; Shaaban, S.M.; Lazar, M.; Lapenta, G.
Particle-in-Cell Simulations of the Effects of the Electron Temperature Anisotropy on the Development of the Proton Firehose Instability in the Solar Wind conditions
AGU Fall Meeting, San Francisco, California, USA, 9-13 December 2019 (poster)

104. Micera, A.; Boella, E.; Zhukov, A.N.; Shaaban, S.M.; Lazar, M.; Lapenta, G.
Particle-in-Cell Simulations of the Effects of the Electron Temperature Anisotropy on the Development of the Proton Firehose Instability in the Solar Wind
61st Annual Meeting of the APS, Fort Lauderdale, USA, 21-25 October 2019 (poster)

105. Mierla, M.; D'Huys, E.; Janssens, J.; Wauters, L.; West, M.; Seaton, D.; Berghmans, D.; Podladchikova, E.
Long-term evolution of the solar corona using PROBA2 data
ESWW16, Liège, Belgium, 18-22 November 2019 (poster)

106. Mierla, M.; Inhester, B.; Zhukov, A.N.
Calculation of polarization angle deviations for different coronal conditions
PROBA-3 Science Working Team Meeting 8, Göttingen, Germany, 25-26 September 2019

107. Mierla, M.
3D Reconstruction of Solar Eruptions using PROBA2/SWAP and STEREO/EUVI Data
PROBA-2 Symposium: 9 Years of Proba-2 Operations, Redu, Belgium, 7-8 February 2019

108. Mierla, M.; Rodriguez, L.; Samara, E.
Coronal holes and space weather consequences
Workshop FReSWeD 2019 Towards Future Research on Space Weather Drivers, San Juan, Argentina, 2-7 July 2019 (invited talk)

109. Mierla, M.
On 3D reconstruction and propagation of Coronal Mass Ejections

Workshop FReSWeD 2019 Towards Future Research on Space Weather Drivers, San Juan, Argentina, 2-7 July 2019 (invited talk)

110. Morel, L; Durand, F.; Abbondanza, C.; Pottiaux, E.; Follin, J.-M.; Durand, S.; Van Baelen, J.
Global validity and behaviour of tropospheric gradients estimated by GPS
27th IUGG General Assembly, Montreal, Canada, 8-18 July 2019

111. Mueller, D.; Fleck, B.; Nicula, B.; Verstringe, F.; Bourgoignie, B.; Berghmans, D.; Felix, S.; Csillaghy, A.; Ireland, J.; Osuna, P.; Jiggens, P.
3D Visualisation of Solar Data: Preparing for Solar Orbiter and Parker Solar Probe
Workshop FReSWeD 2019 Towards Future Research on Space Weather Drivers, San Juan, Argentina, 2-7 July 2019 (poster)

112. Nicula, B.; Verstringe, F.; Bourgoignie, B.; Berghmans, D.
jHelioviewer for Solar Orbiter
SPICE consortium meeting, MPS Göttingen, Germany, 15 May 2019 (invited talk)

113. Nicula, B.; Rodriguez, L.
Jhelioviewer News
Solar Orbiter Modelling and Data Analysis Working Group (MADAWG), Madrid, Spain, 23 January 2019 (invited talk)

114. Palmerio, E.; Witasse, O.; Nieves-Chinchilla, T.; Barnes, D.; Mierla, M.; Weiss, A.; Moestl, C.; Zhukov, A.N.; Jian, L.; Sanchez-Cano, B.; Rodriguez, L.; Guo, J.; Roussos, E.; Masters, A.; Provan, G.; Isavnin, A.; Lowrance, P.; Turc, L.; Kilpua, E.
Following the evolution of coronal mass ejections across the heliosphere
AGU Fall Meeting, San Francisco, California, USA, 9-13 December 2019

115. Palmerio, E.; Scolini, C.; Barnes, D.; Magdalenic, J.; West, M.; Zhukov, A.N.; Rodriguez, L.; Mierla, M.; Good, S.; Morosan, D.; Kilpua, E.; Pomoell, J.; Poedts, S.
Multipoint study of successive CMEs driving moderate disturbances at 1 AU
EGU General Assembly 2019, Vienna, Austria, 7-12 April 2019

116. Pinat, E.; Bergeot, N.; Chevalier, J.-M.
Introduction to GNSS and its geophysical applications
Workshop: Interhemispheric Comparison of the Ionosphere-Plasmasphere System, SANSA, Hermanus, South Africa, 19-21 November 2019

117. Pinat, E.; Bergeot, N.; Defraigne, P.; Chevalier, J.-M.
Seasonal variation of snow height in East Antarctica using GNSS Interferometric Reflectrometry
7th international colloquium on scientific and fundamental aspects of GNSS, Zurich, Switzerland, 4-6 September 2019

118. Podladchikova, O.; Marqué, C.; Podladchikova, T.; Veronig, A.; Stegen, K.
Comparison of Different Approaches for the Real Time Forecast of the F10.7 index at the Space Weather Forecasting Centres
EGU General Assembly 2019, Vienna, Austria, 7-12 April 2019

119. Podladchikova, O.; Vourlidas, A.; Mierla, M.; West, M.; D'Huys, E.; Stegen, K.; O'Hara, J.; Wauters, L.
Automated EUV Wave Catalogue For Solar Cycle 23 And 24: EUV Global Wave Rotation Sense Follows Hale Magnetic Cycle
CESPM 2019, Hvar, Croatia, 6-10 May 2019

120. Podladchikova, T.; Veronig, A.; Podladchikova, O.; Dissauer, K.; Vršnak, B.; Saqri, J.; Piantschitsch, I.; Temmer, M.
Multiple EUV wave reflection from a coronal hole
EGU General Assembly 2019, Vienna, Austria, 7-12 April 2019

121. Podladchikova, T.; Veronig, A.; Podladchikova, O.; Dissauer, K.; Vršnak, B.; Saqri, J.; Piantschitsch, I.; Temmer, M.
Multiple EUV wave reflection from a coronal hole
ESWW16, Liège, Belgium, 18-22 November 2019 (poster)

122. Podladchikova, T.; Podladchikova, O.; Veronig, A.
Development of adaptive Kalman filter for short-term forecasts of the F30 and F10.7 cm radio flux
ESWW16, Liège, Belgium, 18-22 November 2019

123. Pottiaux, E.; Bruyninx, C.; Fabian, A.; Legrand, J.; Miglio, A.; Pacione, R.; Kenyeres, A.
Pan-European GNSS CORS Infrastructures: Complementarity and Mutual Benefits
E-GVAP Joint Expert Team Meeting 2019, 28-29 November 2019, Offenbach, Germany

124. Pottiaux, E.; Bruyninx, C.
ROB's Analysis Centre: Contribution to E-GVAP
E-GVAP Joint Expert Team Meeting 2019, 28-29 November 2019, Offenbach, Germany

125. Pottiaux, E.; Van Malderen, R.; Klos, A.; Alshawaf, F.; Bock, O.; Bogusz, J.; Chimani, B.; Domonkos, P.; Elias, M.; Guijarro, J.A.; Ning, T.; Tornatore, V.; Zengin Kazanci, S.
Towards the Homogenization of GNSS Tropospheric Delay Time Series: Status and Recent Developments
EGU General Assembly 2019, Vienna, Austria, 7-12 April 2019

126. Poyraz, D.; Van Malderen, R.; De Backer, H.; De Muer, D.; Delcloo, A.; Verstraeten, W.; Mangold, A.; De Bock, V.; Laffineur, Q.
50 years of balloon borne ozone profile measurements at Uccle, Belgium
EGU General Assembly 2019, Vienna, Austria, 7-12 April 2019 (poster)

127. Ranvier, S.; Anciaux, M.; De Keyser, j.; Lebreton, J.P.
SLP, the Sweeping Langmuir Probe instrument
Workshop on Instruments for ESA Distributed Space Weather Sensor System (D3S), Darmstadt, Germany, 23-24 October 2019

128. Ranvier, S.; Anciaux, M.; De Keyser, J.; Pieroux, D.; Baker, N.; Lebreton, J.P.
SLP: The Sweeping Langmuir Probe Instrument to Monitor the Upper Ionosphere on Board the PICASSO Nano-Satellite
70th International Astronautical Congress (IAC), Washington D.C., USA, 21-25 October 2019

129. Ranvier, S.; Anciaux, M.; De Keyser, J.; Cipriani, F.; Lebreton, J.P.
Monitoring of the Upper Ionosphere with SLP on Board PICASSO
Grenoble NewSpace Week, Grenoble, France, 14-17 May 2019

130. Ranvier, S.; Hess, S.; Matéo Vélez, J.C.; Rodríguez Gómez, J.; Alvaro Sanchez, A.; De Keyser, J.
Dust Study, Transport and Electrostatic Removal for Exploration Missions: the DUSTER Project
7th European Lunar Symposium, Manchester, UK, 21-23 May 2019 (poster)

131. Rochus, P.; Auchère, F.; Berghmans, D.; Harra, L.; Schmutz, W.; Schühle, U.
The Solar Orbiter EUI instrument: The Extreme Ultraviolet Imager
AGU Fall Meeting, San Francisco, California, USA, 9-13 December 2019 (poster)

132. Rodriguez, L.
Validation of EUHFORIA and K_p, Dst models in VSWMC
Virtual Space Weather Modelling Center Final Review Meeting, ESTEC (online), 18 February 2019 (invited talk)

133. Rodriguez, L.
Validation for EUHFORIA 2.0
EUHFORIA 2.0 Kick Off Meeting, Leuven (KUL), Belgium, 19 December 2019 (invited talk)

134. Rodriguez, L.; Scolini, C.
Meteorología espacial: observaciones, modelos y su predicción
61st annual meeting of the Argentinian Association of Astronomy, Viedma, Argentina, 17 September 2019 (invited talk)

135. Rupiewicz, J.; and the Tech-TIDE consortium (including Verhulst, T. and Stankov, S.)
TechTIDE project: how technology can support space weather applications
2nd TREASURE Workshop, Toulouse, France, 21-22 May 2019

136. Ryan, A.; Gallagher, P.; Carley, E.; Morosan, D.; Brentjens, M.; Zucca, P.; Fallows, R.; Vocks, V.; Mann, G.; Breitling, F.; Magdalenic, J.; Kerdraon, A.; Reid, H.
Imaging the Solar Corona during the 2015 March 20 Eclipse using LOFAR
CESRA 2019, Potsdam, Germany, 8-12 July 2019

137. Samara, E.; Magdalenic, J.; Rodriguez, L.; Poedts, S.; Heinemann, S.; Hinterreiter, J.
Developing fast solar wind modeling with EUHFORIA
ESWW16, Liège, Belgium, 18-22 November 2019

138. Samara, E.; Magdalenic, J.; Rodriguez, L.; Hinterreiter, J.; Poedts, S.
Statistical analysis of coronal hole properties during 2018 within the frame of fast solar wind modeling with EUHFORIA
CESPM 2019, Hvar, Croatia, 6-10 May 2019 (poster)

139. Samara, E.; Magdalenic, J.; Rodriguez, L.; Heinemann, S.; Poedts, S.
Developing fast solar wind modeling with EUHFORIA
SHINE 2019, Boulder, Colorado, USA, 4-9 August 2019 (poster)

140. Samara, E.; Magdalenic, J.; Rodriguez, L.; Heinemann, S.; Poedts, S.
Developing fast solar wind with EUHFORIA
AGU Fall Meeting, San Francisco, California, USA, 9-13 December 2019 (poster)

141. Sapundjiev, D.; Stankov, S.
Refurbishing the 9-NM-64 neutron monitor at Dourbes, Belgium
NMDB meeting, Athens, Greece, 5-7 March 2019

142. Scolini, C.
Constraining 3D MHD models via remote-sensing and in-situ measurements: the heliosphere
SHINE 2019, Boulder, Colorado, USA, 4-9 August 2019 (invited talk)

143. Scolini, C.; Rodriguez, L.; Temmer, M.; Guo, J.; Dumbovic, M.; Kilpua, E.K.J.; Veronig, A.; Palmerio, E.; Pomoell, J.; Poedts, S.
Investigating the evolution and interactions of the September 2017 CME events with EUHFORIA
SHINE 2019, Boulder, Colorado, USA, 4-9 August 2019 (poster)

144. Scolini, C.; Poedts, S.; Rodriguez, l.; Temmer, M.; Dumbovic, M.; Guo, J.; Veronig, A.; Dissauer, K.; Palmerio, E.; Kilpua, E.; Pomoell, J.
A study of the role of CME-CME interactions on CME geo-effectiveness with EUHFORIA
AGU Fall Meeting, San Francisco, California, USA, 9-13 December 2019 (poster)

145. Scolini, C.; Temmer, M.; Guo, J.; Dumbovic, M.; Kilpua, E.K.J.; Pomoell, J.; Chane, E.; Rodriguez, L.; Poedts, S.
Investigating the evolution and interactions of the September 2017 CMEs with EUHFORIA
CESPM 2019, Hvar, Croatia, 6-10 May 2019 (poster)

146. Scolini, C.; Chane, E.; Temmer, M.; Kilpua, E.K.J.; Dissauer, K.; Veronig, A.; Palmerio, E.; Pomoell, J.; Dumbovic, M.; Guo, J.; Rodriguez, L.; Poedts, S.
Investigating the evolution and interactions of the September 2017 CMEs with EUHFORIA
ESWW16, Liège, Belgium, 18-22 November 2019 (poster)

147. Scolini, C.; Chane, E.; Temmer, M.; Kilpua, E.K.J.; Dissauer, K.; Veronig, A.; Palmerio, E.; Pomoell, J.; Dumbovic, M.; Guo, J.; Rodriguez, L.; Poedts, S.
Investigating the evolution and interactions of the September 2017 CMEs with EUHFORIA
AGU Fall Meeting, San Francisco, California, USA, 9-13 December 2019 (poster)

148. Scolini, C.; Rodriguez, L.; Temmer, M.; Guo, J.; Dumbovic, M.; Pomoell, J.; Chane, E.; Poedts, S.
Investigating the evolution and interactions of the September 2017 CMEs with EUHORIA
EGU General Assembly 2019, Vienna, Austria, 7-12 April 2019

149. Scolini, C.; Dasso, S.; Rodriguez, L.; Zhukov, A.N.; Poedts, S.
Characterising the radial evolution of the solar wind and Coronal Mass Ejections using EUHFORIA
ESWW16, Liège, Belgium, 18-22 November 2019

150. Seaton, D.; Alzate, N.; Berghmans, D.; Caspi, A.; D'Huys, E.; Golub, L.; Hurlburt, N.; Mason, J.; Rachmeler, L.; Savage, S.; Tadikonda, S.; West, M.
The Present and Future of EUV Observations of the Corona on Large Scales
L5 Consortium Meeting, Palo Alto, California, USA, 1-3 October 2019 (invited talk)

151. Shestov, S.; Van Doorsselaere, T.; Zhukov, A.N.
Simulation of dynamics of hot plasma in postflare loops
9th Coronal Loop Workshop, St. Andrews, UK, 11-14 June 2019 (poster)

152. Shestov, S.; Zhukov, A.N.
Scattered light in ASPIICS: comparison of various approaches
PROBA-3 Science Working Team Meeting 8, Göttingen, Germany, 25-26 September 2019

153. Shestov, S.; Zhukov, A.N.
Discussion of the ASPIICS calibration
PROBA-3 Science Working Team Meeting 8, Göttingen, Germany, 25-26 September 2019

154. Shestov, S.
Calibration accuracy of Proba-3/ASPIICS white-light coronagraph
Degradation and Inter-calibration of EUV instruments (Solar EUV Irradiance Workshop), Uccle (BISA), Brussels, 14-18 October 2019

155. Shestov, S.; Voitenko, Y.; Zhukov, A.N.
Initiation of Alfvénic turbulence by Alfvén wave collisions: a numerical study
5th UK-Ukraine-Spain Meeting on solar physics and space science, Kyiv, Ukraine, 26-30 August 2019

156. Shestov, S.; Voitenko, Y.; Zhukov, A.N.
Do Alfvén-Wave Collisions Generate the Critically Balanced Turbulence?
5th UK-Ukraine-Spain Meeting on solar physics and space science, Kyiv, Ukraine, 26-30 August 2019

157. Smit, H.G.J.; Van Malderen, R.; Hendrick, F.; Piters, A.; Wang, Y.; Thouret, V.; Godin-Beekmann, S.; Skrivankova, P.; Franke, P.; Costa, M.J.; Kostadinov, I.; Belegante, L.; Vigouroux, C.; Van Roozendael, M.; Veefkind, P.; Eskes, H.; Wagner, T.; Tarasick, D.; Stauffer, R.; Querel, R.
HELSTOP: A Project Design for the Harmonization and Evaluation of Lower Stratospheric and Tropospheric Ozone Vertical Profiles
EGU General Assembly 2019, Vienna, Austria, 7-12 April 2019 (poster)

158. Talpeanu, D.-C.; Poedts, S.; D'Huys, E.; Roussev, I.; Mierla, M.; Hosteaux, S.
Numerical Simulations of Shear-Induced Consecutive Coronal Mass Ejections
ESWW16, Liège, Belgium, 18-22 November 2019 (poster)

159. Talpeanu, D.-C.; Chané, E.; Poedts, S.; D'Huys, E.; Hosteaux, S.; Mierla, M.; Roussev, I.
Numerical Modelling of Stealth Solar Eruptions and Comparison with In-Situ Signatures
CESPM 2019, Hvar, Croatia, 6-10 May 2019 (poster)

160. Talpeanu, D.-C.; Chané, E.; Poedts, S.; D'Huys, E.; Hosteaux, S.; Mierla, M.; Roussev, I.
Numerical Simulations of Stealth CMEs: How Are They Different From "Usual" CMEs?

AOGS 16th Annual Meeting, Singapore, 28 July - 2 August 2019 (poster)

161. Talpeanu, D.-C.; Chané, E.; Poedts, S.; D'Huys, E.; Hosteaux, S.; Mierla, M.; Roussev, I.
Stealth CME Initiation and In-Situ Signatures: What Can We Learn from Modelling?
Workshop FReSWeD 2019 Towards Future Research on Space Weather Drivers, San Juan, Argentina, 2-7 July 2019

162. Talpeanu, D.-C.; Chané, E.; Poedts, S.; D'Huys, E.; Hosteaux, S.; Mierla, M.; Roussev, I.
Initiation of Stealth CMEs: Clues from Numerical Modelling and In-Situ Comparisons
EGU General Assembly 2019, Vienna, Austria, 7-12 April 2019 (poster)

163. Taktakishvili, A.; Mays, M.L.; Andries, J.; Bingham, S.; Dierckxsens, M.; Jones, J.T.; Kuznetsova, M.M.; Marsh, M.S.; Murray, S.A.; Mullinix, R.; Owens, M.J.; Riley, P.; Semones, E.; Wiegand, C.
Community-wide Space Weather Scoreboards: Facilitating the Validation of Real-time CME, Flare, and SEP Forecasts
AGU Fall Meeting, San Francisco, California, USA, 9-13 December 2019 (poster)

164. Van Laeken, L.
Development of experimental benches doe Radiometric Characterization, Application to Space Instrument MAJIS VIS-NIR on JUICE
Master Thesis, Liège, Belgium, 9 September 2019

165. Van Malderen, R.; Pottiaux, E.; Bock, O.; Klos, A.; Pacione, R.
Using GNSS ZTD retrievals for Climate
7th international colloquium on scientific and fundamental aspects of GNSS, Zurich, Switzerland, 4-6 September 2019 (invited talk)

166. Van Malderen, R.; Pottiaux, E.; Stankunavicius, G.; Beirle, S.; Wagner, T.; Brenot, H.; Bruyninx, C.
Interpreting the time variability of integrated water vapour retrievals using local meteorological data and teleconnection indices
EGU General Assembly 2019, Vienna, Austria, 7-12 April 2019 (poster)

167. Van Lil E., Van Malderen R.
A statistical study of atmospheric circumstances on microwave links
IRACON 11th Technical Meeting, Gdansk, Poland, 4-6 September 2019 (talk and paper)

168. Vansintjan, R.; De Patoul, J.; Andries, J.; Chabanski, S.; Calogera, A.; De Donder, E.; Glover, A.
Provision of space weather bulletins in support to Spacecraft Operations
ESWW16, Liège, Belgium, 18-22 November 2019 (poster)

169. Verbeeck, C.; Kraaikamp, E.; Ryan, D.F.; Podladchikova, O.
Solar flare parameters: evidence for lognormal rather than power law distributions
ESWW16, Liège, Belgium, 18-22 November 2019 (poster)

170. Verbeeck, C.
Finetuning the Near Earth Commissioning Phase plan
24th EUI Consortium Meeting, Brussels (ROB), Belgium, 17 September 2019

171. Verbeeck, C.
EUI observing programs
23rd EUI Consortium Meeting, Paris (IAS), France, 29 January 2019

172. Verbeeck, C.; Lamy, H.; Calders, S.; Martínez Picar, A.; Calegaro, A.
BRAMS forward scatter observations of major meteor showers in 2016-2019
International Meteor Conference 2019, Bollmannsruh, Germany, 3-6 October 2019

173. Verhulst, T.; Blanch, E.; and the Tech-TIDE consortium
Tech-TIDE project: Techniques for detecting TIDs
ESWW16, Liège, Belgium, 18-22 November 2019

174. Verhulst, T.; Blanch, E.; and the Tech-TIDE consortium
Tech-TIDE project: TID warning system
ESWW16, Liège, Belgium, 18-22 November 2019

175. Verhulst, T.
Science and engineering of sensing TIDs with Digisonde
XV International GIRO Forum, Lowell, Massachusetts, USA, 21-24 May 2019

176. Voitenko, Y.; Gogoberidze, G.; De Keyser, J.; Machabeli, G.
Multi-Scale Turbulence and Turbulent Spectra in the Solar Wind
5th UK-Ukraine-Spain Meeting on solar physics and space science, Kyiv, Ukraine, 26-30 August 2019

177. Wauters, L.; Dominique, M.; Dammash, I.E.; Meftah, M.
Evolution of periodicities with solar cycle for long-term solar time series
ESWW16, Liège, Belgium, 18-22 November 2019 (poster)

178. West, M.; Seaton, D.; Davies, J.; Kintziger, C.; Rodriguez, L.; Mierla, M.; Scolini, C.; Haberreiter, M.; D'Huys, E.
EUV Observations of the Middle Corona From the L5 Perspective
AGU Fall Meeting, San Francisco, California, USA, 9-13 December 2019 (poster)

179. West, M.; Seaton, D.; O'Hara, J.; Mierla, M.; Podladchikova, O.; D'Huys, E.
Unique SWAP Observations of the Middle Corona
SHINE 2019, Boulder, Colorado, USA, 4-9 August 2019 (poster)

180. West, M.; Seaton, D.
Session 1: Exploring the Middle Corona - Deface this Poster
SHINE 2019, Boulder, Colorado, USA, 4-9 August 2019 (poster)

181. West, M.
Proba-2 Guest Investigators, Summary of Scientific Activities
PROBA-2 Symposium: 9 Years of Proba-2 Operations, Redu, Belgium, 7-8 February 2019 (invited talk)

182. West, M.
Proba-2 as a Pathfinder to the SSA Lagrange Mission
PROBA-2 Symposium: 9 Years of Proba-2 Operations, Redu, Belgium, 7-8 February 2019 (invited talk)

183. West, M.; Golub, L.; Savage, S.
Improving Space Weather Forecasting With EUV Spectroscopic Imaging
Preparing for When the Sun Wakes Up: Workshop on Deep-Space Sun-Earth L5/L1 Space-Weather Missions, London, UK, 27-28 June 2019

184. West, M.; Berghmans, D.; Andries, J.
ESA Solar Expert Service Centre
Preparing for When the Sun Wakes Up: Workshop on Deep-Space Sun-Earth L5/L1 Space-Weather Missions, London, UK, 27-28 June 2019

185. West, M.; Kintziger, C.; Haberreiter, M.
LGRRS-II-EUVI Instrument
Preparing for When the Sun Wakes Up: Workshop on Deep-Space Sun-Earth L5/L1 Space-Weather Missions, London, UK, 27-28 June 2019

186. West, M.; Kintziger, C.; Gyo, M.; Haberreiter, M.; Berghmans, D.; Pfiffner, D.; Koller, S.; Gissot, S.
The EUV Imager on Lagrange
ESWW16, Liège, Belgium, 18-22 November 2019

187. Wilken, V.; Kriegel, M.; Berdermann, J.; Cesaroni, C.; Spogli, L.; Romano, V.; Bergeot, N.; Chevalier, J.-M.; Stanislawska, I.; Tomasik, L.; van den Oord, B.
PECASUS - GNSS Service Domain
AGU Fall Meeting, San Francisco, California, USA, 9-13 December 2019 (poster)

188. Zychova, L.; Dierckxsens, M.; Crosby, N.; Perry, C.; Glover, A.
ESA SSA Space Radiation Expert Service Centre: Spacecraft Operation Domain
ESWW16, Liège, Belgium, 18-22 November 2019 (poster)

Public Outreach: Talks and publications for the general public

1. Bergeot, N.
Inter-comparison between the Earth and Mars Ionospheres
SANSA, South-Africa, 2019

2. Bergeot, N.
Volcanoes: where, how, when?
Clès pour l'Univers ASBL, La Porte Bleue, Auderghem, 2019

3. Bergeot, N.
STCE Research & services in support of PECASUS: GNSS
STCE Annual Meeting, Uccle, 6 June 2019 (invited talk)

4. Berghmans, D.
Space Weather: the biggest natural risk in the solar system
Zitting KSB - KBIRA - KMI, Uccle, Belgium, 6 May 2019 (invited talk)

5. Berghmans, D.; De Donder, E.; Andries, J.
The PECASUS constellation
STCE Annual Meeting, Uccle, 6 June 2019 (invited talk)

6. Calders, S.
Radio Meteor Zoo: current status & future plans
BRAMS annual meeting, Genk, 9 March 2019

7. Calders, S.
The Radio Meteor Zoo: identifying meteor echoes using artificial intelligence
BRAMS annual meeting, Grimbergen, 2 November 2019

8. Calders, S.
BRAMS observations of major meteor showers in 2018-2019
BRAMS annual meeting, Grimbergen, 2 November 2019

9. Calders, S.
BRAMS & de Radio Meteor Zoo
Lemon, Kontich, 15 November 2019

10. Calders, S.; Lamy, H.; Martinez Picar, A.; Verbeeck, C.; Anciaux, M.; Ranvier, S.
Towards an autonomous BRAMS network
Proceedings of IMC2018, Pezinok, Slovakia, 30 August - 2 September 2018, 2019

11. Chevalier, J.-M.
GNSS Expert Centre
SWIC, Uccle, 13 March 2019

12. Chevalier, J.-M.
GNSS Expert Centre
SWIC, Uccle, 29 October 2019

13. Chevalier, J.-M.
GNSS Expert Centre
SWIC, Uccle, 10 December 2019

14. Cisneros, M.; Bolsée, D.
Presentation of the MAJIS project at BIRA-IASB
Asgard - Scientific balloons for space education, Space Pole, 25 April 2019

15. Cisneros, M.; Bolsée, D.
Presentation of the MAJIS project at BIRA-IASB
Visit students from the University of Twente, Uccle, 9 July 2019

16. Cisneros, M.; Bolsée, D.
The MAJIS project and the development of the VIS-NIR facility
The Moon, between Dream and Reality, Exhibition at the Royal Palace, Brussels, 23 July-25 August 2019

17. Clette, F.
L'activité solaire à long-terme: Une surveillance continue!
Astronomy Day, Uccle (ROB), 21 September 2019

18. Decraemer, B.
Op ontdekkingsreis naar onze ster
Astronomy Day, Uccle (ROB), 21 September 2019

19. De Donder, E.
Space Particle Radiation and Effects
SWIC, Uccle, 13 March 2019

20. De Donder, E.
Cosmic Rays and Space Weather Services for Aviation
STCE Cosmic Rays workshop, BIRA-IASB, 23 April 2019

21. De Donder, E.
Space Weather services
Visit students from University of Twente, SSCC room, Uccle, 9 July 2019

22. De Donder, E.; Dierckxsens, M.
Effective dose
Training for PECASUS Operators - MeteoWing, Uccle, 22 October 2019

23. De Donder, E.
Radiation Expert Centre
SWIC, Uccle, 29 October 2019

24. Dierckxsens, M.
Oorzaak en gevolgen van energetische zonnedeeltjes
Volkssterrenwacht Armand Pien, Gent, 28 September 2019

25. Dierckxsens, M.
PECASUS - a Pan-European Consortium for Aviation Space Weather User Services
EURAVIA visit to BIRA-IASB, Uccle, 23 October 2019

26. Dierckxsens, M.; De Donder, E.
Radiation Expert Centre
SWIC, Uccle, 10 December 2019

27. Dolla, L.
Preparation de nouvelles missions spatiales
Stage d'observation pour étudiants du secondaire, Uccle, 1 March 2019

28. Dolla, L.
Préparation de nouvelles missions spatiales
Stage d'observation pour étudiants du secondaire, Uccle, 1 April 2019

29. Dominique, M.
Observatoire Royal de Belgique - Département 4: Physique solaire
Stage d'observation pour étudiants du secondaire, Uccle, 29 February 2019

30. Dominique, M.
Using cubesats for investigating the possible effects of long-term solar variability over the climate
Belgian Cubesat Industry Day, Brussels, 20 May 2019

31. Dominique, M.
L'Observatoire et l'étude du soleil: un voyage dans le temps et l'espace
Astronomy Day, Uccle (ROB), 21 September 2019

32. Janssens, J.; Marqué, C.
Sensors
SWIC, Uccle, 12-14 March 2019

33. Janssens, J.
Drivers of space weather
SWIC, Uccle, 12-14 March 2019

34. Janssens, J.
Earth environment - Magnetosphere
SWIC, Uccle, 12-14 March 2019

35. Janssens, J.
Earth environment - Ionosphere
SWIC, Uccle, 12-14 March 2019

36. Janssens, J.
Space weather impacts on the earth environment
SWIC, Uccle, 12-14 March 2019

37. Janssens, J.
SIDC/RWC and URSIgram + exercises
SWIC, Uccle, 12-14 March 2019

38. Janssens, J.; Bourgoignie, B.; Lemaitre, O.; Vanlommel, P.
Knowledge and Situations Quiz
SWIC, Uccle, 12-14 March 2019

39. Janssens, J.; Marqué, C.
Sensors
SWIC, Uccle, 28-30 October 2019

40. Janssens, J.
Drivers of space weather
SWIC, Uccle, 28-30 October 2019

41. Janssens, J.
Earth environment - Magnetosphere
SWIC, Uccle, 28-30 October 2019

42. Janssens, J.
Earth environment - Ionosphere
SWIC, Uccle, 28-30 October 2019

43. Janssens, J.
Space weather impacts on the earth environment
SWIC, Uccle, 28-30 October 2019

44. Janssens, J.
SIDC/RWC and URSIgram + exercises
SWIC, Uccle, 28-30 October 2019

45. Janssens, J.; Bourgoignie, B.; Lemaitre, O.; Vanlommel, P.
Knowledge and Situations Quiz
SWIC, Uccle, 28-30 October 2019

46. Janssens, J.; Marqué, C.
Sensors
SWIC, Uccle, 9-11 December 2019

47. Janssens, J.
Drivers of space weather
SWIC, Uccle, 9-11 December 2019

48. Janssens, J.
Earth environment - Magnetosphere
SWIC, Uccle, 9-11 December 2019

49. Janssens, J.
Earth environment - Ionosphere
SWIC, Uccle, 9-11 December 2019

50. Janssens, J.
Space weather impacts on the earth environment
SWIC, Uccle, 9-11 December 2019

51. Janssens, J.
SIDC/RWC and URSIgram + exercises
SWIC, Uccle, 9-11 December 2019

52. Janssens, J.; Bourgoignie, B.; Lemaître, O.; Vanlommel, P.
Knowledge and Situations Quiz
SWIC, Uccle, 9-11 December 2019

53. Janssens, J.
An introduction to space weather
Visit NATO, Uccle, 10 January 2019

54. Janssens, J.
An introduction to space weather
Tractebel Visit, Uccle, 26 April 2019

55. Janssens, J.
De kunst van het zonnewaarnemen
MIRA Public Observatory, Grimbergen, 5 June 2019

56. Janssens, J.
Space Weather Training Course
TRACTEBEL Training, Uccle, 21 October 2019

57. Janssens, J.
Een nieuwe bril voor een nieuwe zonnecyclus
MIRA Public Observatory, Grimbergen, 27 December 2019

58. Marqué, C.; Martínez Picar, A.
Radio-astronomy & Space Weather
SWIC, Uccle, 13 March 2019

59. Marqué, C.; Martínez Picar, A.
Solar radio observations
SWIC, Uccle, 29 October 2019

60. Marqué, C.; Martínez Picar, A.
Solar radio observations
SWIC, Uccle, 10 December 2019

61. Marqué, C.
Radio communication
PECASUS training, 11 October 2019

62. Martínez Picar, A.; Marqué, C.
Radio Astronomy & Space Weather
STCE Annual Meeting, Uccle, 6 June 2019

63. Martınez Picar, A.; Marqué, C.
Using SPADE for radio meteor observations - status update
Proceedings of IMC2018, Pezinok, Slovakia, 30 August - 2 September 2018, 2019

64. O'Hara, J., Andries, J., De Patoul, J.
RWC and SSCC
SWIC, Uccle, 12 March 2019

65. O'Hara, J., Andries, J., De Patoul, J.
RWC and SSCC
SWIC, Uccle, 28 October 2019

66. O'Hara, J., Andries, J., De Patoul, J.
RWC and SSCC
SWIC, Uccle, 9 December 2019

67. Rodriguez, L.
Solar weather, K_p, solar x-rays
Training for PECASUS Operators - MeteoWing, Uccle, 22 October 2019

68. Sapundjiev, D.
Development of the Cosmic Rays Space Weather Observatory in Dourbes
STCE Cosmic Rays workshop, BIRA-IASB, 23 April 2019

69. Sapundjiev, D.
STCE Research & services in support of PECASUS: Dourbes neutron monitor network
STCE Annual Meeting, Uccle, 6 June 2019 (invited talk)

70. Vanlommel, P.; Janssens, J.
STCE Newsletters
Weekly newsletter, https://www.stce.be/ , 2019

71. Vanlommel, P.
Space Weather Drivers
Training for PECASUS Operators - MeteoWing, Uccle, 22 October 2019

72. Vanlommel, P.; Berghmans, D.
Structures and Tasks
Training for PECASUS Operators - MeteoWing, Uccle, 22 October 2019

73. Vanlommel, P.
Storm parameters - thresholds
Training for PECASUS Operators - MeteoWing, Uccle, 5 November 2019

74. Vanlommel, P.
Drivers of Space Weather
Training for PECASUS Operators - MeteoWing, Uccle, 5 November 2019

75. Vanlommel, P.
Het noorderlicht, hoe zit het nu echt?
Asgard - Scientific balloons for space education, Space Pole, Uccle, 25 April 2019

76. Vanlommel, P.
De Zon
Summer School VVS, Leuven, 26 August 2019

77. Vanlommel, P.
Zon, satellieten en vliegtuigen
Urania, Hove, 19 October 2019

78. Vanlommel, P.
PECASUS - wanneer is de zon een gevaar voor vliegtuigen?
Elcker-Ik, Antwerpen, 5 December 2019

79. Vanlommel, P.
Introduction to space weather
SWIC, Uccle, 9-11 December 2019

80. Vanlommel, P.
Introduction to space weather
SWIC, Uccle, 28-30 October 2019

81. Vanlommel, P.
Introduction to space weather
SWIC, Uccle, 12-14 March 2019

82. Vanlommel, P.
Ursigram Exercise
SWIC, Uccle, 12-14 March 2019

83. Vanlommel, P.
Ursigram Exercise
SWIC, Uccle, 28-30 October 2019

84. Vanlommel, P.
Ursigram Exercise
SWIC, Uccle, 9-11 December 2019

85. Verbeeck, C.; Lamy, H.; Calders, S.; Tétard, C.; Martínez Picar, A.
BRAMS radio observations: activity of some recent major meteor showers
Proceedings of IMC2018, Pezinok, Slovakia, 30 August - 2 September 2018, 2019

86. Verbeeck, C.
Solar Orbiter launch in 2020: studying the Sun from closer than ever
Astronomy Day, Uccle (Planetarium), 21 September 2019

87. Verbeeck, C.
Ruimteweer: de impact van zonnestormen op aarde
Astronomy Day, Uccle (ROB), 21 September 2019

88. West, M.
A decade probing the Sun
ESA webpage, 2019

89. West, M.
Ten Suns for 10 years
ESA webpage, 2019

90. West, M.
Voici la première image du pole nord du soleil
Science & Vie, 2019

91. West, M.
The Sun in 2018
ESA Space In Images, 2019

92. Zychova, L.
Space Weather - how does it influence life on Earth
Trebic observatory, Trebic, the Czech Republic, 18 January 2019

93. Zychova, L.
Exploring the universe
Czech Embassy in Belgium (children workshop), Brussels, 24 March 2019

94. Zychova, L.
Space Weather - how does it influence life on Earth
Brno observatory, Brno, the Czech Republic, 9 May 2019

95. Zychova, L.
Space Weather - how does it influence life on Earth
Jihlava observatory, Jihlava, the Czech Republic, 10 May 2019

96. Zychova, L.
Space Weather - how does it influence life on Earth
Jicin observatory, Jicin, the Czech Republic, 3 November 2019

97. Zychova, L.
Space workshop - Julie goes to space
Czech Embassy in Belgium (children workshop), Brussels, 1 December 2019

List of abbreviations

~	About, proportional to
1D	One dimensional
2D	Two dimensional
3D	Three dimensional
Å	Ångstrom (0.1 nm)
A	Article
AAS	American Astronomical Society
ABL	Atmospheric Boundary Layer
ACE	Advanced Composition Explorer
ACFJ	Australia, Canada, France and Japan consortium
ADA	Astronomical Data Analysis
AFFECTS	Advanced Forecast For Ensuring Communications Through Space
AGU	American Geophysical Union
AIA	Atmospheric Imaging Assembly (SDO)
ALC	Automatic LIDAR Ceilometer
ALF	faint narrow-band radio bursts from sources propagating with velocities close to the local Alfvén velocity
AOGS	Asia Oceania Geosciences Society
AP-RASC	Asia-Pacific Radio Science Conference
APS	American Physical Society
AR	Active Region
ARCAS	Augmented Resolution Callisto Spectrometer
ASGARD	An educational space programme for schools (no acronym)
ASEC	Applied Space Environments Conference
ASOPOS	Assessment of Standard Operating Procedures for OzoneSondes
ASPIICS	Association of Spacecraft for Polarimetric and Imaging Investigation of the Corona of the Sun (PROBA-3)
AT-RASC	Atlantic Radio Science meeting
AU, au	Astronomical Unit; about 150 million km
B_0	Heliographic latitude of the central point of the solar disk (The range of B_0 is $\pm$7.23°)
BE	Belgium
BELSPO	Belgian Science Policy Office
BeNELux	Belgium, The Netherlands, and Luxembourg
BIRA	Koninklijk Belgisch Instituut voor Ruimte-Aëronomie
BISA	Royal Belgian Institute for Space Aeronomy
BRAIN-be	Belgian Research Action through Interdisciplinary Networks (BELSPO)
BRAMS	Belgian RAdio Meteor Stations
BUKS	Belgium, UK, and Spain
B.USOC	Belgian User Support and Operation Centre
Bz	Component of the IMF perpendicular to the ecliptic ("north-south" component)
C	Capacitor
C-class flare	Common x-ray flare
C/N_0	Carrier-to-Noise density
CA	COST Action (COST)
Ca II H	A blue line in the solar spectrum at 396.85 nm
Ca II K	A blue line in the solar spectrum at 393.37 nm
CACTus	Computer Aided CME Tracking software
CALLISTO	Compound Astronomical Low frequency Low-cost Instrument for Spectroscopy and Transportable Observatory
CAMS	Copernicus Atmosphere Monitoring Service
CCMC	Community Coordinated Modeling Center
CCSOM	Constraining CMEs and Shocks by Observations and Modelling
CESPM	China-Europe Solar Physics Meeting
CESRA	Community of European Solar Radio Astronomers
CH	Coronal Hole
CHARM	Contemporary physical challenges in Heliospheric and AstRophysical Models

CIR	Co-rotating Interaction Region
Cluster	ESA/NASA mission to study the Earth's magnetosphere (no acronym)
cm	centimeter
CME	Coronal Mass Ejection
CMOS	Complementary Metal-Oxide-Semiconductor
CNES	Centre national d'études spatiales (France)
CNRS	Centre national de la recherche scientifique (France)
CO_2	Carbon Dioxide
COMESEP	COronal Mass Ejections and Solar Energetic Particles
COPUOS	COmmittee on the Peaceful Uses of Outer Space (UN)
COR (1/2)	Coronagraph (Inner/Outer) onboard STEREO
CORS	Continuously Operating Reference Stations (GNSS)
COSPAR	COmmittee on SPAce Research
COST	(European) COoperation in Science & Technology
COTS	Commercial off-the-shelf
CR	Carrington Rotation
CSL	Centre Spatial de Liège
CubeSat	A small satellite measuring 10cm x 10cm x 10cm
Δ	Delta (difference)
D/SCI	ESA Science Directorate
D/TEC	ESA Technology, Engineering and Quality Directorate
D2D	Digisonde-to-Digisonde
D3S	Distributed Space weather Sensor System
dB-Hz	decibel-Hertz (bandwidth relative to 1 Hz)
Digisonde	Digitally Integrating Goniometric IonoSONDE
DIGISUN	A software application for digitization of scanned sunspot drawings
DKIST	Daniel K. Inouye Solar Telescope
DLR	German Aerospace Center
DOI	Digital Object Identifier
DoY	Day of Year
DPS	Division for Planetary Sciences (EPSC)
Dr.	Doctor
DSCOVR	Deep Space Climate Observatory
Dst	Disturbance Storm Time index (geomagnetic)
DUSTER	Dust Study, Transport and Electrostatic Removal (for exploration missions)
E	East
e-Callisto	extended Compact Astronomical Low-cost Low-frequency Instrument for Spectroscopy and Transportable Observatory
E-GVAP	EUMETNET GNSS water Vapour Programme
EC	European Commission
ECS	European CubeSat Symposium
ECSIM(-CYL)	Energy Conserving Semi-Implicit Method (Cylindrical)
ed.	Edition
Eds.	Editors
EGNOS	European Geostationary Navigation Overlay Service
EGNSS	European GNSS
EGU	European Geosciences Union
EISCAT	European Incoherent SCATter scientific association
EIT	Extreme ultraviolet Imaging Telescope (SOHO)
EM	(1) Electromagnetic (2) Engineering Model
EPN	EUREF Permanent Network
EPOS(-PL)	European Plate Observing System (- Poland)
E-PROFILE	EUMETNET Profiling Programme
EPSC	European Planetary Science Congress
EPT	Energetic Particle Telescope (PROBA-V)
erg	10^{-7} Joule
Es	Sporadic E-layer (ionosphere)
ES	Earth System (Science and Environmental Management (COST)
ESA	European Space Agency
ESAC	European Space Astronomy Centre
ESC	Expert Service Centre
ESD	ElectroStatic Discharge

ESCAPE	European SpaceCraft for the study of Atmospheric Particle Escape
ESERO	European Space Education Resource Office
ESOC	European Space Operations Centre
ESPM	European Solar Physics Meeting
ESTEC	European Space Research and Technology Centre
ESWW	European Space Weather Week
EU	European Union
EUHFORIA	European Heliospheric Forecasting Information Asset
EUI	Extreme-Ultraviolet Imager (Solar Orbiter)
EUMETNET	Network of European Meteorological Services
EUMETSAT	European Organisation for the Exploitation of Meteorological Satellites
EURAVIA	European Association of Aerospace Students
EUREF	EUropean Reference Frame
EUV	Extreme Ultraviolet
EUVI	Extreme Ultraviolet Imager (STEREO/SECCHI; LGRRS)
EUVM	EUV Monitor (MAVEN)
EVE	Extreme ultraviolet Variability Experiment (SDO)
ExoMars	Exobiology on Mars (ESA, Roscosmos)
$F_{10.7\ cm}$	Solar radio flux at 10.7 cm wavelength
F10.7P	Proxy for $F_{10.7\ cm}$ solar radio flux
F_2	Main ionospheric layer
F_{30}	Solar radio flux at 30 cm wavelength
FITS	Flexible Image Transport System
FM	Flight Model
FMI	Finnish Meteorological Institute
FNRS	Fonds National de la Recherche Scientifique
foF2	Critical frequency F2-layer
FOV	Field-Of-View
FP7	Framework Programme 7 (EU)
FReSWeD	Future Research on Space Weather Drivers
FRS	Fonds de la Recherche Scientifique
FTE	Full-Time Equivalent
FUV	Far Ultraviolet
Galileo	European GNSS
GAW	Global Atmospheric Watch (WMO)
GB	Gigabyte (10^9 bytes)
GBO	Ground-Based Observatory
GCR	Galactic Cosmic Rays
GEANT-4	GEometry ANd Tracking (simulation platform)
GeV	Giga electronvolt ($10^9 . 1.6 . 10^{-19}$ Joule)
GFZ	Deutsches GeoForschungsZentrum (German Research Centre for Geosciences)
GHz	Gigahertz (10^9 Hz)
GIRO	Global Ionosphere Radio Observatory
GLE	Ground Level Enhancement
GLONASS	GLObal NAvigation Satellite System (Russia)
GNSS	Global Navigation Satellite System
GNSS4SWEC	Advanced GNSS tropospheric products for the monitoring of Severe Weather Events and Climate
GOES	Geostationary Operational Environmental Satellite
GOME	Global Ozone Monitoring experiment (SCIAMACHY)
GOMESCIA	GOME/SCIAMACHY/GOME-2
GONG	Global Oscillation Network Group
GPS	Global Positioning System (USA)
GRETSI	Groupe d'Etudes du Traitement du Signal et des Images
GSFC	Goddard Space Flight Center
h	(1) hour ; (2) Planck's constant ($6.62607004 \times 10^{-34}$ m^2 kg / s)
H	(1) Hydrogen ; (2) Heat flux
H-alpha (Hα)	A red visible spectral line at 656.28 nm created by Hydrogen

H2020	Horizon 2020 (EU)
HEK	Heliophysics Events Knowledgebase
HELSTOP	Harmonization and Evaluation of Lower Stratospheric and Tropospheric Ozone Vertical Profiles
HESPERIA	High Energy Solar Particle Events forecasting and Analysis project
HF	High Frequency
HI	Heliospheric Imager (STEREO)
h_mF_2	peak density height of F_2-layer
HMI	Heliospheric and Magnetic Imager (SDO)
HSRS	Humain Solar Radio Spectrograph
HSS	High Speed Stream
HuRAS	Humain Radio Astronomy Station
HXR	Hard x-rays
Hz	Hertz (per second)
I/Ps	Ionosphere-Plasmasphere system
I-V	Current-Voltage
IAC	International Astronautical Congress
IAG	International Association of Geodesy
IAGA	International Association of Geomagnetism and Aeronomy
IAS	Institut d'Astrophysique Spatiale (France)
IASB	Institut royal d'Aéronomie Spatiale de Belgique
IASC	International Arctic Science Committee
IAU	International Astronomical Union
ICAO	International Civil Aviation Organization
ICME	Interplanetary CME
ICT	Information and Communication Technologies
i.e.	"id est" (that is)
IEEE	Institute of Electrical and Electronics Engineers
IGS	International GNSS Service
IMC	International Meteor Conference
IMF	Interplanetary Magnetic Field
INGV	Istituto nazionale di geofisica e vulcanologia
InSight	Interior Exploration using Seismic Investigations, Geodesy and Heat Transport
INSPIRE	International Satellite Program in Research and Education
IOP	Institute of Physics
IPAG	Institut de Planétologie et d'Astrophysique de Grenoble
IPF	International Polar Foundation
IPIM	IRAP Plasmasphere Ionosphere Model
IR	Infrared
IRACON	Inclusive Radio Communication Networks for 5G and beyond
IRAP	Institut de Recherche en Astrophysique et Planetologie (France)
IRENE	International Radiation Environment near Earth
IRI	International Reference Ionosphere
IRM	Institut Royal Météorologique
ISAS	Institute of Space and Astronautical Science
ISC	(1) International Science Council; (2) International Steering Committee
ISN	International Sunspot Number
ISS	International Space Station
ISSI	International Space Science Institute
ISSS	(1) International School of Space Science; (2) International School/Symposium for Space Simulations
ISTP	International Symposium on Tropospheric Profiling
IT	Information Technology
ITU	International Telecommunication Union
IUGG	International Union of Geodesy and Geophysics
IVOA	International Virtual Observatory Alliance
jHV	jHelioViewer

JOSIE	Jülich Ozonesonde Intercomparison Experiment
JPEG	Joint Photographic Experts Group
JSWSC	Journal of Space Weather and Space Climate
JUICE	JUpiter ICy moons Explorer
K	(1) Local K-index: A 3-hour geomagnetic index, ranging from 0 (quiet) to 9 (extremely severe storm); (2) degrees Kelvin
K*	Local 1-minute resolution K index
Ka-band	"Kürz above": Radio frequency band from 27-40 GHz
KAW	Kinetic Alfvén Waves
keV	kilo electronvolt ($10^3 . 1.6 . 10^{-19}$ Joule)
kHz	kilo Hertz (10^3 /second)
km	kilometer
km/s	kilometers per second
KMI	Koninklijk Meteorologisch Instituut
KNMI	Koninklijk Nederlands Meteorologisch Instituut
K_p	A geomagnetic index, ranging from 0 (quiet) to 9 (extremely severe storm)
KSO	Kanzelhöhe Solar Observatory
KSB	Koninklijke Sterrenwacht van België
KUL	Katholieke Universiteit Leuven
kV	kiloVolt (10^3 Volt)
λ	wavelength
l/m^2	Liter per square meter
L-class	Large class satellite (ESA)
L	Letter (manuscript)
L*	Set of Earth's magnetic field lines which cross the Earth's magnetic equator at * earth radii from the centre of the Earth (e.g. L = 2)
L_0	Heliographic longitude of the central point of the solar disk
L1, … , L5	First, … , fifth Lagrangian point
L1, L2	GPS frequencies: L1 = 1575.42 MHz, L2 = 1227.60 MHz
LaRa	Lander Radio science (ExoMars)

LASCO	Large Angle Spectrometric Coronagraph (SOHO); small (C2) and wide (C3) field of view
Lat	Latitude
LATMOS	Laboratoire ATmosphères, Milieux, Observations Spatiales (France)
LDE	Long Duration Event
LEO	Low Earth Orbit
LGGRS-EUVI	LaGRange Remote Sensing instruments (EUVI)
LIDAR	LIght Detection And Radar
LIEDR	Local Ionospheric Electron Density profile Reconstruction
LMSAL	Lockheed Martin Solar and Astrophysics Laboratory
LOC	Local Organizing Committee
LOFAR	Low-Frequency Array
Lon	Longitude
Ls	Solar longitude
LT	Local Time
Ly-α	Lyman-alpha, a spectral line in the VUV at 121.6 nm
LYRA	Large Yield Radiometer, formerly called Lyman Alpha Radiometer (PROBA2)
LW	Langmuir Wave
LWS	Living With a Star
µm	micrometer (10^{-6} meter)
M-class	Medium class satellite (ESA)
M-class flare	Medium x-ray flare
m^3	Cubic meter
MADAWG	Modelling and Data analysis Working Group (Solar Orbiter)
MAJIS	Moons And Jupiter Imaging Spectrometer (JUICE)
MAVEN	Mars Atmosphere and Volatile EvolutioN (NASA)
MB	Megabyte (10^6 bytes)
mbar	millibar
MER	Mars Exploration Rover
MeV	Mega electronvolt ($10^6 . 1.6 . 10^{-19}$ Joule)
MHD	Magnetohydrodynamics
MHz	Megahertz (10^6/s)
MIT	Massachusetts Institute of Technology
MJD	Modified Julian Day
ML-Helio	Machine Learning in Heliophysics

MLT	Magnetic Local Time
mm	millimeter (10^{-3} meter)
mm/s	millimeter per second
MoMo	Model of Mars Ionosphere
MPS	Max Planck Institute for Solar System Research
ms	millisecond (10^{-3} second)
MUV	Mid Ultraviolet
ν	Frequency
N	North
N-S	North-South
n-SEU	neutron induced SEU
N_2	Nitrogen
nA	nano Ampère (10^{-9} meter)
NASA	National Aeronautics and Space Administration
NASU	National Academy of Sciences of Ukraine
NATO	North Atlantic Treaty Organization
NeQuick	Electron density Quick calculation model (ionospheric model)
Net-TIDE	Pilot Network for Identification of Travelling Ionospheric Disturbances in Europe
NIR	Near IR
NL	The Netherlands
NM	Neutron Monitor
No.	Number of
nm	nanometer (10^{-9} meter)
NMDB	Neutron Monitor DataBase
N_mF_2	peak density of F_2-layer
NOAA	National Oceanic and Atmospheric Administration
NRT	Near Real Time
ns	nanosecond (10^{-9} second)
NSO	National Solar Observatory
nT	nano-Tesla (10^{-9} Tesla)
NUV	Near Ultraviolet
NWP	Numerical Weather Prediction
O	Oxygen
O_3	Ozone
ODC	On Duty Center (PECASUS)
OGSE	Optics Ground Support Equipment
OML	Orbital-Motion-Limited
ORB	Observatoire Royal de Belgique
ORFEES	Observation Radio Fréquences pour l'Etude des Eruptions Solaires
P	The position angle between the geocentric north pole and the solar rotational north pole measured eastward from geocentric north. The range in P is $\pm$26.3°
P2SC	PROBA2 Science Center
PB	Petabyte (10^{15} bytes)
PBC	Primary Backup-Center (PECASUS)
PEA	Princess Elisabeth Antarctic
PECASUS	Pan-European Consortium for Aviation Space weather User Services
PFSS	Potential Field Source Surface
pfu	particle (proton) flux unit: the number of particles registered per second, per square cm, and per steradian
PhD	Doctor of Philosophy
PI	Principal Investigator
PICASSO	PICo-satellite for Atmospheric and Space Science Observations
PRESTO	Fast warning message for important SWx events
PROBA	PRoject for OnBoard Autonomy
PROBA-V	PROBA-Vegetation
PROBE	PROfiling the atmospheric Boundary layer at European scale (COST)
PRODEX	PROgramme for the Development of scientific Experiments
ps	picosecond (10^{-12} second)
PSF	Point Spread Function
PTB	Physikalish-Technische Bundesanstalt (Germany)
Q&A	Questions and Answers
QPP	Quasi-periodic pulsation
R	Resistor
R&D	Research and Development
R-ESC	Space Radiation ESC
RAS	Royal Astronomical Society
RC circuit	An electric circuit composed of resistors and capacitors
RC time	The time constant (in seconds) of an RC circuit

ReSourCE	Radio Sciences Research on AntarCtic AtmosphEre
RF	Radio Frequency
RHESSI	Reuven Ramaty High Energy Solar Spectroscopic Imager
RISE	Rotation and Interior Structure Experiment (InSight)
RMI(B)	Royal Meteorological Institute (of Belgium)
RMS	Root Mean Square
ROB	Royal Observatory of Belgium
Roscosmos	Russian Space Agency
RSSB	Royal Statistical Society of Belgium
R_{sun}	Solar radius (~ 696,000 km)
RTIM	Real Time Ionosphere Monitoring
RWC	Regional Warning Center
σ	sigma (confidence level)
s	second
S	South
S-band	Radio frequency band from 2-4 GHz
S/C	Spacecraft
S-class	Small class satellite (ESA)
S-SAIL	Solar System Atmospheres' Investigation and exopLanets
SAFIRE	SolAr Flux monItoRing Equipment
SANAE-IV	South African National Antarctic Expedition IV (Antarctic research base)
SANSA	South African National Space Agency
SBC	Secondary Backup-Center (PECASUS)
SC24, SC25	Solar Cycle 24, Solar Cycle 25
SCAR	Scientific Committee on Antarctic Research
SCIAMACHY	SCanning Imaging Absorption spectroMeter for Atmospheric CHartographY (ENVISAT)
SCK-CEN	Studiecentrum voor Kernenergie - Centre d'Etude de l'Energie Nucléaire
SCOPE	Solar Coronagraph for OPErations
SDO	Solar Dynamics Observatory
SDR	Software Defined Radio
SECCHI	Sun Earth Connection Coronal and Heliospheric Investigation (STEREO)
SEP	Solar Energetic Particle
SEPEM	Solar Energetic Particle Environment Modelling
SEU	Single Event Upset
SFU, sfu	Solar Flux Unit (10^{-22} W m^{-2} Hz^{-1})
SHADOZ	Southern Hemisphere Additional Ozonesondes (JOSIE)
SHINE	Solar Heliospheric & Interplanetary Environment
SIDC	Solar Influences Data analysis Center
SILSO	Sunspot Index and Long-term Solar Observations
SKA	Square Kilometre Array
SLP	Sweeping / Segmented / Single/ Split / Spherical Langmuir Probe
SLT	Solar Local Time
SM	Spare Model
sms	short message service
SN	Sunspot Number
SN	Space weather and Near-earth objects
SOC	Science Operations Centre
SOHO	SOlar & Heliospheric Observatory
SOLARNET	European network of solar physics researchers and facilities (H2020)
SOLIS	Synoptic Optical Long-term Investigations of the Sun (NSO)
SolO	Solar Orbiter
SOLSPEC	SOLar SPECtrum
SPADE	Small Phased Array DEmonstrator
SPD	Solar Physics Division (AAS)
SPENVIS (-NG)	SPace ENVironment Information System (- Next Generation)
SPICE	Spectral Imaging of the Coronal Environment (SolO)
SPIE	Society of Photo-Optical Instrumentation Engineers
SPRING	Solar Physics Research Integrated Network Group (SOLARNET)

SPS	Science for Peace and Security (NATO)
sr	steradian
SRAM	Static Random-Access Memory
SRB	Solar Radio Burst
SREM	Standard Radiation Environment Monitor (Integral, Rosetta)
SSA	Space Situational Awareness
SSCC	SSA Space Weather Coordination Centre
SSI	Solar Spectral Irradiance
SSN	SunSpot Number
STAFF	Solar Timelines viewer for AFFECTS
STCE	Solar-Terrestrial Centre of Excellence
STCL	Space Technology & Calibration Laboratories
STEREO	Solar-TErrestrial RElations Observatory
STM	Structural Model
SUVI	Solar Ultraviolet Imager (GOES)
SWAP	Sun Watcher using APS detector and image Processing (PROBA2)
SWAVES	STEREO WAVES
SWE	Space Weather
SWEK	Space Weather Event Knowledgebase
SWIC	Space Weather Introductory Course
SWPC	Space Weather Prediction Center (USA)
SWT	Science Working Team
SWx	Space weather
SXR	Soft x-rays
SXT	Soft X-Ray Telescope (Yohkoh)
SZA	Solar Zenith Angle
τ	Time
TB	Terabyte (10^{12} bytes)
TEC	Total Electron Content
Tech-TIDE	Warning and Mitigation Technologies for TIDs Effects
TECu	TEC unit ($10^{16} e \cdot m^{-2}$)
TGSE	Thermic Ground Support Equipment
THEMIS	Time History of Events and Macroscale Interactions during Substorms (NASA mission)
TID	Travelling Ionospheric Disturbance
TRACTEBEL	International company for consultancy and engineering; merger from Tractionel and Electrobel
TREASURE	Training Research and Applications Network to Support the ultimate real-time high-accuracy EGNSS solution
TSI	Total Solar Irradiance
UCL	Université Catholique de Louvain
UHF	Ultra High Frequency (0.3 - 3 GHz)
UK	United Kingdom
ULB	Université libre de Bruxelles
UNCOPUOS	United Nations Committee on the Peaceful Use of Outer Space
URAN	Ukrainian Radio Interferometer of NASU
URSI	International Union of Radio Science - Union Radio-Scientifique Internationale
US(A)	United States (of America)
USET	Uccle Solar Equatorial Table
UT(C)	(Coordinated) Universal Time
UV	Ultraviolet
v	Velocity (speed)
V	Volt
V1, 2, …	Version 1, 2, …
VarSITI	Variability of the Sun and Its Terrestrial Impact
VBI	Visible Broadband Imager (DKIST)
VHF	Very High Frequency
VIP	Very Important Person
VIS	Visible
VKI	Von Karman Institute
VLF	Very Low Frequency
VSWMC	Virtual Space Weather Modelling Centre
VTEC	Vertical TEC
VUB	Vrije Universiteit Brussel
VUV	Vacuum Ultraviolet
VVS	Vereniging Voor Sterrenkunde
W	(1) Watt; (2) West
W/m^2	Watt per square meter

WAVES	Radio and plasma wave investigation (WIND, STEREO)
WDC	World Data Center
WG	Working Group
W_L	Energy of a Longmuir wave
WMO	World Meteorological Organization
WP	Work Package
WRC	World Radiation Center
WS	Workshop
WSA	Wang-Sheeley-Arge (model for solar wind)
X-band	Radio frequency band from 8-12 GHz
X-class flare	Extreme x-ray flare
XRT	X-Ray Telescope (Hinode)
ZTD	Zenith Total Delay